

**Crosstalk of ancient pathways:
Phosphoinositides link receptor-triggered MAP-kinase signalling to
membrane trafficking in Arabidopsis**

Dissertation

Zur Erlangung
des Doktorgrades der Naturwissenschaften
„doctor rerum naturalium“

der

Naturwissenschaftlichen Fakultät I
– Biowissenschaften –
der Martin-Luther-Universität Halle-Wittenberg



Vorgelegt von Herrn Wilhelm Menzel
geboren am 20. November 1987
in Frankfurt an der Oder, Deutschland

Gutachter:

1. Prof. Dr. Ingo Heilmann
2. Prof. Dr. Sabine Rosahl
3. Prof. Dr. Ralph Hückelhoven

Dissertationsschrift eingereicht am: Donnerstag, 1. August 2019

Datum der Dissertationsverteidigung: Freitag, 13. Dezember 2019

Inhalt

1	Introduction	1
1.1	Plant cells perceive environmental cues	1
1.1.1	Exogenous cues can be perceived by surface receptors and trigger signalling cascades to influence cellular processes	2
1.1.2	A limited number of signal transduction cascades amplifies signals and elicits stress-appropriate responses	4
1.1.3	Signal transduction modules mediate cell-specific responses in different signalling contexts	4
1.2	The plant MAPK system is involved in innate immunity.....	5
1.2.1	Pathogen-associated molecular pattern-triggered immunity	5
1.2.2	RbohD and reactive oxygen burst	6
1.2.3	RbohD is subject to membrane trafficking.....	8
1.3	Structural and functional properties of eukaryotic membranes	9
1.3.1	Membrane trafficking and its importance for the physiology of eukaryotic cells.....	10
1.4	The plant phosphoinositide system	12
1.4.1	Phosphoinositide formation and degradation	12
1.4.2	Phosphoinositides control membrane-associated cellular processes	15
1.4.3	Regulation of PI4P 5-kinases	17
1.5	Raison d'être	18
2	Results	20
2.1	PIP5K6 is expressed in somatic tissue and interacts physically with MPK6 in vegetative tissue	20
2.2	PIP5K6 is phosphorylated upon PAMP-perception	23
2.3	Effects of flg22 treatment on cellular PtdIns(4,5)P ₂ levels in Arabidopsis.....	26
2.3.1	Flg22-perception leads to relocalization of a PtdIns(4,5)P ₂ biosensor	26
2.3.2	PtdIns(4,5)P ₂ levels are not changed upon activation of PTI	29
2.4	Flg22 perception does not affect PIP5K6 turnover.....	32
2.5	Flg22 treatment inhibits PI4P 5-kinase activity in mesophyll protoplasts.....	34

2.6	Flg22 perception or chemically induced activation of MKK5-MPK3/6 module affects PtdIns(4,5)P ₂ -dependent processes in Arabidopsis	37
2.6.1	Endocytosis of PIN2 is inhibited upon flg22 perception or chemically induced activation of the MAPK module MKK5-MPK3/6	39
2.6.2	Flg22 perception inhibits endocytosis of RbohD in root protoplasts expressing PIP5K6-mCherry	40
2.7	PtdIns(4,5)P ₂ -dependent CME of RbohD correlates with extracellular ROS production	43
3	Discussion	46
3.1	MAPK signalling and PIs are interconnected throughout different tissues.....	46
3.2	Phosphorylation of PIP5K6 by MPK6 and inhibition of catalytic activity upon flg22 treatment	48
3.3	Protoplast expression system: a matter of control	50
3.4	Flg22-treatment or activation of the MKK5-MPK3/6 module attenuate PtdIns(4,5)P ₂ -dependent membrane trafficking.....	51
3.5	PtdIns(4,5)P ₂ may impact on RbohD recycling from the plasma membrane and on ROS production.....	53
3.6	A model to be completed: Further complexity and open questions.....	56
4	Material and methods	58
4.1	Chemical compounds and antibiotics	58
4.2	Enzymes and molecular size markers	58
4.3	Kits and single-use material	59
4.4	Equipment.....	59
4.5	Software and online tools	60
4.6	Antibodies	60
4.7	Microorganisms	60
4.8	Plant material.....	61
4.9	cDNA manipulation and molecular biology techniques	61
4.9.1	RNA isolation from plant material	61
4.9.2	cDNA synthesis from Arabidopsis total RNA preparation.....	62

4.9.3	cDNA amplification by polymerase-chain reaction (PCR)	62
4.9.4	Analysing transcript levels by quantitative real time PCR (qPCR).....	63
4.9.5	Analytical and preparative electrophoretic separation of cDNA	63
4.9.6	Measuring the concentration of nucleic acid solutions.....	64
4.9.7	Assembly of DNA constructs	64
4.9.8	DNA sequencing	64
4.9.9	Preparation of competent <i>E. coli</i> cells	64
4.9.10	Transformation of competent <i>E. coli</i> with plasmid DNA	65
4.9.11	Plasmid DNA extraction from <i>E. coli</i> cells	65
4.10	Cloning strategies.....	65
4.10.1	Epitope-tagged protoplast expression and BiFC clones.....	65
4.10.2	Plasmid constructs for protoplast expression of fluorescence-tagged PI4P 5-kinases..	67
4.10.3	Plasmid constructs for protoplast expression of EYFP-tagged RbohD.....	67
4.11	Seed sterilization.....	68
4.12	Plant growth conditions.....	68
4.13	GUS assay	68
4.14	Protoplast preparation and transformation	68
4.15	Treatment of Arabidopsis seedlings and protoplasts	69
4.15.1	FM4-64 staining of Arabidopsis seedlings.....	69
4.15.2	Pharmacological treatment.....	70
4.15.3	Elicitor treatment	70
4.15.4	Chemical induction of MKK5 KR and MKK5 DD expression	70
4.16	Bimolecular fluorescence complementation assay (BiFC).....	70
4.17	Microscopy and image analysis	71
4.18	Electrophoretic separation of ectopically expressed proteins	72
4.19	Analysing protein phosphorylation by gel shift assay	73
4.20	Immunodetection of epitope-tagged proteins	73
4.21	Immunoprecipitation of epitope-tagged proteins from transgenic protoplasts.....	74

4.22	PI4P 5-kinase activity assay.....	74
4.23	Lipid analysis	75
4.23.1	Acidic phospholipid extraction.....	75
4.23.2	Lipid separation by thin-layer chromatography (TLC).....	76
4.23.3	Isolation and transesterification of separated PIs from silica plates	76
4.23.4	FAME quantification by analytical gas chromatography.....	76
4.24	Statistical evaluation.....	77
5	Summary	78
6	Zusammenfassung	80
7	Literature	82
8	Appendix	97
8.1	Plasmids, constructs and primer.....	97
8.2	Fluorophores.....	100
8.3	Supplementary figures.....	101
9	Abbreviations	104
	Acknowledgement	107
	Curriculum vitae	109
	Publications	110
	Eidesstattliche Erklärung	111

1 Introduction

Plants are challenged by numerous environmental changes and they continuously perceive vital information on their surroundings. To be able to respond effectively to variable environmental conditions, cellular processes are coupled to mechanisms, which monitor multiple exogenous factors. Partially due to their sessile nature, plants have developed highly structured signalling networks to perceive and process stimuli and permit appropriate metabolic responses. In this thesis, the control of phosphoinositides - regulatory phospholipids with profound effects on different aspects of plant metabolism - by a receptor-triggered mitogen-activated protein kinase (MAPK) cascade is investigated. Even though phosphoinositides are highly conserved in all eukaryotic species, it is still poorly understood how the network of regulatory lipids and their coplayers are linked to other signalling pathways. Based on recently identified links between PI-metabolism and a MAPK cascade in pollen tubes, this thesis provides evidence that MAPKs and PIs can act in a common signalling pathway triggered by the activation of a cell-surface receptor by its ligand. The data on the interconnection of the MAPK and PI pathways enables a more comprehensive view of signalling events occurring during pathogen defence in vegetative tissue of *Arabidopsis thaliana* (*Arabidopsis*) plants, spanning processes from receptor-activation upstream of MAPKs and PIs all the way to PI-controlled downstream responses.

1.1 Plant cells perceive environmental cues

Biological stress is the confrontation of an organism with unfavourable environmental conditions that demand a response in order to grant survival and procreation. In the course of evolution, the sessile live style of plants has resulted in tight network mechanisms to perceive and process environmental cues and transduce the information to modulate appropriate cellular responses. As environmental stress can be detrimental to plant growth, it is an important research topic to study how plants perceive their environment and initiate responses. As plants furthermore are the basis of every food chain, to understand how crop plants respond to environmental changes is of great importance to ensure humankind's primary source of nutrition. Environmental stresses can be divided into two major categories, biotic and abiotic stress. Abiotic stress is caused by environmental changes regarding physical factors limiting or depleting vital resources, such as drought stress, hyperosmotic or salt stress, hypoxia or anoxia and temperature or light conditions. Biotic stress requires the interaction with other biological systems, including other plants, herbivores or pathogenic microorganisms. In this thesis, certain aspects of plant responses to microbial infection are investigated. Pathogenic microorganisms include infectious bacteria, fungi or oomycetes. Plants can detect and differentiate microorganisms to

induce an immune response, if necessary. The first stages of plant immune responses is the perception of pathogens at the cell surface by specific receptor proteins, and the subsequent signal transduction events that initiate early aspects of plant immune responses.

1.1.1 Exogenous cues can be perceived by surface receptors and trigger signalling cascades to influence cellular processes

The plasma membrane separates the intracellular space from the environment. Exogenous cues that derive from exogenous stresses need to be perceived at the cell surface and are converted into biochemical signals that can broadcast into the cell. Thus, surface receptors provide an important link between the extra- and intracellular space. The Arabidopsis genome encodes more than 500 receptor-like kinases (RLK) (Fritz-Laylin et al., 2005) that are involved in signal transduction events mediating downstream responses. RLKs are composed of an extracellular domain that specifically and reversibly binds to its ligand, a transmembrane domain, and a cytosolic domain that can contain a protein kinase domain. The largest family with over 170 genes possess an extracellular domain composed of leucine-rich repeats (LRR) (Memon and Durakovic, 2014). LRR-RLKs bind to specific targets enabling plant cells to perceive numerous types of elicitors. A subset of LRR-RLKs called somatic embryogenesis receptor kinase (SERK) serve as coreceptors in a hetero-dimer complex with other LRR-RLKs to modulate signalling specificity (Ma et al., 2016). LRR-RLK-mediated signalling in plant cells follows a common theme independent of the respective stimulus (**figure 1.1**). Upon ligand-binding, the LRR-RLK forms a hetero-dimer with the SERK coreceptor and is activated by phosphorylation. Activation of the receptor complex triggers downstream signalling cascades that transduce the signal onto target sites to reprogram cell metabolism. Elicitors that are perceived by LRR-RLKs include phytohormones, endogenous peptides and the molecular signatures of microorganisms, illustrating the broad variety of cellular pathways in which LRR-RLKs can be involved. For instance, the LRR-RLK CLAVATA1 (CLV1) is involved in the regulation of shoot apical meristem maintenance and binds to a regulatory peptide ligand CLAVATA3 (CLV3) (Brand et al., 2000; Ogawa et al., 2008). The phytohormone family of brassinosteroids is recognized by the LRR-RLK BRASSINOSTEROID INSENSITIVE 1 (BRI1), which associates with SERK1 or SERK4 to control plant growth (Li and Chory, 1997). In pollen tube guidance, receptors at the surface of the pollen tube cell play an important role in navigating the growing cell towards the female gametophyte for sexual reproduction. Synergid cells in the embryo sac produce cysteine-rich peptide (CRP) attractants, so called LUREs that can bind to LRR-RLKs at the plasma membrane of the growing pollen tube cell. The attractant LURE1 binds to and activates the LRR-RLK complex composed of POLLEN RECEPTOR-LIKE KINASE (PRK) 3 and PRK6 (Takeuchi and Higashiyama, 2016), which affects downstream processes like endocytosis and actin dynamics to control directional

pollen tube germination and growth (Higashiyama and Yang, 2017). RLKs are also involved in the recognition of pathogens and the initiation of the plant immune response. Plant cells have developed a set of LRR-RLKs that can recognize molecular signatures of non-plant surface structures of infectious microbes (pathogen-associated molecular patterns, PAMPs). These PAMPs include peptides, carbohydrates or lipopolysaccharides that are specific for microorganisms, and can also be referred to as microbe-associated molecular patterns (MAMP), as they can derive not only from pathogenic but also from non-pathogenic organisms. The binding of a PAMP to its surface receptor represents the initial perception of the microbe and triggers multiple cellular events, including the expression of defence genes, regulation of membrane trafficking, and the regulation of other cytosolic or nuclear proteins. In general, the activation of signalling pathways by a stimulus leads to the reprogramming of cellular metabolism towards adaptation to generate stress resistance, if possible.

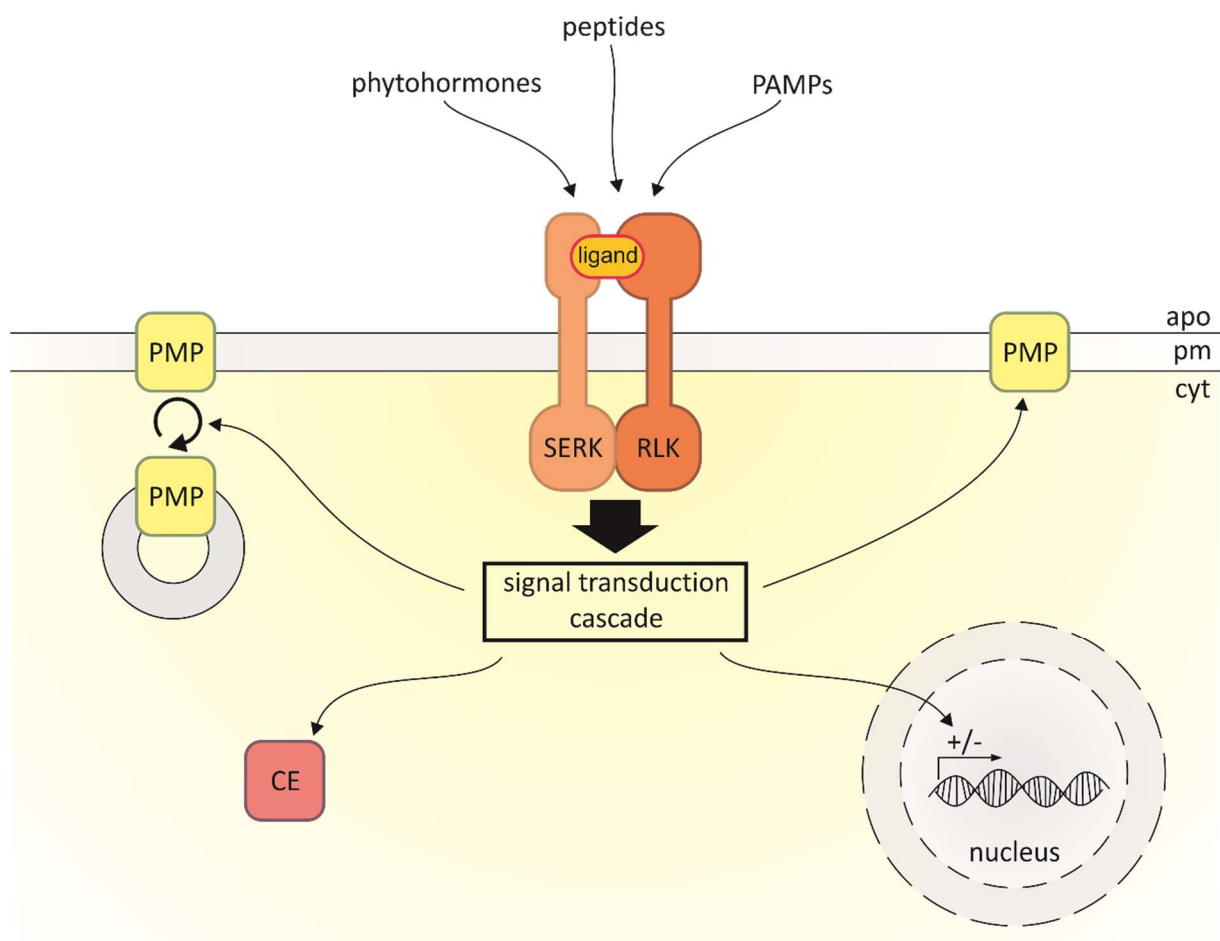


Figure 1.1: Principle of RLK-mediated signalling in plants. Association and activation of an RLK and a SERK coreceptor upon ligand-binding triggers downstream signalling cascades to transduce the signal onto cellular processes including gene expression, the regulation of membrane trafficking and recycling of plasma membrane proteins (PMP) and the regulation of activity and abundance of plasma membrane-localized and/or cytosolic target proteins (cytosolic enzymes; CE).

1.1.2 A limited number of signal transduction cascades amplifies signals and elicits stress-appropriate responses

Once an elicitor is perceived by a surface receptor, a signal is transduced to the inside of the cell and amplified via signalling cascades. Plants utilize a complex signalling network involving calcium, nucleotides, reactive oxygen species and signalling lipids as well as proteins with roles in signalling. The function of signalling proteins can be modulated by posttranslational modification (PTM), especially phosphorylation. Reversible phosphorylation of certain residues can affect protein stability, subcellular localization and enzymatic activity (Olsen et al., 2006). The Arabidopsis genome encodes approximately 1000 protein kinases and 300 protein phosphatases (Abe et al., 2003, Koyama et al., 2010, Seki et al., 2002), a majority of which is directly involved in signal transduction. Protein kinase cascades of multiple layers provide signal amplification for effective response. Besides phosphorylation, the localization and abundance of target proteins can also be influenced by other PTMs, such as ubiquitination, sumoylation, glycosylation, methylation and acetylation. The majority of enzyme-catalyzed PTMs is reversible. Multiple PTMs can occur at the same protein at the same time, enabling dynamic modes of regulation of protein function by PTMs (Chalkley et al., 2014). Another signalling system is the modulation of the intracellular concentration of small ions by transmembrane ion channels. Ions like K^+ , Cl^- and H^+ determine pH and global electrostatic properties within the cell to regulate downstream processes. In the case of Ca^{2+} , ions can serve as ligands. A set of calcium sensing threonine/serine kinases, calcium-dependent protein kinases (CDPK), are activated rapidly upon Ca^{2+} binding and phosphorylate downstream targets (Harper et al., 2004). The different signalling cascades present in a plant cell are tightly interconnected and influence each other.

1.1.3 Signal transduction modules mediate cell-specific responses in different signalling contexts

As mentioned above, plant cells possess a set of modules that enable the processing of signals derived from exogenous and endogenous cues. Which module is activated depends on the cue and cell type. However, numerous examples have shown that individual components or even complete modules of signalling factors can contribute to different cellular processes. In these cases, the same set of enzymes can trigger response to different stimuli in different tissues. One key example with relevance to experiments in this thesis MAPKs. The MAPK MPK6, for instance, has been the subject of countless studies and was shown to be involved in numerous signalling contexts, including cold and salt stress where MPK6 is activated by the same upstream kinases during both kinds of stress (Teige et al., 2004). MPK6 has also been shown to be involved in the control of pollen tube guidance, i.e. the polar tip growth of pollen tubes towards the female ovules (Guan et al., 2014). In addition to these functions,

the most widely-known role of MPK6 is in plant defense against pathogens. To provide more background, the plant MAPK system is introduced in more detail in the following section.

1.2 The plant MAPK system is involved in innate immunity

MAPKs are highly conserved throughout eukaryotic kingdoms and can be found prominently in plants, fungi and animals. MAPK cascades are composed of at least three layers of protein kinases and are essential signals during the transduction of environmental and developmental cues into cellular processes. When a surface receptor is triggered by binding to its ligand, oftentimes a MAPK kinase kinase (MP3K, MEKK) is activated, resulting in the subsequent phosphorylation of a MAPK kinase (MP2K) and then a MAPK (MPK). The Arabidopsis genome encodes 80 MP3Ks, 10 MKKs and 20 MPKs (Colcombet and Hirt, 2008). MP3Ks display the most heterogeneous group of MAPKs (Danquah et al., 2015). Upon activation, MP3Ks phosphorylate an S/T-X₃₋₅-S/T motif within MKKs (Chang and Karin, 2001). The thus activated MKKs then target a T-X-Y motif within the activation loop of MPKs for phosphorylation (Rodriquez et al., 2010, Hettenhausen et al., 2014). Activated MPKs phosphorylate a variety of downstream target proteins, including transcription factors, cytosolic enzymes (CE) and cytoskeletal proteins as well as plasma membrane proteins (PMP) (Rodriquez et al., 2010, Jia et al., 2016). MAPKs are involved in the transduction of a variety of extracellular stimuli including abiotic stresses, such as drought, salt, cold and osmotic stress as well as biotic stresses like interaction of bacterial or fungi pathogens, which can activate the innate immune system. The role of MAPKs in PAMP-triggered immunity (PTI) is well studied and described in detail in the following section.

1.2.1 Pathogen-associated molecular pattern-triggered immunity

The plant immune system is composed of several defence layers, of which PTI is the first layer (Jones & Dangl, 2006). PTI is triggered upon the perception of a PAMP by pathogen-recognition receptors (PRR), which are receptor kinases (RK) or RLKs (Zipfel et al., 2004). As mentioned above, PAMPs can derive from different bacterial and fungi derived molecules. A prominent PRR/PAMP pair is represented by the LRR-RLK FLAGELLIN-SENSING 2 (FLS2), which can bind the conserved N terminus of bacterial flagellin (Gomez-Gomez & Boller, 2000). Upon binding of bacterial flagellin or the artificial elicitor peptide flg22, FLS2 associates with its coreceptor, the BRI1-associated receptor kinase 1 (BAK1), resulting in the rapid phosphorylation and activation of both proteins (Chinchilla et al., 2007). The activation of FLS2 upon binding of flg22 triggers the activation of the MAPK module MKK4/MKK5-MPK3/MPK6 (Meng and Zhang, 2013). However, the initial steps of this activation are still not fully understood, and no MAP3K is identified yet that links the FLS2/BAK1 receptor complex to the MAPK cascade (Asai et al, 2002, Ren et al, 2002).

A fully functional flg22-triggered activation of MKK4/MKK5-MPK3/MPK6 in Arabidopsis *mekk1* mutant plants indicates that MEKK1 is not the responsible upstream MP3K (Ichimura et al., 2006; Suarez-Rodriguez et al., 2007). A known element of early signal transduction of the flg22 stimulus is BOTRYTIS-INDUCED KINASE1 (BIK1), a cytosolic protein kinase associated with the FLS2/BAK1 co-receptor complex. Upon flg22 perception, BIK1 is activated by phosphorylation and dissociates from the co-receptor complex (Lu et al., 2010). *Bik1 pbl1* double mutant plants show no changes in flg22-triggered MPK3/MPK6 activity, indicating that BIK1 is not necessary for the activation of this particular MAPK cascade (Feng et al., 2012). However, in protoplasts expressing the bacterial effector protein AvrAC, MPK3/MPK6 activity was decreased. AvrAC is an inhibitor of BIK1 and can probably also prevent activation of BIK1-related protein kinases, which indicates these kinases as candidates for protein kinases upstream from the MKK4/MKK5-MPK3/MPK6 module (Feng et al., 2012). Although Ca²⁺ seem to trigger MPK3/MPK6 activation, no calcium-dependent protein kinase CDPK has been identified yet to act as an upstream activator (Bodsocq et al., 2010). Even though these early steps still require clarification, it is well accepted that flg22 perception by FLS2 results in the activation of several MAPKs, including MPK3 and MPK6. Activated MPK3 and MPK6 phosphorylate downstream target proteins to reprogram metabolism towards pathogen defence, resulting in the activation of innate immunity. MPK3 and MPK6 act partially redundant and share some target proteins, while other targets are specifically phosphorylated by either MPK3 or MPK6 (Rayapuram et al., 2018). An overview of different signalling events occurring upon PAMP perception in plant cells is illustrated in **figure 1.2**.

Whereas PTI can display an effective mechanism to prevent infection, some pathogenic organisms have evolved a setup of effector proteins that are transferred into the host cell to suppress plant defence response (Cui et al., 2015). To counteract immune suppression by bacterial effectors, plants deploy a second layer of defence that is called effector triggered immunity (ETI), which is mediated by the recognition of bacterial effectors by intracellular nucleotide-binding/leucine-rich-repeat (NLR) receptors (Cui et al., 2015). Due to the limited scope of this thesis, ETI is not discussed further in detail.

1.2.2 RbohD and reactive oxygen burst

Reactive oxygen species (ROS) regulate a variety of cellular processes in plants, including biotic and abiotic stress responses and development. During plant immune responses, transient ROS production is rapidly and massively induced (Doke et al., 1983) (**figure 1.2**). PAMP-induced production of apoplastic ROS executes a wide range of functions to increase plant immunity, including oxidative stress to the pathogen, stomatal closure and cell wall strengthening via glycoprotein crosslinking and callose deposition (Lambeth, 2004, Bradley et al. 1992, Mersmann et al. 2010, Luna et al. 2011, Macho

et al. 2012). Additionally, apoplastic ROS has been described to trigger ROS production in neighbouring cells to induce defence in distal tissues (Dubella et al. 2013).

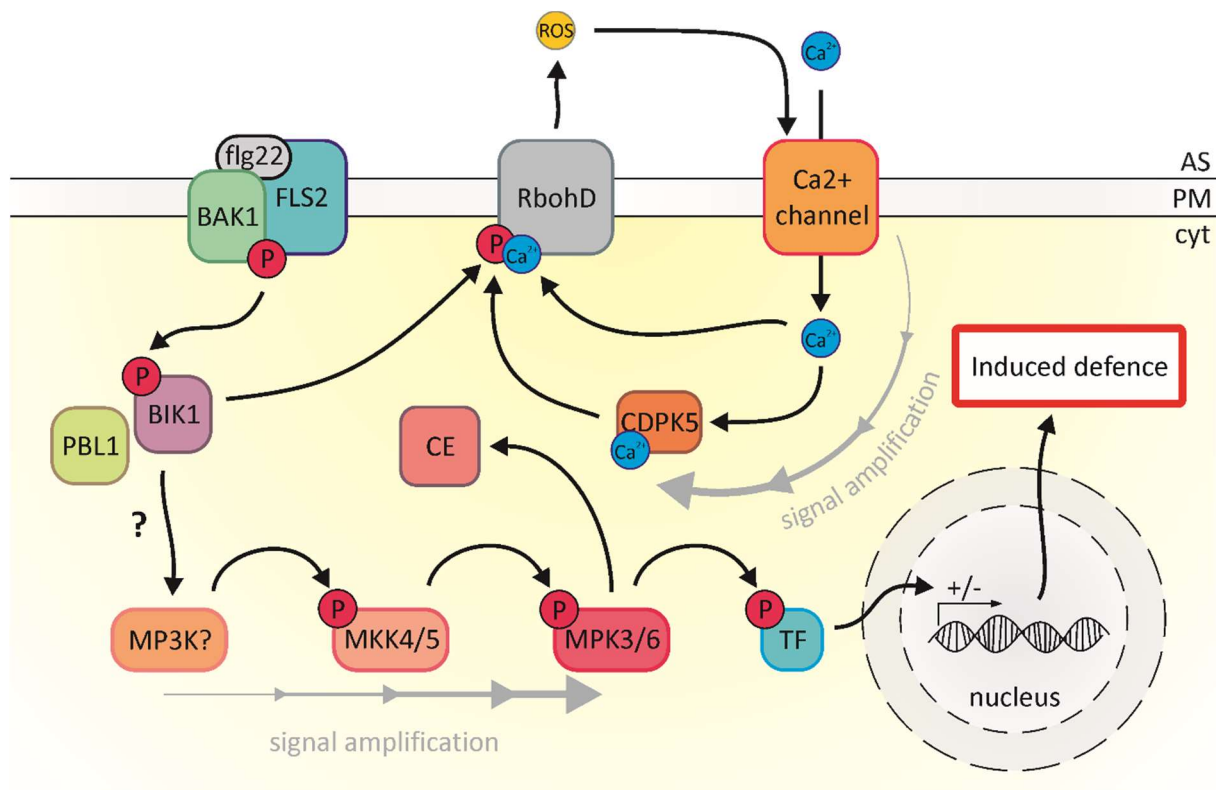


Figure 1.2: Flg22-triggers downstream kinase signalling cascades. Binding of the N-terminal region of the bacterial flagellum or flg22 to FLS2 leads to the activation of two independent signalling pathways: 1. a MAPK-mediated regulation of gene expression and regulation of cytosolic targets and 2. the activation of RbohD-mediated ROS production. Activation of RbohD requires multiple layers of regulatory events including phosphorylation and calcium-binding. Cytosolic enzyme (CE), transcription factor (TF), apoplastic space (AS), plasma membrane (PM), cytosol (cyt). Scheme according to Bigeard et al., 2015.

ROS are produced in different cellular compartments including the plasma membrane, mitochondria, chloroplasts and peroxisomes (Singh et al., 2016). Apoplastic ROS are produced by plasma membrane localized nicotinamide adenine dinucleotide phosphate (NADPH)-oxidases also called reactive oxygen burst homologues (Rboh). The Arabidopsis genome encodes ten *RBOH* genes, of which *RBOHD* encodes an isoform mainly responsible for apoplastic ROS-production upon pathogen recognition (Torres et al., 2002). The central ferric oxidoreductase domain of the RbohD protein is comprised of 6 trans-membrane domains (**figure 1.3**). The N-terminus contains a binding domain for the signalling lipid phosphatidic acid (PtdOH) and two copies each of an EF-hand and an EF-like-hand domain, while the C-terminus is responsible for FAD and NADPH binding (Kadota et al., 2015). RbohD is rapidly activated upon PAMP-perception within a few minutes (**figure 1.2**). Two signalling pathways control elicitor-triggered activation of RbohD. Perception of flg22 triggers influx of apoplastic Ca²⁺, which can

directly bind the EF hand domains of RbohD and is required for activation (Ogasawara et al. 2008). Additionally, CDPKs are activated upon the increased intracellular Ca^{2+} concentration. CDPK5 phosphorylates the N-terminal cytosolic domain of RbohD at specific serine residues (Dubiella et al. 2013). Beside Ca^{2+} -dependent regulation, PAMP-induced RbohD activation is also affected by BIK1-mediated phosphorylation (Li et al., 2014). RbohD interacts physically with the FLS2/BAK1 PRR complex and is phosphorylated by BIK1 upon flg22 perception (Kadota et al. 2014, Li et al. 2014). Furthermore, investigations on *rbohD* null mutants expressing an RbohD variant that cannot be phosphorylated by BIK1 anymore, showed that decreased PAMP-triggered ROS production correlates with a higher susceptibility of plants to hypovirulent bacteria (Kadota et al., 2014).

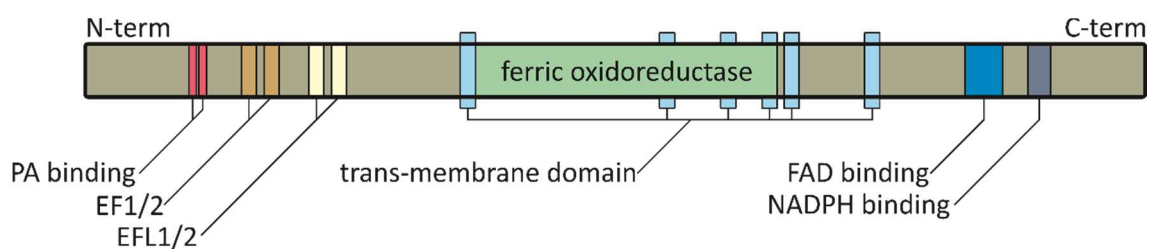


Figure 1.3: The domain structure of RbohD reflects its complex modes of regulation. The cytosolic N-terminal region of RbohD contains two phosphatidic acid binding (PtdOH) domains, two EF-hand and two EF-like-hand domains. The ferric oxidoreductase is located in the six central trans-membrane domains. The cytosolic C-terminus harbours two domains that bind FAD and NADPH, respectively. Figure modified from Kadota et al. (2014).

1.2.3 RbohD is subject to membrane trafficking

All plasma membrane proteins (PMPs) are subject to recovery from the plasma membrane to the endomembrane system composed of trans-Golgi network (TGN) and early endosomes (EE). As an integral plasma membrane protein, RbohD is thought to undergo constant rounds of endo- and exocytosis, and the balance of these processes defines the lifetime of the protein at the plasma membrane. It has recently been shown that RbohD colocalizes with clathrin and the protein Flot1 (Hao et al., 2014) at the plasma membrane and upon inhibition of exocytosis accumulates in endosomal bodies that can be stained by the lipophilic dye, FM 4-64. The accumulation of RbohD in endosomal bodies is amplified upon application of salt stress and accompanied by increased intracellular ROS production (Hoa et al., 2014). These observations indicate that RbohD undergoes clathrin-mediated endocytosis and its localization correlates directly with the NADPH-oxidase activity to determine the level and specific localization of ROS production. Besides recycling processes, Hoa et al. performed experiments to elucidate the dynamics of RbohD at the plasma membrane. By using variable-angle total internal reflection fluorescence microscopy (VA-TIRFM) imaging GFP-tagged RbohD was observed in a spot-like pattern rather than with uniform distribution within the plasma membrane plane (Hoa

et al., 2014). Quantification of GFP-RbohD foci revealed accelerated lateral mobility and higher levels of oligomerization upon flg22 perception (Hao et al., 2014). In contrast to salt stress, PAMP perception triggers the production of apoplastic ROS (Torres et al., 2002), suggesting RbohD to be stabilized at the plasma membrane, which would require a decreased endocytotic rate of the NADPH-oxidase. However, the rates of endocytosis of RbohD during PTI have never been reported, and it is unclear whether RbohD is recycled from the plasma membrane at a constant rate or may be stabilized upon PAMP perception for more efficient production of apoplastic ROS. As some results from this thesis suggest the latter scenario, it is important to become familiar with the contribution of regulatory membrane lipids and phosphoinositides in the control endocytosis and exocytosis of plasma membrane proteins in plants.

1.3 Structural and functional properties of eukaryotic membranes

All cells are surrounded by membranes that create permeability barriers to limit the exchange of substances and information between the intra- and extracellular space (Gerth et al., 2017). In eukaryotic cells, membranes also form intracellular compartments to provide enclosed spaces within the cell that can execute functions independently from each other. The body of cellular membranes is built from a variety of amphiphilic lipids with polar hydrophilic head groups and hydrophobic backbones. The amphiphilic nature of these lipids favors the formation of bilayer structures in aqueous surroundings. Within bilayers, the hydrophobic portion of the lipids is oriented to the center of the membrane, while the hydrophilic head groups are displayed to the cytosolic or apoplastic spaces, respectively. While this general principle of membrane structures is shared by all membranes, the specific lipid composition of membranes can vary between compartments but also between areas of the same membrane in time and space. Except for chloroplastic thylakoids, structural glycerophospholipids represent the major lipid class in membranes, including phosphatidylcholine (PtdCho), phosphatidylethanolamine (PtdEtn) and Phosphatidylinositol (PtdIns). Sphingolipids display the second most abundant lipid class and are represented by glycosylceramides (GCers), glycosylinositolphosphorylceramides (GIPCs), ceramide species (Cers) or free long-chain bases (Gerth et al., 2017). Together with sterol-based lipids, these major constituents define the physical properties of membranes and provide the matrix that hosts protein factors.

Functional properties of a membrane are mainly defined by the associated or embedded proteins that mediate membrane-associated processes, such as altering a membrane area via endo- and exocytosis, directional transport of chemical compounds or the perception and transduction of environmental signals (Heilmann, 2016). Similar to lipid species, membrane protein composition differs between cell types, membrane areas or can change upon environmental cues. With reference to plant surface

receptors, plasma membrane proteins are subject to continuous rounds of recycling between the plasma membrane and a complex endomembrane system mediated by the adjustable balance of endo- and exocytosis. The entirety of dynamic movement of membrane vesicles between the plasma membrane, endomembranes, the endoplasmic reticulum (ER), the Golgi, the tonoplast and endosomal compartments, is summarized by the term membrane trafficking.

1.3.1 Membrane trafficking and its importance for the physiology of eukaryotic cells

The exchange of membrane material and/or membrane embedded proteins between different compartments requires a tightly regulated trafficking system. Plasma membrane proteins and membrane material are inserted into the plasma membrane via the fusion of secretory vesicles (SV) with the plasma membrane. This process is called exocytosis. SVs can origin from at least three different exocytotic pathways. A complex endomembrane compartment called TGN is considered the most prominent among all possible donor compartments for the formation of exocytotic vesicles (Zarsky et al., 2009, Gendre et al., 2015). As the TGN not only serves as a sorting and packaging machinery for Golgi-derived cargoes but is also involved in PMP recycling and trafficking, the term TGN/early endosome (TGN/EE) has previously been suggested. The TGN/EE derives from the maturation of trans-most Golgi cisterna (Kang et al., 2011) and displays a highly dynamic structure, including a contribution of secretory and endocytotic vesicles (Viotti et al., 2010). From the TGN/EE, protein cargoes can be delivered directly to the plasma membrane or to vacuole (Griffiths and Simons, 1986). The second exocytotic pathway is also associated to the TGN/EE, from where internalized PMPs can alternatively recycle to the plasma membrane via the recycling endosome (RE). This pathway depends on the ARF-guanine exchange factor GNOM and is sensitive to the toxin, Brefeldin A (BFA). BFA is a fungi-derived substance that inhibits GNOM and causes the aggregation of endosomal material in so-called BFA-induced endosomal bodies (BFA-bodies) (Langhans et al., 2011). As an experimental tool, BFA is applied to study the endocytotic rate of protein cargoes that undergo plasma membrane recycling. Auxin-efflux carriers of the PIN-FORMED (PIN) family have been shown to recycle via the GNOM/RE pathway (Geldner et al., 2003) to control their highly polarized subcellular localization. Another compartment possibly contributing to the exocytosis in eukaryotic cells is the late endosome (LE) or multivesicular body (MVB). In plants, the role of LE/MVBs in exocytosis is poorly understood, but emerging evidence indicates that pathogen-triggered cell wall strengthening might be supported by LE/MVB trafficking (Meyer et al., 2009).

Endocytosis is the antagonistic process to exocytosis and starts with the internalization of membrane material and extracellular substances from the plasma membrane to form the endocytotic vesicle. These vesicles are transported to and fused with the TGN/EE. Depending on the fate of the cargo, the

endocytosis-derived TGN/EE domains can be delivered to a number of destinations, including the plasma membrane, via recycling and the LE/MVB that fuses with vacuoles or lysosomes to exhibit degradation of the cargo protein. Besides others, clathrin-mediated endocytosis (CME) is the most prominent and best studied endocytotic pathway in eukaryotes (Valencia et al., 2016). CME of plasma membrane cargoes is executed in 5 steps: nucleation, cargo selection, clathrin coat assembly, membrane scission and uncoating of the vesicle (McMahon and Boucrot, 2011). The nucleation starts with the activation of adaptor proteins, such as AP-2 or TPLATE (Gadeyne et al., 2014), which bind to the cargo protein and forms the adapter protein complex. Cargo proteins are selected by endocytotic sorting signals in the form of motifs within the primary and/or secondary structure, or by posttranslational modifications like phosphorylation or ubiquitination (Traub and Bonifacio, 2013). Once the cargo protein is selected, the adaptor complex starts to recruit clathrin-heavy chain (CHC) and clathrin-light chain (CLC) subunits from the cytosol to the forming vesicle (Tebar et al., 1996). Three subunits of each CHC and CLC form clathrin triskelia that assemble into a polymeric protein coat and help to stabilize the vesicle and support membrane curvature (Tebar et al., 1996). After the clathrin coat is fully assembled, GTPases or the DYNAMIN RELATED PROTEIN (DRP) family are recruited to initiate the scission of the nascent vesicle from the plasma membrane (Chappie and Dyda, 2013). Upon release of the vesicle from the plasma membrane, the disassembly of the clathrin coat starts and the free vesicle can fuse with the TGN/EE membrane (Valencia et al., 2016).

The balance of exo- and endocytosis determines the intracellular distribution, activity and the membrane-half-life of PMPs. For example, RLKs like FLS2 recycle from the PM in a GNOM-dependent manner and accumulate in endosomal bodies upon BFA application (Geldner et al., 2003, Beck et al., 2012). Although surface receptor internalization was originally proposed to be mediated by clathrin-independent endocytosis (CIE) (Li et al., 2012), recent studies indicate also CME to play a role in the internalization of FLS2 (Mbengue et al., 2016). In contrast to the receptor in its unbound state, flg22-bound FLS2 is not recycled anymore (Beck et al., 2012). Endocytotic vesicles containing activated FLS2 are directed to the LE/MVB for receptor degradation (Beck et al., 2012, Lu et al., 2011). Efficient cellular sensitivity to the flg22 elicitor has been correlated to the function of membrane trafficking of FLS2, including its internalization and recycling, and the insertion of *de novo* synthesised FLS2 protein (Smith et al., 2014). Besides surface receptors, other PMPs are also subject to membrane recycling. For instance, the contribution of membrane trafficking of PIN proteins has been studied extensively. PIN proteins show polarized localization, and PIN1 and PIN2, for instance, are localized at apical and basal plasma membrane regions of Arabidopsis root cells, respectively. It has been shown that PIN1 and PIN2 are constantly recycled from the PM via CME and that this process is sensitive to BFA treatment (Geldner et al., 2001). Furthermore, investigations on Arabidopsis *gnom* null mutants revealed a severe phenotype including impaired establishment of cell polarity, which correlates with a mislocalization of

PIN1 (Steinmann et al., 1999). These data underline the importance of recycling for the correct localization and functionality of PMPs. Besides protein factors, phosphoinositides (PIs), a minor class of regulatory membrane phospholipids, have moved into the focus of scientists as important regulators of endocytosis and exocytosis as well as numerous other membrane-associated cellular processes.

1.4 The plant phosphoinositide system

The majority of all lipids present in eukaryotic membranes are structural lipids that are important for the basic architecture of the respective membrane. However, a minor proportion of little abundant lipids serves to regulate cellular processes. PIs have been shown to be of significant importance for the regulation of various processes that are associated with the plasma membrane and the endomembrane system.

1.4.1 Phosphoinositide formation and degradation

PIs are derivatives of the glycerophospholipid PtdIns, which is composed of an inositol head group linked via a phosphodiester bond to a diacylglycerol (DAG) backbone. An overview of the formation and degradation of all PIs present in Arabidopsis is displayed in **figure 1.4**. The *de novo* synthesis of PtdIns is catalyzed by phosphatidylinositol synthases (PISs) from D-myo-inositol and cytidine diphosphate DAG (CTP-DAG) substrates. In Arabidopsis, two isoforms of PIS (PIS1, PIS2) are present that show unique substrate specificity in terms of the unsaturation status of the acyl chains of CTP-DAG (Löfke et al., 2008). The hydroxyl groups at the positions D3, D4 and D5 of the inositol head group of PtdIns can be subject to sequential phosphorylation, leading to a variety of different mono- or bisphosphorylated derivatives of PtdIns. Phosphatidylinositol 3-phosphate (PtdIns3P) is formed by the phosphorylation of the D3 position. In Arabidopsis, this reaction is catalyzed by a single PtdIns 3-kinase, VACUOLAR PROTEIN SORTING 34 (AtVPS34) (Welters et al., 1994, Mueller-Roeber and Pical, 2002). PtdIns3P can be further phosphorylated by a PtdIns3P 5-kinase at the position D5 to generate phosphatidylinositol 3,5-bisphosphate (PtdIns(3,5)P₂). The Arabidopsis genome encodes four PtdIns3P 5-kinases, FAB1A-D (Mueller-Roeber and Pical, 2002). Both PtdIns3P and PtdIns(3,5)P₂ are substrates for a PI phosphatase family called PHOSPHATASE AND TENSIN HOMOLOGUE DELETION ON CHROMOSOME 10 (PTEN) (Pribat et al., 2012). Three copies of PTENs are present in Arabidopsis (PTEN1-3). PTEN1-3 display specific phosphatase activity against the phosphorylated D3 position in PtdIns3P and PtdIns(3,5)P₂. In case of the monophosphate PtdIns3P, this reaction leads to the formation of PtdIns. For PtdIns(3,5)P₂, the depletion of D3 phosphate group is discussed as a possible pathway for the plant to generate the monophosphate phosphatidylinositol 5-phosphate (PtdIns5P).

Although plants have been shown to contain PtdIns5P, its biogenesis remains unclear, since no enzyme has been identified yet that displays D5 kinase activity and accepts PtdIns as a substrate. PtdIns(3,5)P₂ can also convert back to PtdIns3P by dephosphorylation of the D5 position.

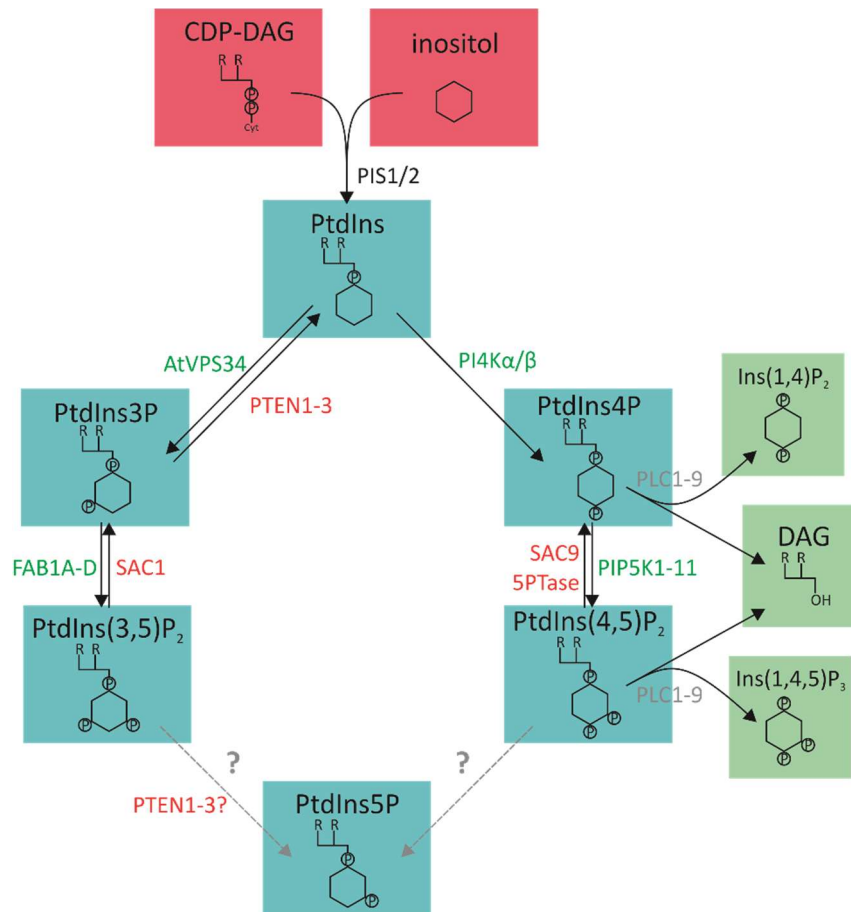


Figure 1.4: Formation and degradation of PIs in Arabidopsis. The glycerophospholipid phosphatidylinositol (PtdIns) is formed by the PtdIns synthase (PIS, black)-catalysed condensation of cytidyl triphosphate diacylglycerol (CTP-DAG) and D-myoinositol. A set of kinases (green) and phosphatases (red) reversibly catalyses the phosphorylation and dephosphorylation of the inositol head group respectively to form different PI derivatives: Monophosphates: phosphatidylinositol-3-phosphates (PtdIns3P), phosphatidylinositol-4-phosphates (PtdIns4P), phosphatidylinositol-5-phosphates (PtdIns5P), Bisphosphates: phosphatidylinositol 3,5-bisphosphates (PtdIns(3,5)P₂), phosphatidylinositol 4,5-bisphosphates (PtdIns(4,5)P₂). PtdIns4P and PtdIns(4,5)P₂ are targeted by phosphatidylinositol-specific phospholipase 1-9 (PLC1-9, grey). R = acyl chain. The scheme was created from Gerth et al., 2017.

SUPPRESSOR OF ACTIN (SAC) represents a protein family of lipid phosphatases, that is comprised of nine members and some display activity against the phosphorylated D3 position (Zhong and Ye, 2003). The third monophosphate, which is present in Arabidopsis, is phosphatidylinositol 4-phosphate (PtdIns4P), which results from the phosphorylation of PtdIns at the D4 position. Two PtdIns 4-kinase subfamilies are known in Arabidopsis, PI4Kα1/2 and PI4Kβ1/2 (Mueller-Roeber and Pical, 2002). Similar to PtdIns3P, PtdIns4P is a substrate for further phosphorylation, and PI4P 5-kinases (PI4P 5-kinases)

convert PtdIns4P to phosphatidylinositol 4,5-bisphosphate (PtdIns(4,5)P₂). The structure of PtdIns(4,5)P₂ is displayed in **figure 1.4 A**.

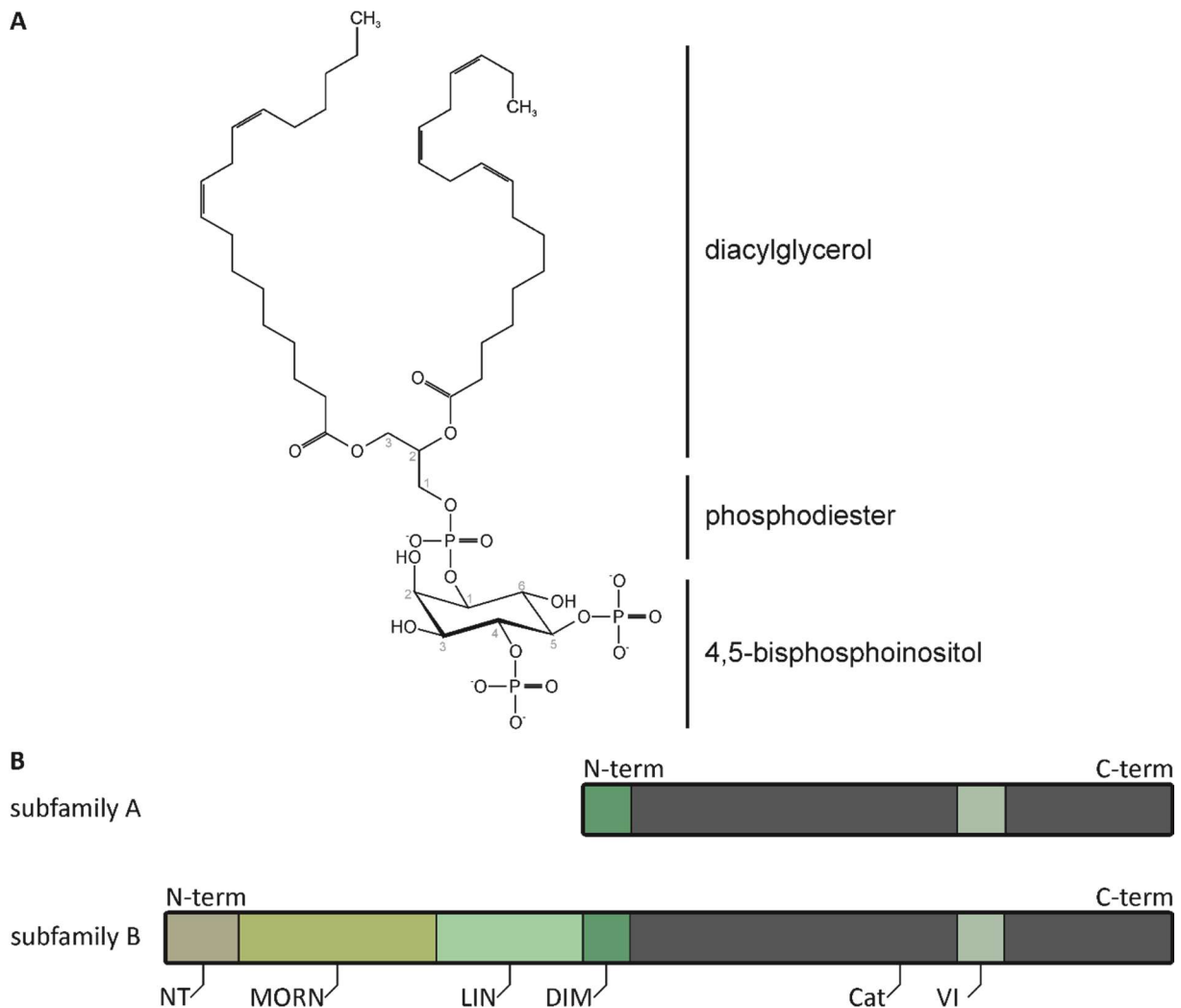


Figure 1.5: Overview of the domain structure of Arabidopsis PtdIns4P PI4P 5-kinases and the structure of PtdIns(4,5)P₂. A) PtdIns(4,5)P₂ is the phosphodiester of diacylglycerol (DAG) and a d-myo-inositol harbouring two phosphoryl moieties at the D4 and D5 positions. In this image, the acyl chains are represented by linoleic acid (at C3 position) and linolenic acid (at the C2 position). B) Arabidopsis PI4P 5-kinases comprise 11 isoforms. Subfamily A kinases (PIP5K10 and PIP5K11) are composed of a catalytically active lipid kinase domain (CAT) with a variable unconserved region (variable insert; VI) and a dimerization domain (DIM). Subfamily B kinases (PIP5K1-9) possess additional N-terminal domains: N-terminal domain (NT), membrane occupation and recognition nexus (MORN) and linker domain (LIN).

Arabidopsis encodes 11 isoforms of PI4P 5-kinase, PIP5K1-11, which can be divided into subfamily A and B according to their domain structure. While PIP5K10 and PIP5K11, comprising PI4P 5-kinase subfamily A, only possess catalytic (Cat) and N terminal dimerization (DIM) domains, the N terminus of PI4P 5-kinases of subfamily B (PIP5K1-9) includes an additional N-terminal domain (NT), a membrane occupation and recognition nexus (MORN) domain, and a variable linker (LIN) domain (**figure 1.4 B**).

These domains are unique to PI4P 5-kinases from the plant kingdom and their function is still debated. The PtdIns(4,5)P₂ is formed can be converted back to PtdIns4P by lipid phosphatases, including SAC7/ROOT HAIR DEFECTIVE 1 (RHD1) or SAC9, which dephosphorylate the D5 position of PtdIns(4,5)P₂ (Thole et al., 2008, Williams et al., 2005). This reaction can also be catalyzed by phosphoinositide 5-phosphatases (5PTases) (Zhong et al., 2005, Ercetin et al., 2008). However, none of the 15 members of the 5PTase protein family present in Arabidopsis has yet been characterized in terms of substrate specificity. PtdIns4P and PtdIns(4,5)P₂ can be further processed by a family of phosphoinositide-specific phospholipase Cs (PLCs) to form DAG and soluble Inositol(1,4)P₂ or Inositol(1,4,5)P₃, respectively (Mueller-Roeber and Pical, 2002). The Arabidopsis genome encodes nine isoforms of PLC. Among the phosphorylated PIs, PtdIns(4,5)P₂ is the best studied, and in recent years PI4P 5-kinases involved in its biogenesis have emerged as a prominent object for research (Heilmann 2016, Gerth et al., 2017).

1.4.2 Phosphoinositides control membrane-associated cellular processes

Although the importance of PIs for the regulation of various cellular processes is undebated in plants, little is known about the mechanistic details by which PIs exert their regulatory roles in certain processes. PIs are thought to act predominantly through direct protein-lipid-interaction between PIs and potential factors to be regulated, as proposed for all eukaryotic cells (Lemmon, 2003). In Arabidopsis, several PI binding domains have been identified that can bind the head group of different PI species, sometimes with a high degree of specificity (van Leeuwen et al., 2004). Examples for PI binding domains are Pleckstrin homology (PH) domains, Fab1/YOTB/Vac1/EEA1 (FYVE) domains and phagocytic oxidase (PX) domains (Lemmon, 2003). The high degree of specificity of some lipid binding domains for particular PI species has been exploited to design fluorescent probes for analyzing the subcellular distribution of these lipids: By expressing fluorescence-tagged fusions of PI-binding domains in plant cells, the localization of PIs can be microscopically visualized (Varnai & Balla, 1998; Kost et al., 1999; van Leeuwen et al., 2007; Vermeer et al., 2006, 2009; Simon et al., 2014). One highly specific PI-binding domain is the PH domain of phospholipase C δ 1 (PLC δ 1) from human or rat (Varnai & Balla 1998), which binds to PtdIns(4,5)P₂. *In vivo*, by binding to their target proteins, PIs are thought to regulate protein activity and localization directly (by recruitment to a membrane) or indirectly (by influencing membrane insertion or recycling) (Heilmann, 2016). Based on the current literature, PIs appear to be involved in all kinds of membrane-associated cellular processes in plants, including membrane trafficking and PMP recycling. Experiments using the tobacco pollen tube system revealed that pectin deposition is regulated by PIs (Ischebeck et al., 2008). Overexpression of different enzymes from the PI metabolism including PIP5K4, PIP5K5, PIS and PI4K β 1 results in aberrant cell morphologies

of pollen tubes (Ischebeck et al., 2008, Ischebeck et al., 2010, Sousa et al., 2008), indicating that PIs and especially PtdIns(4,5)P₂ act as regulators of secretion in pollen tube cells. However, the role of PIs in maintaining cell polarity is not restricted to pollen tubes. Overexpression of the PI4P 5-kinase PIP5K3 leads to a loss of polarity in Arabidopsis root hairs, whereas Arabidopsis *pip5k3* mutants displayed reduced root hair growth (Stenzel et al., 2008; Kusano et al., 2008). Besides exocytosis, some endocytotic events have also been shown to depend on PIs, including CME. In *Saccharomyces cerevisiae*, AP-2 is known to bind to PtdIns(4,5)P₂ and this protein-lipid-interaction serves as a sorting signal to initiate CME in yeast (Honing et al., 2005). In addition, the scission of the clathrin-coated vesicle (CCV) from the membrane also seems to be partially controlled by PIs. DRP2A and DRPB2B from Arabidopsis possess PH domains that bind to PtdIns(4,5)P₂, indicating that both proteins may be recruited to their site of action by PtdIns(4,5)P₂ (Seaman et al., 1998). The uncoating of CCVs is the final step before fusion of the vesicle with the compartments of the endomembrane system. The auxilin-like SH3-domain containing protein AtSH3P1 was shown to colocalize with clathrin and to be involved in the process of clathrin disassembly from the vesicle (Lam et al., 2001). As also AtSH3P1 interacts with PtdIns4P and PtdIns(4,5)P₂, these lipids - and especially PtdIns(4,5)P₂ - seem to be important for CME. A *pip5k1 pip5k2* double mutant with reduced PtdIns(4,5)P₂ levels showed a strong phenotype that has been postulated to be related to defects in Auxin distribution. The subcellular distribution of GFP-tagged auxin exporter proteins, PIN1 and PIN2 in *pip5K1 pip5k2* double mutants revealed defects in the polarization of both PMPs (Ischebeck et al., 2013; Tejos et al., 2014). Measuring the internalization of PIN2-GFP in the mutant plant showed that the endocytotic rate was significantly reduced compared to wild type plants (Ischebeck et al., 2013). These results indicate the importance of PtdIns(4,5)P₂-regulated recycling of PMPs for their functionality. However, when displaying the endocytotic rate of the membrane dye FM4-64 in the *pip5k1 pip5k2* double mutant, the effect was less severe, suggesting that either CIE may not be affected by the altered PI metabolism, or that PtdIns(4,5)P₂ regulates only the endocytosis of specific cargoes, possibly depending on the responsible PI4P 5-kinase (Ischebeck et al., 2013). Besides the transport of membrane cargo proteins, CME controls the membrane area during hyperosmotic or salt stress. The treatment of Arabidopsis seedlings with high concentrations of sodium chloride leads to a transient increase in global as well as CCV-associated PtdIns(4,5)P₂ (DeWald et al., 2001, König et al., 2008), consistent with a role of PtdIns(4,5)P₂ in the responses to these stresses.

Similar to numerous PMPs, the subcellular distribution of PIs themselves has been shown to be polar rather than uniform. PtdIns(4,5)P₂ has been mainly detected at the apex of tobacco pollen tube and root hair cells (Ischebeck et al., 2008, Ischebeck et al., 2013, Tejos et al., 2014). Circumstantial evidence (Furt et al., 2010) and recent experiments using high resolution microscopy techniques in combination with specific fluorescent markers for PIs indicate that PIs are enriched in distinct areas of the plasma

membrane (Prof. Dr. Ingo Heilmann, personal communication). These microdomains display diameters below 200 nm and have been shown to be involved in trafficking processes including CME (Konopka et al., 2008, Wang et al., 2013). The data so far suggest that PI formation is highly dynamic and requires a tight network for spatiotemporal regulation. While numerous cellular functions and associated plant phenotypes have been attributed to PtdIns(4,5)P₂ and PI4P 5-kinases (Heilmann 2016; Gerth et al., 2017), there is only limited information about the integration of PI4P 5-kinases into the greater plant signalling network and in particular on how PtdIns(4,5)P₂ production might be regulated. In this context, it has recently been reported that PI4P 5-kinases can be targets for upstream protein kinases and for regulation by phosphorylation.

1.4.3 Regulation of PI4P 5-kinases

Although the complex interplay of PI signalling requires precise regulation, knowledge on how the abundance of PIs is controlled is rather limited. Evidences from all eukaryotic systems indicates that PI4P 5-kinases can be targeted by protein kinases to regulate enzyme activity and/or localization. For instance, the sole PI4P 5-kinase in *S. cerevisiae* is multicopy suppressor of *stt4* (MSS4). The MSS4 protein can localize at the plasma membrane. Upon casein kinase I (CKI)-mediated phosphorylation, MSS4 dissociates from the plasma membrane and is now targeted to the nucleus (Audhya and Emr, 2003), suggesting either an additional function of MSS4 in the nucleus or a mechanism to reduce PI4P 5-kinase abundance at the plasma membrane. There is also evidence for post-translational modification (PTM) directly affecting the activity of PI4P 5-kinases, and - for instance - the human PI4P 5-kinase Type I (PIP5K1 α) is inhibited by protein kinase A (PKA)-mediated phosphorylation (Park et al., 2001). Recombinant PIP5K1 from Arabidopsis can also be inhibited by PKA-mediated phosphorylation *in vitro* (Westergren et al., 2001), and whereas there is no PKA in Arabidopsis, further analyses demonstrated that Arabidopsis contains soluble protein kinase activities capable of phosphorylating PIP5K1 (Westergren et al., 2001). A proteome-wide screen for phosphorylation sites in proteins from Arabidopsis pollen tubes (Mayank et al., 2012) indicates the presence of phosphopeptides that can be attributed to PI4P 5-kinases. A recent, focused study on PTM-mediated regulation of PI signalling, describes a new link between MAPKs and a PI4P 5-kinase to regulate the production of PtdIns(4,5)P₂ and membrane trafficking in growing pollen tube cells. Using an in-gel protein kinase assay and mass spectrometry for non-targeted identification of protein kinase candidates that can phosphorylate the PI4P 5-kinase PIP5K6, MPK6 was identified as a potential upstream regulator of PIP5K6 (Hempel et al., 2017). Further characterization confirmed that MPK6 phosphorylates PIP5K6 at T590 and T597 *in vitro*, and this phosphorylation inhibits the catalytical activity of PIP5K6 (Hempel et al., 2017). In tobacco pollen tube cells, the overexpression of MPK6 reduces plasma membrane association of a

fluorescence-tagged PtdIns(4,5)P₂ reporter as well as the internalization of the membrane dye FM4-64 (Hempel et al., 2017). Furthermore, coexpression of MPK6 attenuates pollen tube growth defects caused by overexpression of PIP5K6 (Hempel et al., 2017). Together, these results indicate that MPK6-mediated phosphorylation inhibits enzymatic activity of PIP5K6 in growing pollen tube cells to reduce PtdIns(4,5)P₂ production and membrane trafficking at the site of action. As Arabidopsis *mpk6* mutants display a pollen tube guidance defect (Guan et al., 2014), it can be assumed that a MAPK-cascade involving MPK6 is part of the receptor-mediated pollen tube guidance to the ovules. In this context, MPK6-mediated phosphorylation of PIP5K6 and subsequent effects on membrane trafficking might be part of a signalling pathway to link the receptor-activated MAPK cascade to the machinery for cell expansion (Hempel et al., 2017). In this sense, the following model for the integration of signalling events in pollen tubes was proposed (**figure 1.6**), but not experimentally proven.

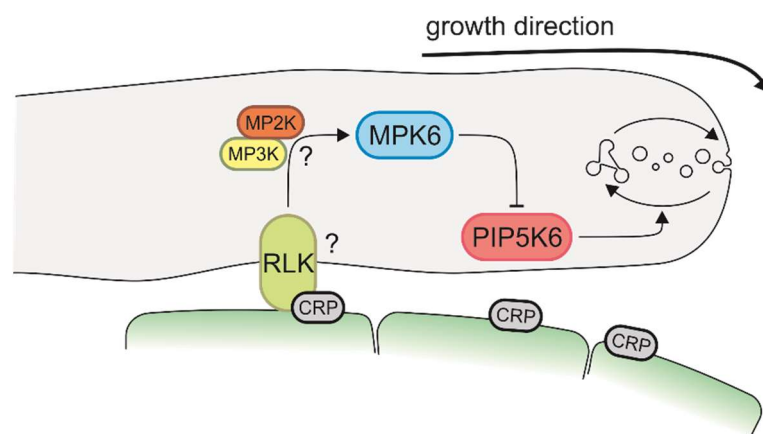


Figure 1.6: Model: interconnection of MAPKs and PI signalling in pollen tube cells. MPK6 phosphorylates PIP5K6 and inhibits PtdIns(4,5)P₂ production by this enzyme in pollen tube cells. Decreased local PtdIns(4,5)P₂ abundance leads to reduced membrane trafficking at the site of action, which leads to an imbalance in trafficking level at the pollen tube. The uneven integration of membrane material and secretion of cell wall compounds forces the growing pollen tube to turn in a certain direction. Surface receptors in the plasma membrane of the pollen tube cell are discussed to function as triggers for this phosphorylation event. A set of RLKs encoded by the Arabidopsis genome are known to bind to attractant peptides (CRP) synthesised by synergid cells to navigate the growing pollen tube towards the female gametophyte. Scheme was modified from Hempel et al., 2017.

1.5 Raison d'être

The network of interacting signalling pathways in plants is not fully understood. Due to the complex nature of plant signal transduction, for a long time signalling cascades were studied separately from each other and significant progress was made over the past decades. However, the interconnection of the different signalling pathways moves more and more into the focus of plant research. To fully understand how plants perceive their environment and initiate proper responses, future studies must

contemplate multiple signalling pathways and their interconnection. This thesis tries to add a new element to our understanding how signalling pathways influence each other. MAPKs and PIs respectively have been shown to act as key regulators in several cellular processes in generative and vegetative tissues in plants. A recent study suggests that those two ancient cellular pathways cooperatively regulate the navigation of pollen tube growth, raising the question if there is a connection of MAPKs and PIs as well in vegetative tissues.

Therefore, this thesis aimed 1) to test whether the relation between MPK6 and PIP5K6 also occurred in vegetative tissues of Arabidopsis. 2) A second goal was to test whether MPK6-mediated regulation of PtdIns(4,5)P₂ production could be triggered by activating the cell surface receptor FLS2. 3) The third goal of this thesis was to further test whether receptor-mediated signalling events transduced through phosphorylation of PIP5K6 had an effect on relevant physiological downstream responses. At a larger scale, the goal of this thesis was, thus, to delineate the central role of PI4P 5-kinases and PtdIns(4,5)P₂ production in the context of a signal transduction pathway spanning the full range from upstream receptor activation at the cell surface to the downstream effects on membrane trafficking and the biochemical performance of particular cargo proteins.

2 Results

A functional interaction of MPK6 and PIP5K6 was described previously to occur upon heterologous expression in tobacco pollen tube cells (Hempel et al., 2017). In the pollen tube cells, a PtdIns(4,5)P₂ overproduction phenotype caused by strong expression of PIP5K6 was attenuated when MPK6 was coexpressed, indicating an inhibitory effect of MPK6 on PIP5K6. The *in vivo* effect was consistent with *in vitro* data demonstrating the interaction between MPK6 and PIP5K6, the phosphorylation of PIP5K6 by MPK6 and the effect of the phosphorylation on catalytic activity and folding of PIP5K6 (Hempel et al., 2017). While thus, a functional interplay of MPK6 and PIP5K6 was concluded, it remained unclear how relevant this interaction might be for the overall physiology of Arabidopsis plants. As the native expression of the two proteins is not limited to pollen tubes, it was a main goal of this thesis to assess the relevance of a functional relation between MAPKs and PI signalling in somatic tissue. MPK6 is a well-described component of a PAMP-triggered MAPK cascade, which promotes PTI against bacterial pathogens. Therefore, in this thesis experiments were conducted to elucidate potential effects of the PAMP triggered activation of the MAP kinase cascade on the functionality of PIP5K6, PtdIns(4,5)P₂-production, and on PtdIns(4,5)P₂-mediated downstream processes.

2.1 PIP5K6 is expressed in somatic tissue and interacts physically with MPK6 in vegetative tissue

The function of MPK6 as a regulator of PTI in vegetative plant tissues has been the subject of extensive studies. By contrast, investigations on PIP5K6 have so far been restricted to the pollen tube system. Expression data obtained from the eFP Browser (Winter et al., 2007) indicate that MPK6 and PIP5K6 share similar expression pattern (**suppl. figure 8.1**). MPK6 and PIP5K6 are both strongly expressed in mature pollen, while displaying lower overall expression in vegetative tissue. The eFP browser is a computational tool, which visualizes sum gene expression maps for Arabidopsis based on various large-scale transcriptomics data sets (Winter et al., 2007). Since these results largely represent predictions, expression patterns should be experimentally verified.

To test PIP5K6 promoter activity in somatic cells, the activity of a β -glucuronidase (GUS) reporter expressed from a *PIP5K6* promoter fragment was monitored. As a "promoter", a 1500 bp fragment of 5'-UTR immediately upstream of the *PIP5K6* coding sequence was cloned in front of the *uidA* gene, encoding the GUS reporter. The expression cassette was introduced into Arabidopsis Col-0 plants by Agrobacterium-mediated transformation. The transgenic pPIP5K6-GUS Arabidopsis lines were generated and the GUS staining experiments were performed by Dr. Irene Stenzel. Transgenic seedlings were grown for 10 days under long day conditions (16 h light/8 h darkness) and incubated with 5-bromo-4-chloro-3-indolyl glucuronide (X-glcA) staining solution for the GUS reaction (Hamilton

et al., 1992). β -glucuronidase converts X-glcA to glucuronic acid and insoluble blue coloured 5-bromo-4-chloro-3-indol indicating *pPIP5K6* promotor activity in the respective tissue. After fixation of the tissue samples, images were taken using a binocular light microscope. Besides a strong promotor activity in generative tissues like flowers, pollen grains and pollen tube cells, GUS staining revealed *pPIP5K6* promotor activity also in vegetative tissues like roots and the vascular system (**figure 2.1 A-J**).

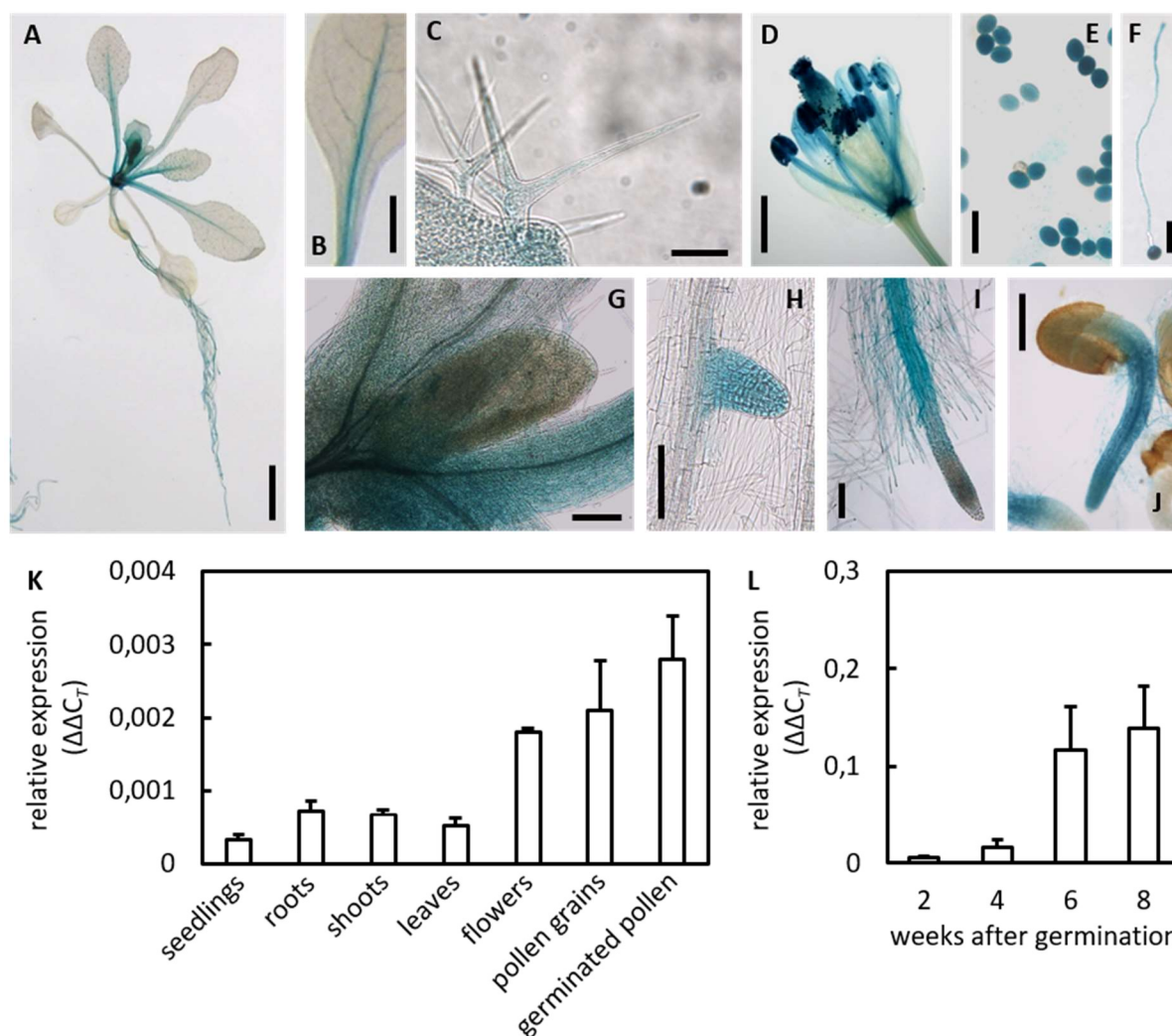


Figure 2.1: PIP5K6 promoter activity and transcript levels in vegetative tissues of Arabidopsis. A-J) *pPIP5K6*-driven glucuronidase activity is detectable in generative and vegetative tissues. Three-week-old Arabidopsis seedling A), leaf vascular tissue cells B), trichomes C), late flower D), pollen grains E), pollen tube cell F), vascular tissue at vegetative rosette centre G), lateral root H), root tip I), 1 day old seedling J). Bars, 1 cm (A); 1 mm (D); 500 μ m (B); 200 μ m (G, I, J); 50 μ m (C, E, F, H). K, L) *PIP5K6* is transcribed in all tissues examined and during all developmental stages. Samples were taken from indicated tissues or from leaf tissue at indicated time points for qPCR analyses. Graphs display mean values and standard deviation from four ($N = 4$; K) and three ($N = 3$; L) independent experiments. The analyses of the promotor-GUS reporter and measurements of organ specific *PIP5K6* transcript levels were performed by Dr. Irene Stenzel. Experiments on the *PIP5K6* transcript levels in different developmental stages were performed by Dr. Praveen Krishnamoorthy.

These results correlate with the data obtained from eFP browser and indicate that PIP5K6 is expressed nearly ubiquitously in Arabidopsis. Nevertheless, promotor GUS assays are not suitable for quantification of expression levels, since the intensity of the staining is affected by various parameters like incubation time and the accessibility of each tissue for perfusion by the staining solution. Therefore, qPCR was used for quantitative analyses of the relative *PIP5K6* transcript levels. Different generative and vegetative tissues were harvested from Arabidopsis seedlings, total RNA was extracted and used for cDNA synthesis and the quantification of transcript levels. All values were normalized to an internal actin control. Consistent with the results from the promotor GUS assays, a strong abundance of *PIP5K6* transcript was observed in germinating pollen, pollen grains and flowers. In addition, *PIP5K6* transcript was also detected in roots, shoots and leaves as well as in not flowering whole seedlings (**figure 2.1 K**). Besides tissue specific expression, developmental changes in PIP5K6 transcript levels were also investigated. Leaf tissue was obtained from Arabidopsis plants at different times after germination, and the abundance of PIP5K6 transcripts was analysed (**Figure 2.1 L**). The results show a strong increase of *PIP5K6* transcript level at late developmental stages, suggesting PIP5K6 to play a role in fully developed cells rather than in seedlings or during early organ development. As the expression patterns indicated the presence of PIP5K6 in vegetative tissues, it was next tested whether the protein-protein interaction of PIP5K6 and MPK6 previously observed in pollen tubes (Hempel et al., 2017) could be confirmed also for vegetative plant tissue. To address this question, Arabidopsis mesophyll protoplasts were used for bimolecular fluorescence complementation (BiFC) experiments. The BiFC assay is based on the reconstitution of the N- and C-terminal halves of yellow-fluorescent protein (YFP) upon close spatial proximity. Such close physical proximity can be supported by an interaction of two proteins partners fused to ^CYFP and ^NYFP, respectively. 3x HA or 3x myc tags were also introduced into the expressed fusion proteins to test enable the immunodetection of the expressed proteins to verify their integrity. The co-expression of HA-^CYFP-PIP5K6 and MPK6-^NYFP-myc resulted in a detectable fluorescence signal at the plasma membrane and in the cytosol, indicating physical interaction of the partner proteins (**figure 2.2**). To rule out auto-reconstitution, fusions of ribulose 1,5-bisphosphate carboxylase/oxygenase large subunit (RBCL) with ^NYFP or ^CYFP were tested as negative controls (**figure 2.2**). A reconstitution of YFP fluorescence was observed for neither control tested, HA-^CYFP-PIP5K6/RBCL-^NYFP-myc and MPK6-^NYFP-myc/HA-^CYFP-RBCL, indicating that the fluorescence reconstitution positively seen for the MPK6 and PIP5K6 was a consequence of their interaction. In all control samples, a weak signal was detected in the YFP channel that was caused by chloroplasts background fluorescence (**figure 2.2**). The integrity of ectopically expressed fusion proteins was verified by immunodetection and all protein fusions were expressed as intact full-length proteins (**suppl. figure 8.2**). Transgenic protoplasts were lysed in 1x Laemmli sample buffer and applied to SDS-PAGE method followed by electrophoretic transfer to

nitrocellulose membrane. Fusion constructs were detected with a primary anti-HA or anti-myc antibody and a secondary anti-mouse antibody conjugated to HRP.

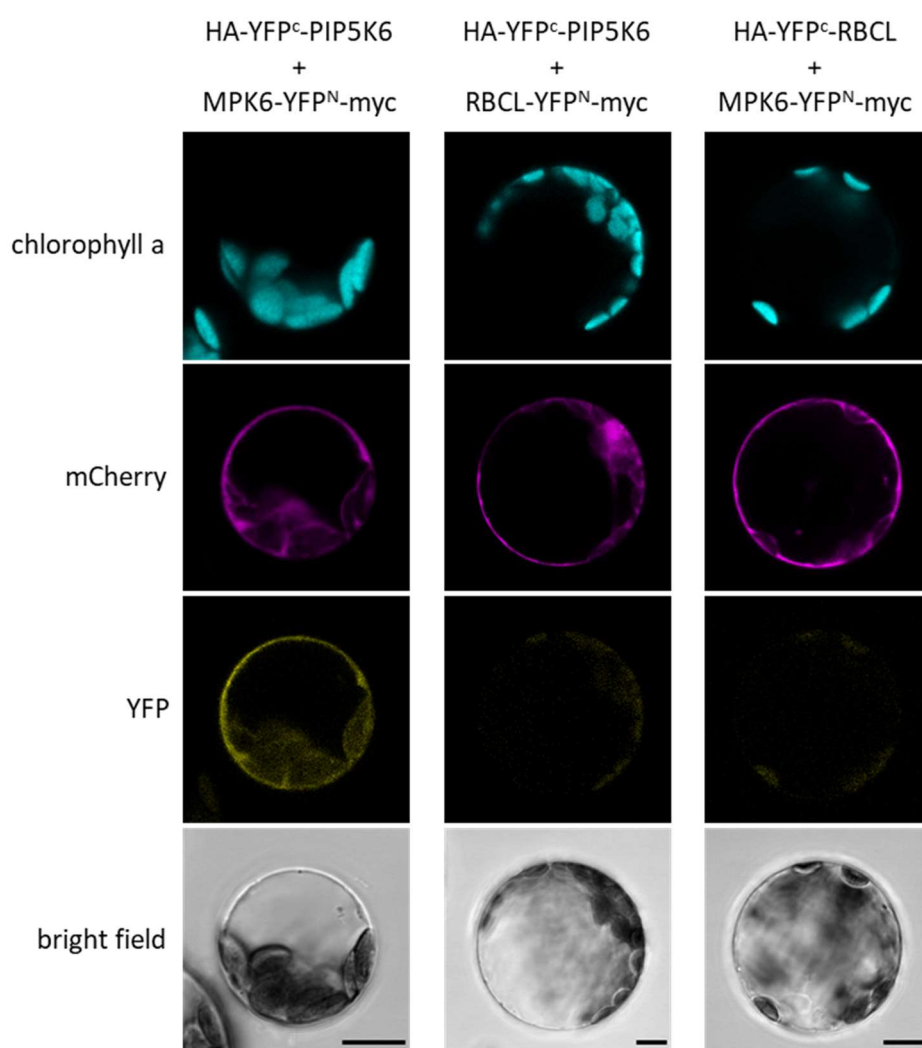


Figure 2.2: PIP5K6 interacts with MPK6 in mesophyll protoplasts. Confocal micrographs show fluorescence complementation upon coexpression of HA-^cYFP-PIP5K6 and MPK6-^NYFP-myc fusion constructs. pENTRY:pCaMV35S::mCherry was cotransformed as a transformation control. No fluorescence was detected for the controls coexpressing HA-^cYFP-PIP5K6/RBCL-^NYFP-myc or MPK6-^NYFP-myc/HA-^cYFP-RBCL. Expression and integrity of all fusion constructs was verified by Western blot-based immunodetection (*supple. figure 8.2*). $N = 3$, For each experiment and transformation 5 cells were imaged minimum. Bars, 10 μm .

2.2 PIP5K6 is phosphorylated upon PAMP-perception

Phosphorylation of PIP5K6 by MPK6 has recently been reported (Hempel et al., 2017). However, all *in vivo* experiments reported by Hempel et al. were limited to the analyses of membrane trafficking and growth dynamics in tobacco pollen tubes. Even though the notion was discussed with reference to surface receptors involved in pollen tube guidance (Hempel et al., 2017), the pollen tube system was

not suitable to investigate whether the phosphorylation could be triggered by the activation of a cell surface receptor. Furthermore, the mechanism of MAP kinase activation and function in pollen tubes is currently unclear. By contrast, the activation of a MAP kinase cascade including MPK6 by the RLK FLS2 upon perception of flg22 is well characterized for vegetative tissues. Since the physical interaction of MPK6 and PIP5K6 in vegetative tissue was confirmed (**figures 2.1 and 2.2**), here transgenic mesophyll protoplasts expressing tagged variants of PIP5K6 were used to test whether phosphorylation of PIP5K6 protein was triggered upon treatment of the cells with the bacterial PAMP flg22. Transgenic protoplasts expressing an HA-tagged PIP5K6 fusion were treated with 100nM flg22 or water (as a mock control) for 30 min. Protoplasts represent a highly sensitive experimental system and respond easily to a number of stresses. Therefore, to rule out unspecific effects by simply handling of the cells, an untreated control was also included. Phosphorylation of PIP5K6-HA from extracts of the transgenic protoplasts was analysed in gel shift assays. These assays were performed using Phos-tag SDS-PAGE, in which the Phos-tag reagent enhances the retarded electrophoretic migration of phosphorylated proteins (Kinoshita et al., 2004). As an internal positive control, a myc-tagged variant of the known substrate MPK3/MPK6 target VQ protein 1 (MVQ1) was coexpressed. MVQ1 is phosphorylated by MPK6 *in vitro* and has been shown to become an MPK6 target *in vivo* upon flg22 treatment (Pecher et al., 2014). After electrophoresis, proteins were blotted to a nitrocellulose membrane and were detected using primary anti-HA or anti-myc antibodies. An anti-mouse antibody conjugated to HRP was used for chemiluminescence detection. For myc-MVQ1, a visible band shift already appeared in the non-treated and mock treated control samples indicating that a substantial proportion of the protein was phosphorylated both in mock-treated or in untreated cells; no gel shift was visible for PIP5K6-HA in these controls (**figure 2.3 A**). A much more prominent shift for myc-MVQ1 was detectable when transgenic cells were treated with flg22, indicating successful elicitation by flg22 and MPK3/MPK6 activation. PIP5K6-HA also showed a gel shift when samples were treated with flg22, indicating that phosphorylation of PIP5K6 was triggered by the flg22 treatment. The more pronounced gel shift for myc-MVQ1 can be explained by its large number of phosphorylation sites. MVQ1 possesses 12 confirmed MPK6 targeted phosphorylation sites, whereas only the two threonine residues T590 and T597 of PIP5K6 have been shown to be phosphorylated by MPK6 (Hempel et al., 2017). To verify that the observed gel shift of the PIP5K6 protein was caused by phosphorylation and not other posttranslational modifications, extract from mesophyll protoplasts coexpressing PIP5K6-HA and myc-MVQ1 was subjected to λ -phage protein phosphatase (λ PPase) treatment before using Phos-tag acrylamide gel for phosphorylation-specific protein separation. For myc-MVQ1, the prominent band shift that appeared in the flg22-treated sample was completely abolished, when cell extracts were incubated with λ PPase (**figure 2.3 B**). A slight band shift appeared in the flg22 treated samples when

PIP5K6-HA was expressed, but was not present after incubation with λ PPase, indicating that the observed band shifts indeed refer to the flg22-triggered phosphorylation of PIP5K6.

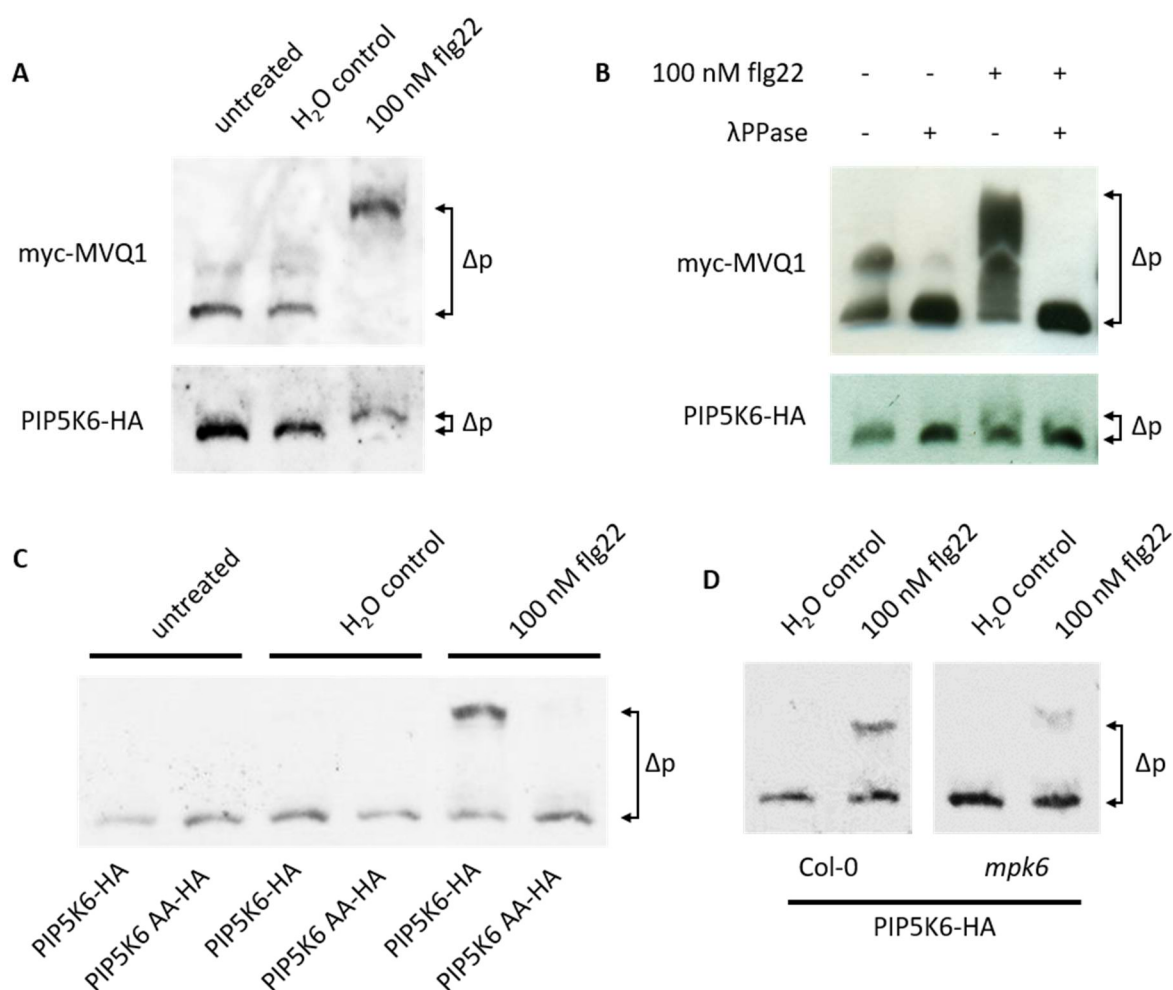


Figure 2.3: Phospho-specific mobility shift analyses. Transgenic protoplasts were treated as indicated. All elicitor and mock treatments were applied for 30 min. Cell extracts containing ectopically expressed HA-tagged PIP5K6 or PIP5K6 AA were subjected to Phos-tag-mediated electrophoretic phosphoprotein separation before Western blot analyses. Epitope-tagged proteins were detected using primary anti-HA and secondary anti-mouse antibody or primary anti-myc and secondary anti-rabbit antibody. Secondary antibodies were HRP-conjugates enabling for luminol-based chemiluminescence detection. **A)** Upon flg22 treatment PIP5K6-HA displays a mobility shift due to triggered phosphorylation (Δp). Myc-MVQ1 was coexpressed as an internal phosphorylation control. $N = 3$. **B)** Phosphatase treatment abrogates mobility shift of PIP5K6-HA. Cell extracts were incubated with λ PPase for 1 h at 37 °C before mobility shift analyses. $N = 1$. **C)** Flg22-treated phosphorylation requires T590 and or T597. $N = 2$. **D)** Flg22-triggered phosphorylation of PIP5K6-HA is reduced in *mpk6* mutant protoplasts. $N = 1$.

For a more detailed analysis, phosphorylation of PIP5K6-HA was compared to the phosphorylation of a PIP5K6 AA-HA variant, which can no longer be phosphorylated by MPK6 due to the substitution of T590 and T597 for alanines (**figure 2.3 C**). PIP5K6-HA showed a distinct gel-shifted band when samples were treated with flg22. A faint shifted band in the mock control may be explained by a weak trigger

of the MAPK cascade by the water treatment, or by additional phosphorylation events, since PIP5K6 is also a target for protein kinases other than MAPKs (Hempel et al., 2017). No gel shift were detected for PIP5K6 AA-HA, indicating that the substitution of T590 and T597 in this protein variant prevented the phosphorylation. The data show that T590 and T597 are necessary for the flg22-triggered phosphorylation of PIP5K6, providing strong evidence that MPK6 was phosphorylating PIP5K6 *in vivo* in somatic cells upon treatment with the flg22 trigger. To further test this hypothesis, phosphorylation of PIP5K6-HA was compared upon expression in protoplasts from either Col-0 wild type or from *mpk6* knock out plants after flg22 treatment (**figure 2.3 D**). In this experiment, a gel shift for PIP5K6-HA protein was still detected for both Col-0 and *mpk6* plants when treated with flg22 while no band shift was visible in the water treated samples. The signal intensities of the shifted band representing phosphorylated PIP5K6-HA protein and the band representing unphosphorylated PIP5K6-HA were quantified and the percentage of phosphorylated protein was calculated. While the relative amount of phosphorylated PIP5K6-HA was at 35 % in the Col-0 cells, only 17.5 % of the PIP5K6-HA protein were phosphorylated in the *mpk6* cell. This observation suggests a reduced degree of phosphorylation in the *mpk6* mutant. However, these results are preliminary, since the experiment was performed only once. In addition to PIP5K6, the ubiquitously expressed PI4P 5-kinase PIP5K2 was tested for flg22-triggered phosphorylation. Although the catalytic domain of PI4P 5-kinases is highly conserved between isoforms, the MPK6-targeted residues T590 and T597 of PIP5K6 are located in a more variable sequence region, and PIP5K2 lacks the corresponding residues (see also **figure 3.1**). In phosphorylation assays using protoplasts expressing an HA-tagged PIP5K2 fusion, a gel shift occurred in the mock and flg22-treated samples (**suppl. figure 8.3**), indicating phosphorylation of the PIP5K2-HA protein, regardless of whether flg22 was applied or not. Thus, whereas PIP5K2-HA was phosphorylated in the protoplasts, there is no evidence for elicitor-triggered phosphorylation of PIP5K2. Still, these data are preliminary.

2.3 Effects of flg22 treatment on cellular PtdIns(4,5)P₂ levels in Arabidopsis

MPK6 has been shown to inhibit PIP5K6 *in vitro* and *in vivo*, thus limiting PtdIns(4,5)P₂ formation and attenuating morphological defects in pollen tube cells caused by PIP5K6 overexpression. Here, the previously reported phosphorylation of PIP5K6 by MPK6 was confirmed for vegetative cells, raising the question whether flg22-triggered activation of MPK6 affects the formation of PtdIns(4,5)P₂.

2.3.1 Flg22-perception leads to relocalization of a PtdIns(4,5)P₂ biosensor

To test possible effects of flg22-perception on PI turnover, a biosensor was used for the indirect investigation of PtdIns(4,5)P₂ abundance at the plasma membrane by confocal microscopy. To this end,

transgenic plants expressing a biosensor consisting of a two-fold (2x) PH domain from rat PLC δ 1 fused to an N-terminal mCITRINE fluorescence tag were used (Simon et al., 2014). Expression of the biosensor was controlled by the constitutively active *pUBQ10* promoter. The PH(PLC δ 1) biosensor specifically detects PtdIns(4,5)P₂ (Simon et al., 2014). The use of two coupled PH(rnPLC δ 1) domains increases plasma membrane localization of the biosensor while reducing cytoplasmic localization (Simon et al., 2014). The transgenic Arabidopsis seedlings were grown in the dark to induce hypocotyl development. Etiolated seedlings were treated for 1 h with 10 μ M flg22 or water as a control for 1h. Micrographs of hypocotyl cells were taken using a confocal microscope. Cells of flg22 treated plants showed relocalization of the biosensor to the cytoplasm (arrow heads) that was not observed in the mock treated plants (**figure 2.4 A**). This pattern indicates a decreased association of the biosensor with the plasma membrane, consistent with reduced abundance of PtdIns(4,5)P₂ available as a binding partner. For further quantification, root tip cells of mCITRINE_{2xPH(PLC δ 1)} expressing plants were also imaged at indicated time points after flg22 or mock treatment. Cells at the root tip are still differentiating and have not expanded yet, thus the vacuole is underdeveloped making imaging and quantification of the cytosolic fluorescence much easier. As in the previous experiments, seedlings were treated with 10 μ M flg22 or water as a control for 1 h prior to microscopic imaging and computational analyses. Fluorescence intensity from cytosol and the plasma membrane were measured, respectively, and the intensity ratio (cyt/PM) was calculated. Cells that were treated with flg22 showed a visible cytosolic fluorescence that was not present in mock treated cells (**figure 2.4 B**). Consistent with this observation, quantification revealed a significant increase of the cyt/PM ratio from 0.1 in the mock treated cells to 0.4 in flg22 treated cells. These results are consistent with a substantial reduction of PtdIns(4,5)P₂ at the plasma membrane, causing a mCITRINE_{2xPH(PLC δ 1)} to relocalize to the cytosol. Together with sphingolipids, sterols and other regulatory membrane compounds, PIs localize to specific domains rather than being distributed throughout the plasma membrane (Furt et al., 2010). Microdomains are formed at specific sites at the plasma membrane, possibly mediating localized functionalities in the respective membrane areas. To better understand the effects of PTI activation on PtdIns(4,5)P₂, the specific distribution of mCITRINE_{2xPH(rnPLC δ 1)} at the plasma membrane was imaged at a high spatiotemporal resolution using spinning disc microscopy. From various studies, PtdIns(4,5)P₂ is known to be formed at higher rates upon salt stress, probably conducting endocytosis for adjusting plasma membrane area and maintaining turgor pressure in the cell (DeWald et al., 2001, König et al., 2008). Using spinning disc microscopy on hypocotyl cells of transgenic plants, mCITRINE_{2xPH(PLC δ 1)} showed a uniform distribution in mock treated cells (**figure 2.4 C**). The observed fluorescence signal probably originates mostly from the cytosol underneath the plasma membrane, which is still within the focal plane. No obvious changes appeared to the reporter distribution when seedlings were treated with flg22. This is consistent with results from this thesis: Assuming that only one layer of reporter

molecules is present at the plasma membrane, whereas contribution of multiple layers of molecules that are localized in the cytosol display a much more prominent fluorescence signal, a decrease in membrane-localized reporter cannot be detected with this particular method.

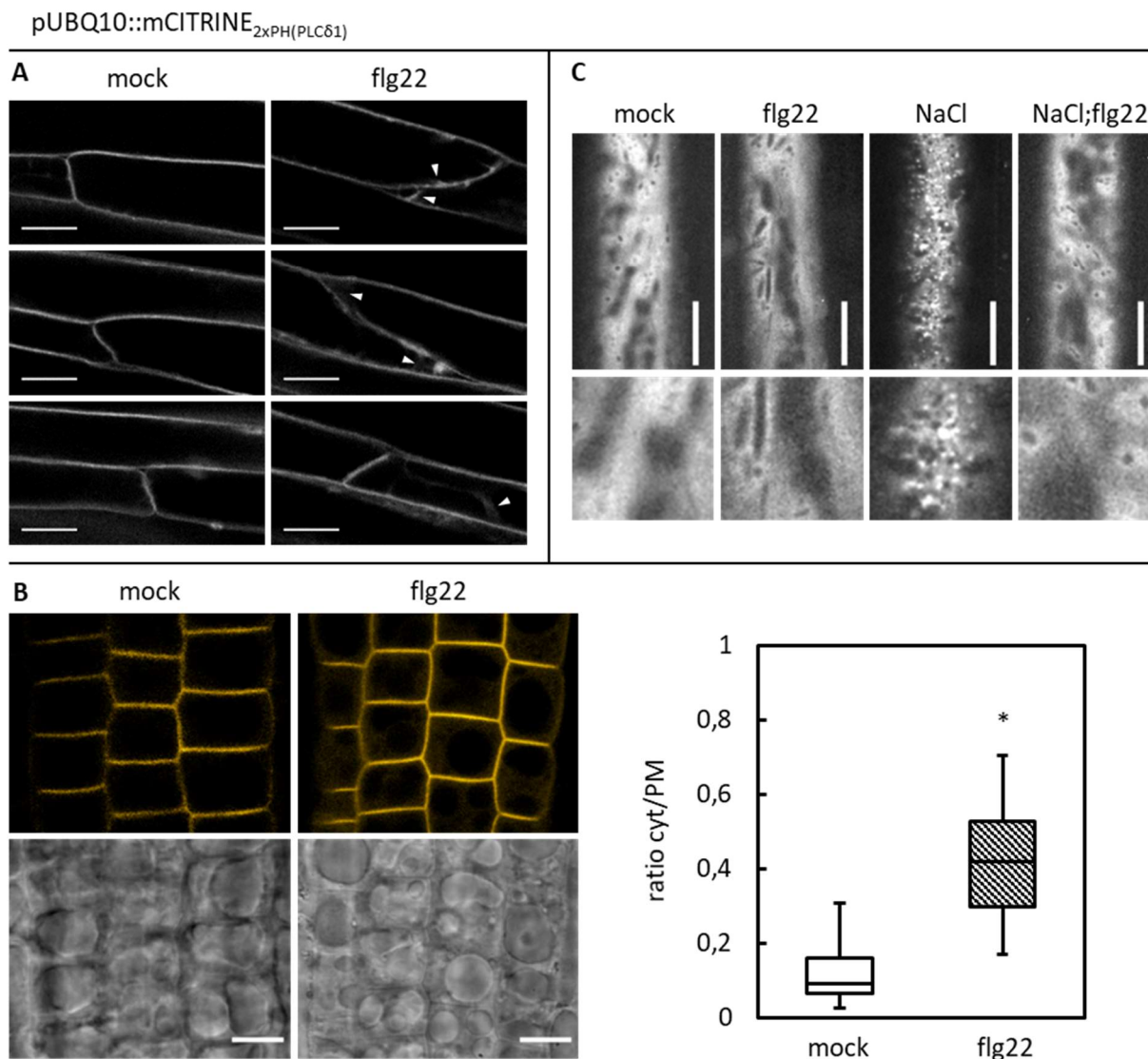


Figure 2.4: Imaging relocation of mCITRINE_{2xPH(PLCδ1)} PtdIns(4,5)P₂ reporter upon flg22 perception. A) mCITRINE_{2xPH(PLCδ1)} shows increased cytosolic localization upon flg22 perception (arrow heads). Stable transgenic P24Y seedlings were grown in the dark for 10 days and treated with 10 μ M flg22 or water as a control 1 h prior confocal microscopic analyses of hypocotyl cells. Bars, 20 μ m. $n = 3$, For each experiment and treatment, 10 cells were imaged minimum. B) Quantification of subcellular distribution of fluorescence intensity revealed an extensive shift in mCITRINE_{2xPH(PLCδ1)} localization from the plasma membrane to the cytosol. Root tips of 10 days old seedlings were imaged after treatment with 10 μ M flg22 or water as a control for 1 h. Bars, 10 μ m. $n = 2$, For each experiment and treatment, 20 seedling were imaged minimum. Student's *t*-test confirmed statistical significance. * $p \leq 0.05$ C) Flg22 pre-treatment prevents salt-induced accumulation of mCITRINE_{2xPH(PLCδ1)} in foci at the plasma membrane. 3 day old seedlings were pretreated with 1 μ M flg22 or water for 1 h as a control before treatment with 200 mM NaCl or water as a control for 15 min. Micrographs were taken using a Zeiss spinning disc system. Bars, 10 μ m. $N = 3$, For each experiment, 10 seedlings were imaged minimum.

However, previous studies have shown that the localization of the reporter is changed drastically upon salt stress (van Leeuwen et al., 2007; König et al., 2008). Treatment of transgenic Arabidopsis seedlings with NaCl at a final concentration of 200 mM caused the mCITRINE_{2xPH(PLCδ1)} biosensor to accumulate in distinct foci in the plane of the plasma membrane, probably due to the rapid formation of PtdIns(4,5)P₂ at these sites (Prof. Dr. Ingo Heilmann, personal communication). These results were confirmed in this study (**figure 2.4 C**). By contrast, when seedlings were pretreated with flg22, NaCl treatment never led to foci formation (**figure 2.4**), indicating that both the NaCl and flg22 treatments affected PtdIns(4,5)P₂ abundance in opposing directions. Activation of the MAPK-cascade by treatment with flg22 seems to attenuate responses to salt treatment at the level of PIs. The combined data of these experiments using the PtdIns(4,5)P₂ reporter mCITRINE_{2xPH(PLCδ1)} suggest that PtdIns(4,5)P₂ abundance is reduced *in vivo* upon perception of flg22.

2.3.2 PtdIns(4,5)P₂ levels are not changed upon activation of PTI

As the indirect microscopic approach using the mCITRINE_{2xPH(PLCδ1)} biosensor in Arabidopsis seedlings indicated decreased PtdIns(4,5)P₂ levels upon PAMP perception, it was next tested whether changes in PI metabolism upon PAMP treatment could be detected by direct biochemical lipid measurements. To this end, a phospholipid fraction was extracted after treatment of Arabidopsis seedlings for for 1 h with flg22. As a control, seedlings were mock-treated with water. After preparative TLC and reisolation of PtdIns4P and PtdIns(4,5)P₂, the lipids were subjected to chemical transesterification of the associated fatty acids. The thus obtained fatty acid methyl-esters (FAMES) derived from PtdIns4P and PtdIns(4,5)P₂ were quantified using gas chromatography (GC) coupled to a flame ionization detector (FID) unit. For both, PtdIns4P and PtdIns(4,5)P₂, no significant changes in the abundance and/or fatty acid composition were detected upon flg22 treatment (**figure 2.5 A and B**), indicating that overall levels of PtdIns4P and PtdIns(4,5)P₂ are not changed upon elicitation. For further analyses on the subject, PtdIns(4,5)P₂ levels were analyzed upon infection with different strains of the pathogenic bacterium *Pseudomonas syringae* pv tomato (PST) infection. Upon infection, PST transfers numerous effector proteins into the host cell to reprogram cell metabolism and suppress immune response (Alfano and Collmer, 1997). While PST pv tomato DC3000 is a virulent strain, PST *hrpA* lacks the large subunit of the Hrp pilus and therefore cannot assemble a functional type III secretion system to translocate effectors (Wei et al., 2000), thus serving as a non-virulent control. Both strains nonetheless can be recognized by FLS2 to trigger an immune response. Bacteria were infiltrated into the leaves of 6 week old Arabidopsis plants. Samples from infected leaves were harvested after the time points indicated (**figure 2.6**) for phospholipid extraction and analysis by combined TLC and GC-FID. Bacterial growth was monitored over the time of treatment. No significant changes in the levels of PtdIns(4,5)P₂ were

detected between samples that were infected with the virulent PST strain compared to samples that were infected with the *hrpA* strain on day 0-4 post infection (**figure 2.6**). The virulent PST strain displayed a higher cell count at day 4 compared to the avirulent *hrpA* strain, indicating that the virulent strain was able to infect the host cells. Increased PtdIns(4,5)P₂ levels and changes in FA composition in both *hrpA* and PST infected samples at day 4 are highly likely to be caused by cell death within the infected tissue rather than a response to infection itself, therefore hard to interpret.

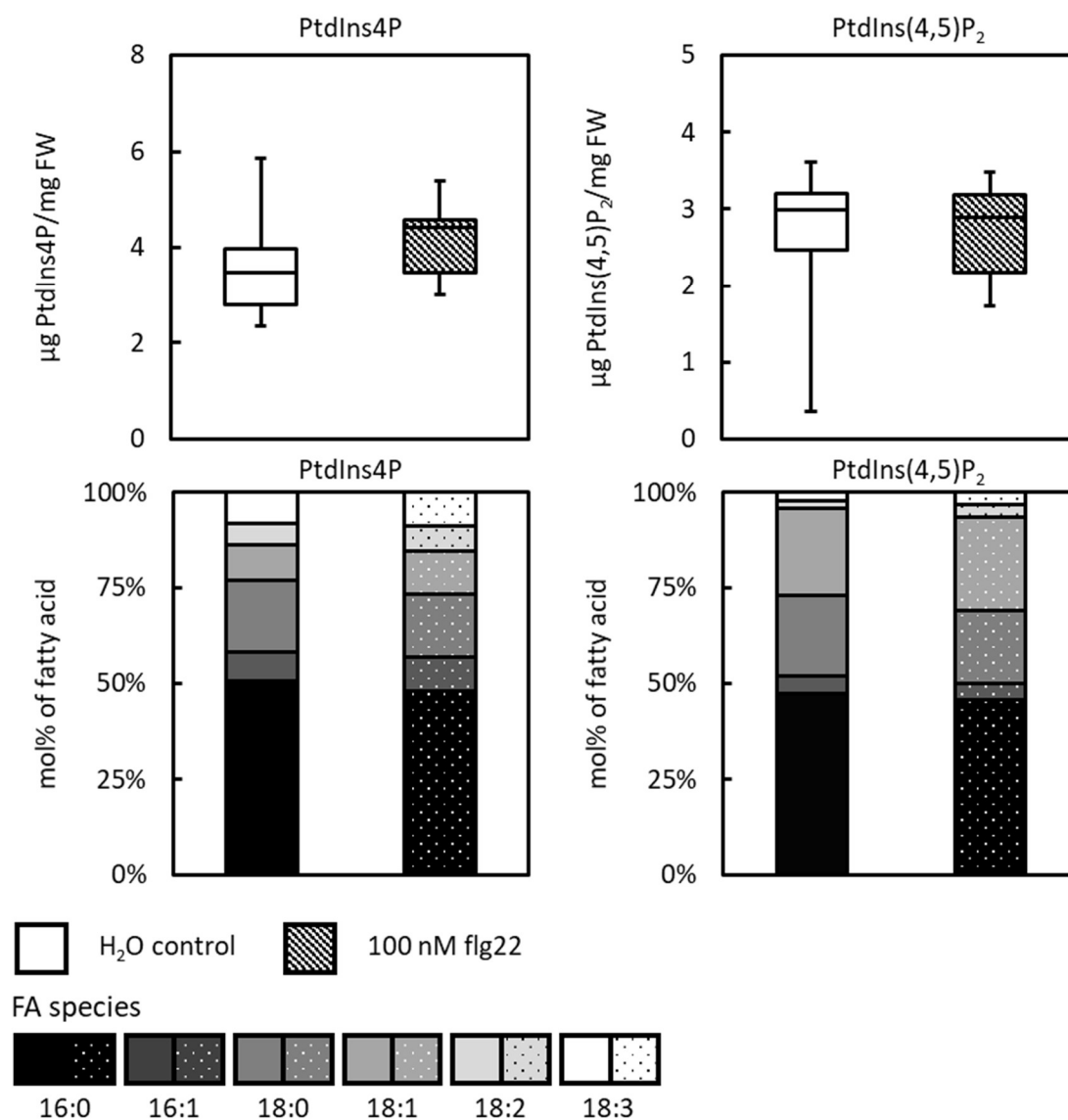


Figure 2.5: Analyses of levels and fatty acid composition of PIs upon flg22 treatment. PtdIns4P and PtdIns(4,5)P₂ levels A) and FA composition B) remained unaltered upon flg22 perception. 10-day-old *Arabidopsis* seedlings were treated with flg22 (patterned bars) or water as a control (plain bars) for 1 h prior phospholipid extraction. FAMES from PtdIns4P and PtdIns(4,5)P₂ fractions were analysed using GC-FID for quantification of total lipid amount per fresh weight and FA composition. $N = 2$. Four technical replicates were performed for each independent experiment. Unpaired student's t-test showed no statistical significance of differences ($p > 0.05$).

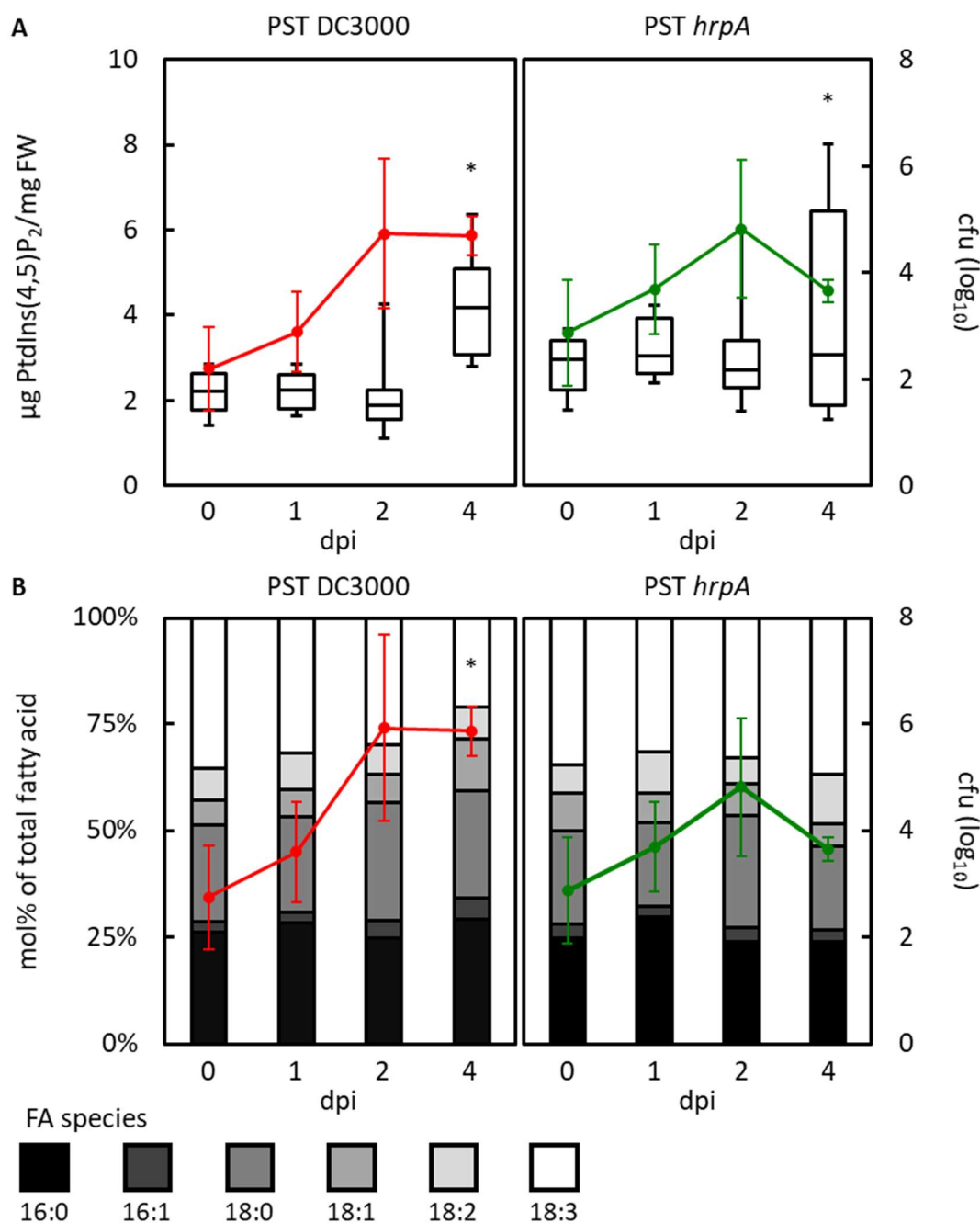


Figure 2.6: Analyses of levels and fatty acid composition of PtdIns(4,5)P₂ upon infection with Pseudomonas. PtdIns(4,5)P₂ levels were not affected upon PST infection. Samples at day four displayed severe tissue damage therefore the contribution of pathogen recognition to the observed changes is hard to estimate. Leaves of 6 weeks old Arabidopsis Col-0 plants were inoculated with virulent PST DC3000 or non-virulent PST *hrpA* cell suspension. Leaf material was harvested and homogenised for phospholipid extraction at the indicated days post infection (dpi). FAMES from PtdIns(4,5)P₂ fractions were analysed using GC-FID for quantification of total lipid amount per fresh weight (A) and FA composition (B). Bacterial growth was monitored as colony-forming units (cfu). Virulent PST DC3000 – red graph. Non-virulent PST *hrpA* – green graph. N = 2. Four technical replicates were performed for each independent experiment. Except for four days dpi, which includes two replicates. An unpaired student's t-test was used to verify statistical significance of differences. *p ≤ 0.05. Experiments were performed by Dr. Lennart Eschen-Lippold (inoculation, harvest and bacterial cell growth) and Dr. Mareike Heilmann (lipid extraction and analysis).

Together these results suggest that the levels of PtdIns4P or PtdIns(4,5)P₂ were not detectably altered upon triggering PTI. While this observation does not support the results from imaging mCITRINE_{2xPH(PLCδ1)} localization (**figure 2.4**), it should be noted that PtdIns4P and PtdIns(4,5)P₂ are regulatory lipids of very low abundance with concentrations that are close to the detection limit of the applied method. Thus, while flg22 perception might well trigger changes in the levels of PtdIns4P or PtdIns(4,5)P₂, these changes may not be easily detected by non-labelled lipid analysis techniques.

2.4 Flg22 perception does not affect PIP5K6 turnover

The data from the microscopic analyses using the PtdIns(4,5)P₂ reporter mCITRINE_{2xPH(PLCδ1)} indicated that flg22 perception affected PI metabolism and might suppress the formation of specific PtdIns(4,5)P₂ pools. To test if this effect is caused by an elicitor-triggered change in PIP5K6 abundance, *pPIP5K6* promoter activity and transcript abundance were analysed upon flg22 treatment. Seedlings of transgenic Arabidopsis pPIP5K6-GUS lines were grown for three weeks under normal light conditions (12 h light/12 h dark) and treated for 1 h with either 10 μM flg22 or water as a control prior to X-Glc staining for GUS activity (**figure 2.7 A-H**). Mock-treated seedlings displayed GUS activity in vascular tissue in leaves and the rosette centre and in root tips and lateral roots (**figure 2.7 A-D**). No differences in GUS activity was observed upon flg22 treatment compared to mock treated seedlings, indicating that *pPIP5K6* promoter activity was not affected by flg22 treatment (**figure 2.7 E-H**). As mentioned before, the promoter GUS assay does not allow the precise quantification of promoter activity. Therefore, *PIP5K6* transcript levels were analysed upon flg22 treatment. Three-week old Arabidopsis Col-0 seedlings were treated for 1 h with either 10 μM flg22 or water as a control, leaf material was harvested and subjected to total RNA extraction and reverse transcription. The abundance of *PIP5K6* transcript was then determined by qPCR relative to the reference gene *ACTIN8*. Besides *PIP5K6*, *PIP5K2* transcript was also included in this assay. The transcription of the gene ETHYLENE RESPONSE FACTOR 1 (ERF1) is activated upon flg22 perception (Denoux et al., 2008) and therefore, this gene was used as a positive control for successful elicitation. Strong transcriptional activation of ERF1 indicated the activation of PTI by flg22 treatment had worked (**figure 2.7 I**). Despite the successful elicitation, no differences were detected for the abundance of *PIP5K6* and *PIP5K2* transcript upon flg22 treatment. Together these data indicate that the expression of PIP5K6 was not affected by flg22 treatment. While these control experiments do not indicate transcriptional regulation of PIP5K6 in response to flg22 treatment, still the observed effect on the distribution of mCITRINE_{2xPH(PLCδ1)} suggested PAMP-triggered regulation of PtdIns(4,5)P₂ turnover that might be promoted by alterations in protein stability. MAPK-mediated phosphorylation can trigger degradation of a target protein via the ubiquitin-proteasome-pathway (Joo et al., 2008, Pecher et al., 2014). To test whether PIP5K6 protein was degraded upon

phosphorylation, *in vivo* degradation assays were performed. Transgenic Arabidopsis mesophyll protoplasts expressing a PIP5K6-HA fusion were treated with flg22 or with water as a control (mock). Cycloheximide (CHX) was added to the samples to inhibit *de novo* protein synthesis, thus enabling the analyses of protein degradation. Lysates from protoplasts harvested after the indicated time points after treatment were subjected to SDS-PAGE and Western blot analyses.

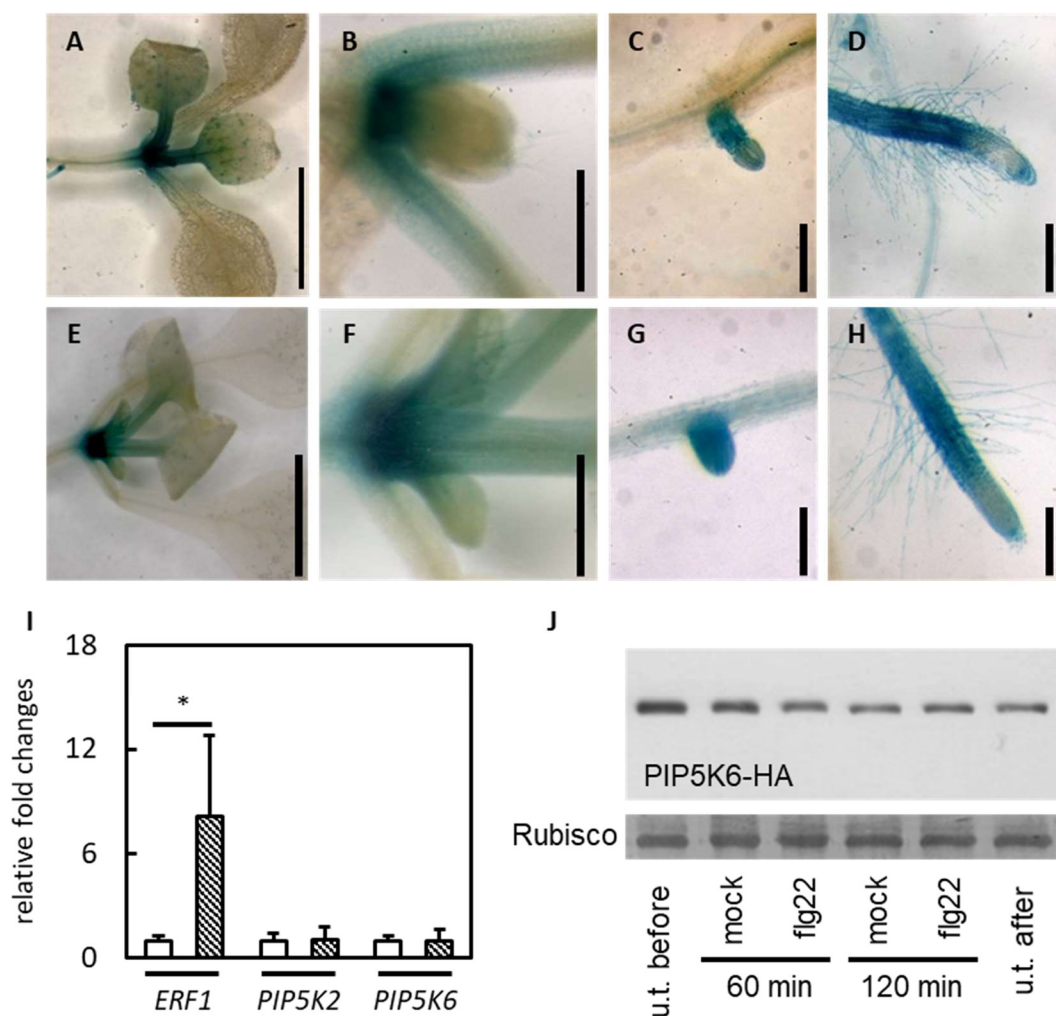


Figure 2.7: Unaltered PIP5K6 promoter activity and protein stability of PIP5K6 upon flg22 treatment. A-H) pPIP5K6 activity in different tissues remained unaltered upon flg22-perception. 3 week old pPIP5K6-GUS Arabidopsis seedlings were treated with 1 μ M flg22 (E-H) or water (A-D) as a control for 1 h. pPIP5K6 driven GUS activity was analysed in leaf rosette, lateral root and root tip. N = 3. Five plants per experiment and treatment. I) PtdIns4P 5-kinase transcript levels were not affected by flg22 perception. PIP5K2 and PIP5K6 transcript level of 3 week old Arabidopsis Col-0 seedlings were analysed by RT-qPCR upon treatment with 10 μ M flg22 (patterned) or water as a control (plain) for 1 h. ERF1 was used as a positive control. An unpaired student's t-test was used to verify statistical significance of differences indicated by asterisks. * $p \leq 0,05$. N = 3. J) PIP5K6 protein stability was not changed upon flg22 perception. Transgenic Arabidopsis Col-0 mesophyll protoplasts were treated with 100 nM flg22 or water as a control (mock). Protein abundance was assayed by Western blot and immunodetection at indicated time points. Amido black staining was used to show equal loading amounts (showing Rubisco large subunit). N = 4. The particular degradation assay was performed by Dr. Lennart Eschen-Lippold.

HA-tagged PIP5K6 was detected using a primary anti-HA antibody and a secondary HRP-conjugated anti-mouse antibody for chemiluminescence-based detection. The patterns suggest a slight decrease in the band intensity for PIP5K6-HA over time of mock treatment or flg22 treatment (**figure 2.7 J**), indicating that PIP5K6 was not subjected to degradation upon flg22 perception. Staining of the nitrocellulose membrane with amido black revealed equal amounts of Rubisco in each sample, indicating equal loading of the protein samples in each lane. The combined data obtained from the analyses of promoter activity, transcript abundance and protein stability did not provide evidence that flg22 treatment would affect the abundance of PIP5K6.

2.5 Flg22 treatment inhibits PI4P 5-kinase activity in mesophyll protoplasts

Experiments so far have shown that the effects of flg22 on the membrane association of the PtdIns(4,5)P₂ reporter mCITRINE_{2xPH(PLCδ1)} cannot be explained by changes in PIP5K6 abundance. Besides localization and turnover, MAPK-mediated phosphorylation has been shown to regulate the activity of target proteins (Nuhse et al., 2007). Consistent with this notion, it was previously shown that MPK6-mediated phosphorylation inhibits the enzymatic activity of PIP5K6 *in vitro* (Hempel et al., 2017). Therefore, experiments were conducted to assess the enzymatic activity of PI4P 5-kinases upon flg22 treatment in Arabidopsis cells. To estimate the global effect of flg22 perception on the intrinsic PI4P 5-kinase activity in Arabidopsis mesophyll cells, untransformed protoplasts were treated with flg22 or water as a control (mock). Equal volumes of protoplast extracts were then tested for PI4P 5-kinase activity using PtdIns4P and γ [³²P]-ATP as substrates. No cold ATP was added to the reaction due to the presence of endogenous ATP in the extracts. Radiolabelled phospholipids were extracted from the reaction volume, separated via TLC and monitored using a phosphor imager. A control reaction contained recombinantly expressed and purified PIP5K2 fused to a maltose binding protein (MBP)-tag. Radiolabelled PtdIns(4,5)P₂ from the latter reaction served as a standard to identify this lipid within the sample lanes on the TLC plate. The respective bands were quantified using the phosphor imager software TINA (Raytest). The results from the lipid phosphorylation assays indicate that radiolabelled PtdIns(4,5)P₂ was formed in all cases. In comparison to the control, extracts from flg22 treated cells showed weaker signals of radiolabelled PtdIns(4,5)P₂, suggesting a decreased intrinsic PI4P 5-kinase activity (**Figure 2.8 A**). Although the quantitative differences between mock and flg22-treated samples appear slight, an unpaired student's t-test indicates the differences to be significant. To test if this effect correlated with the activation of the MAPK cascade represented by the module MKK5-MPK6, transgenic Arabidopsis lines encoding the gene cassette for dexamethasone inducible expression of either an inactive (KR) or a constitutively active (DD) variant of the MP2K MKK5 from *Petroselinum crispum* were used (Lee et al., 2004). MKK5 KR carries a point mutation that changes a lysine to arginine

within the ATP binding pocket of the enzyme, resulting in a “kinase-dead” protein (Lee et al., 2004). By contrast, MKK5 DD has two threonines within the activation loop exchanged for two aspartic acid residues to simulate the phosphorylation of the respective site, which leads to the constitutive activation of MKK5 (Lee et al., 2004). In previous studies, it was shown that the expression of MKK5 DD results in the activation of MPK6 (Lassowskat et al., 2014), whereas the expression of MKK5 KR exerts a dominant negative effect (Lee et al., 2004). Seedlings of transgenic Arabidopsis plants expressing either MKK5 KR or MKK5 DD were treated with dexamethasone for 4 h prior to preparing cell extracts. Equal volumes of extracts were analyzed for PI4P 5-kinase activity as in the previous experiment. A control reaction using recombinant MBP-PIP5K2 again resulted in the formation of a single band for PtdIns(4,5)P₂. The protein extract from seedlings expressing MKK5 DD showed significantly lower intrinsic PI4P 5-kinase activity compared to the extract from MKK5 KR expressing controls (**figure 2.8 B**). This observation is consistent with the results obtained from the elicitor treated protoplasts, indicating a MPK6-dependent flg22-triggered inhibition of intrinsic PI4P 5-kinase activity. However, experiments using stable transgenic MKK5 DD/KR Arabidopsis lines were performed once, which makes them preliminary. Still, the combined experiments suggest that intrinsic PI4P 5-kinase activity is sensitive to the activation of the MKK5-MPK3/6 module. So far, PIP5K6 is the only PI4P 5-kinase isoform that is known to be targeted by MPK6 and phosphorylated upon flg22 perception. To test whether flg22 perception specifically affected the catalytic activity of PIP5K6 in vegetative cells, PIP5K6-HA or PIP5K6 AA-HA were transiently expressed in Arabidopsis mesophyll protoplasts and the cells were treated with flg22 or water as a control (mock). The HA-tagged fusion proteins were then immunoprecipitated from whole cell lysate. Anti-HA protein G beads-bound protein was used to assay the associated PI4P 5-kinase activity. After phospholipid extraction from the reactions, bead suspensions were also analyzed by SDS-PAGE and Western blot to assess the amounts of bound PIP5K6 or PIP5K6 AA protein. HA-tagged proteins were detected in a luminol-based assay using a primary anti-HA antibody from mouse and a secondary anti-mouse antibody coupled to HRP (**suppl. figure 8.4**). The relative protein amounts were then used to normalize the quantified radiolabelling signals from the lipid phosphorylation assay to obtain "specific" PI4P 5-kinase activities. As in previous experiments, a control reaction with recombinant MBP-PIP5K2 resulted in the formation of radiolabelled PtdIns(4,5)P₂ serving as a standard for product identification. The data show that the flg22 treatment resulted in a significant decrease of PI4P 5-kinase activity of immunoprecipitated PIP5K6-HA protein compared to the mock control (**figure 2.8 C**). By contrast, there was no significant difference in PI4P 5-kinase activity between PIP5K6 AA-HA protein immunoprecipitated from flg22-treated or from mock-treated samples. The data indicate that the inhibitory effect of flg22 treatment on the activity of PIP5K6 depends on the presence of T590 and T597, which represent the MPK6 target sites (Hempel et al., 2017).

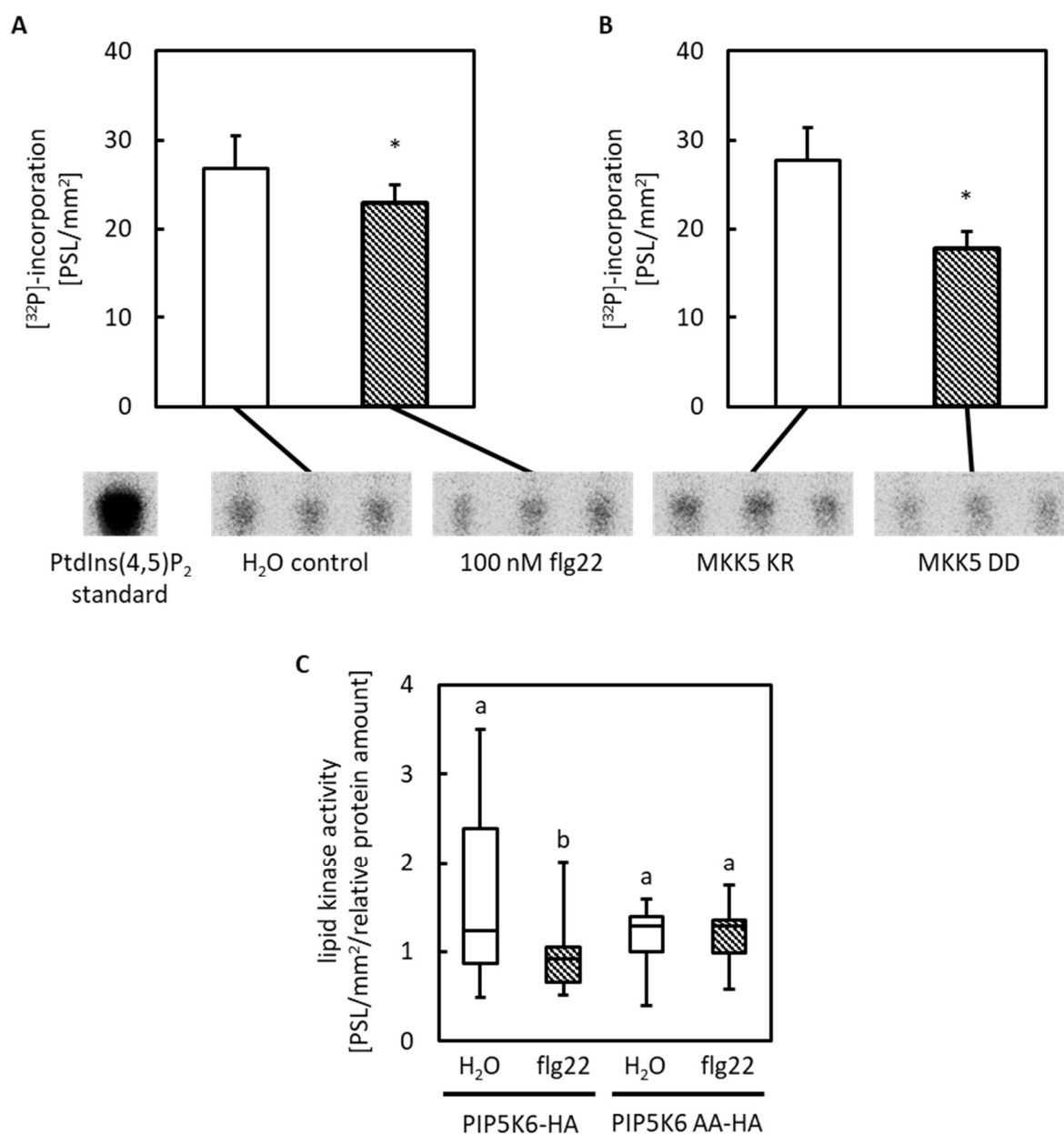


Figure 2.8: Intrinsic PI4P 5-kinase activity in Arabidopsis seedlings upon flg22 perception. Lipid kinase assays were performed using PtdIns4P-containing Triton X-100 micelles and γ [³²P]-ATP. For assaying intrinsic PI4P 5-kinase activity, equal amounts of plant extracts were applied to lipid kinase assay. A) Intrinsic PtdIns4P 5-kinases activity is decreased upon flg22 perception. Untransformed 10 days old Arabidopsis seedlings were treated with 100 nM flg22 or water as a control (mock) for 1 hour. $n = 2$; 3 technical replicates. B) Intrinsic PI4P 5-kinases activity is decreased upon MAP kinas activation. Stably transgenic 10 days old Arabidopsis seedlings were treated with 1 μ M dexamethasone for 4 h to induce MKK5 KR or MKK5 DD expression. $n = 1$; 3 technical replicates. C) Inhibition of the enzymatic activity of ectopically expressed PIP5K6-HA upon flg22 perception requires T590 and T597. Transgenic mesophyll protoplasts expressing PIP5K6-HA or PIP5K6 AA-HA were treated with 100 nM flg22 or water as a control. Immunoprecipitated protein was used for PI4P 5-kinase activity test. [³²P]-incorporation was assayed and was normalized to relative amounts of immunoprecipitated protein that was present in the reaction (**suppl. figure 8.4**). $N = 3$. Three technical replicates were performed for each independent experiment. Statistical significance of measured differences was verified using an unpaired student's t-test. Asterisks and letters indicate statistical significant different values. $*p \leq 0,05$.

These results are consistent with previous data obtained from *in vitro* analyses (Hempel et al., 2017) and show that flg22-triggered phosphorylation of PIP5K6 at T590 and T597 inhibits the catalytic activity of the enzyme. As these observations suggested an effect of flg22 treatment on the *in vivo* formation of PtdIns(4,5)P₂, the effects of flg22 on PtdIns(4,5)P₂-dependent cellular processes were tested.

2.6 Flg22 perception or chemically induced activation of MKK5-MPK3/6 module affects PtdIns(4,5)P₂-dependent processes in Arabidopsis

The previous experiments indicate an inhibitory effect of flg22 perception on PI4P 5-kinase activity. As many PMPs undergo recycling between plasma membrane and TGN/EE, and CME as a prominent endocytotic pathway in plant cells is regulated by PtdIns(4,5)P₂ (König et al., 2008; Ischebeck et al., 2013), experiments were initiated to test whether flg22-mediated inhibition of PtdIns(4,5)P₂ formation would exert an effect on membrane trafficking. To test this, the endocytosis of two CME cargo proteins was analyzed. Endocytosis can be assessed in a quantitative manner upon synchronous pharmacological inhibition of exocytosis and protein *de novo* synthesis. Exocytosis from the RE can be inhibited by BFA, which inhibits the Arf-GEF GNOME (Langhans et al., 2011), resulting in the accumulation of cargo-containing RE bodies (BFA bodies) in the cytoplasm. Additional application of CHX inhibits *de novo* protein synthesis, thus only endocytosis contributes to cargo accumulation in BFA bodies (Vajrala et al., 2014). To estimate the overall endocytotic rate upon PAMP perception, 5-day-old Arabidopsis seedlings were treated overnight with flg22 or water as a control prior to plasma membrane staining with FM4-64. The formation of BFA bodies was then monitored in root tip cells upon application of 50 μM BFA for 30 min by laser-scanning confocal microscopy. Micrographs were evaluated by computer-assisted image analyses for quantification of the cytosolic and plasma membrane fluorescence intensities, and the cyt/PM ratio of intensities was calculated. Seedlings showed slightly elevated uptake of FM4-64-stained membrane material when treated with flg22 compared to the mock treated control (**figure 2.9 A**). An increased endocytotic rate complies with previous studies demonstrating that FLS2 undergoes receptor-mediated endocytosis upon flg22-binding (Robatzek et al., 2006). To further characterize the effects of flg22 on global endocytosis, the internalization of FM 4-64-stained plasma membrane was assayed in root tips of transgenic Arabidopsis seedlings expressing MKK5 DD or MKK5 KR. To this end, 5-day-old seedlings were treated with 20 μM dexamethasone for 4 h to induce the expression of the respective MKK5 variants. Plasma membranes were then stained with 2 μM FM 4-64 for 10 min prior to washout of the dye, and samples were subjected for 30 min to additional treatment with 50 μM BFA. Micrographs of root tip cells were subjected to quantitative image analyses, and the cyt/PM intensity ratios were calculated. In these experiments, tissues that expressed MKK5 DD displayed strongly reduced endocytotic activity

compared to tissues expressing the inactive MKK5 KR variant (**figure 2.9 B**), indicating an inhibitory effect exerted on endocytosis downstream of the MAPK module MKK5-MPK3/6. Together the data on the internalization of FM 4-64-stained plasma membranes suggest that endocytosis is altered in Arabidopsis cells upon flg22-perception in a complex manner.

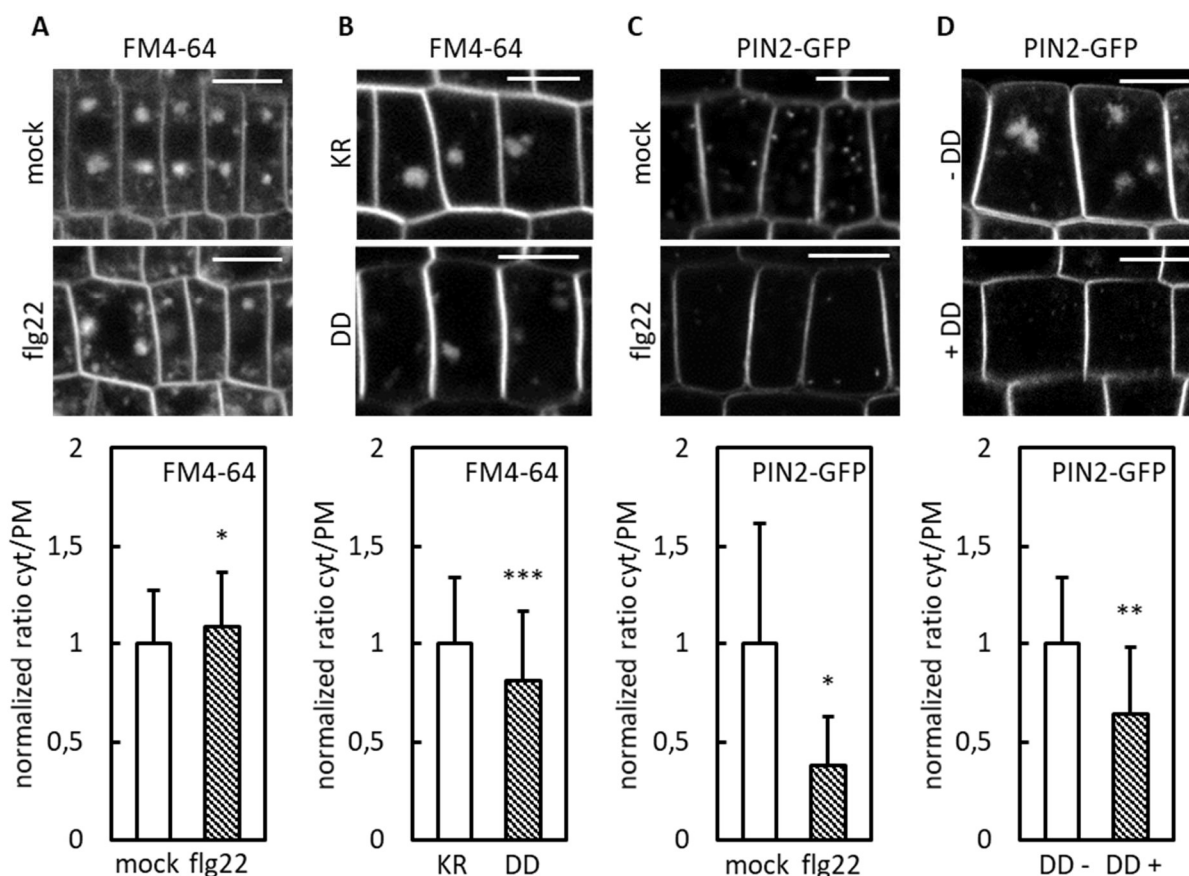


Figure 2.9: Flg22 perception or chemical activation of MKK5 affects endocytosis in Arabidopsis. A, B) Analyses of the overall endocytotic activity in Arabidopsis seedlings. five-days old Arabidopsis seedlings were treated with 10 μM flg22 or water as a control overnight. For chemical-induction of MKK5 KR or MKK5 DD expression, 5-day-old stable transgenic Arabidopsis seedling were incubated in 20 μM dexamethasone for 4 h. Membranes were stained with 2 μM FM4-64 solution for 10 min and washed for 5 min prior to incubation in 50 μM BFA for 30 min. Micrographs were taken using a confocal laser-assisted microscope. Endocytotic rate is displayed as the ratio of cytosolic and plasma membrane fluorescence intensity. Experiments were performed by Dr. Praveen Krishnamoorthy. N = 2, For each experiment and treatment 10 seedlings were analysed. A) Internalization of FM4-64-stained membrane is elevated upon flg22 perception. B) Chemical-induced expression of MKK5 DD inhibits the internalization of FM4-64-stained membrane. C, D) Assessing the endocytotic rate of the CME cargo PIN2-EGFP. Stable transgenic 10-day-old Arabidopsis seedlings were treated with 1 μM flg22 or water as a control overnight (C) or 20 μM dexamethasone for 4 h prior to incubation in 25 μM BFA and 10 μM CHX for 1 h. Micrographs were recorded with a confocal laser scanning microscope. Cytosolic (cyt) and plasma membrane (PM) fluorescence intensity were quantified separately to calculate cyt/PM-ratio. Values were normalized to the water control. PIN2-EGFP endocytosis is reduced upon flg22 perception (C) or expression of MKK5 DD activation (D). N = 3. For each experiment and treatment 10 seedlings were analysed minimum. An unpaired student's t-test was used to verify statistical significance of differences. Asterisks indicate statistical significant differences. *p ≤ 0.05; **p ≤ 0,01; ***p ≤ 0,005. Bars, 10 μm.

The observation that the different treatments used, flg22 perception or direct chemical activation of MKK5-MPK3/6, contrast each other, suggesting that the MAPK module may regulate only a subset of processes controlling endocytotic events that are affected more globally by the elicitor treatment. While these results indicate a general effect of flg22 treatment on endocytosis, these effects are not necessarily linked to a regulatory role of PtdIns(4,5)P₂. For this reason, the endocytosis of particular CME cargo proteins was monitored in more detail.

2.6.1 Endocytosis of PIN2 is inhibited upon flg22 perception or chemically induced activation of the MAPK module MKK5-MPK3/6

The auxin efflux transporter PIN2 recycles from the plasma membrane via CME in a PtdIns(4,5)P₂-dependant manner (Ischebeck et al., 2013; Tejos et al., 2014). In consequence, an Arabidopsis *pip5k1 pip5k2* double mutant with impaired PtdIns(4,5)P₂ formation displayed distinctly decreased endocytosis and perturbed localization of EGFP-tagged PIN2 (Ischebeck., et al. 2013; Tejos et al., 2014). To study the effect of flg22 perception on the CME of PIN2, 10-day-old seedlings of transgenic Arabidopsis expressing PIN2-EGFP were treated for 1 h with 10 μM flg22 prior to treatment for 2 h with 25 μM BFA and 10 μM CHX. Root tip cells were imaged using a confocal microscope and micrographs were subjected to computer-assisted quantitative image analyses to calculate the cyt/PM fluorescence intensity ratios. Quantifications of PIN2-EGFP internalization in flg22-treated intact roots revealed significantly decreased endocytosis of the PIN2-EGFP marker compared to mock treated samples, indicating an inhibition of PIN2-EGFP endocytosis upon elicitor treatment (**figure 2.9 C**). Together with previous data showing a direct influence of PtdIns(4,5)P₂ on the endocytosis of PIN2 (Ischebeck et al., 2013; Tejos et al., 2014), these results correlate well with the detected decrease of intrinsic PI4P 5-kinase activity upon flg22 treatment. However, it is likely that other factors besides PtdIns(4,5)P₂ may also contribute to the observed effect. To test whether the chemically induced expression of the constitutively active MP2K MKK5 DD affected PIN2 endocytosis, the PIN2-EGFP marker was introgressed into the MKK5 DD background. Expression of MKK5 DD in 10-day-old seedlings was induced by treatment with 20 μM dexamethasone for 4 h. A mock control was included that was treated with DMSO without dexamethasone. Treated seedlings were incubated in 25 μM BFA and 10 μM CHX for 1 h and micrographs were taken and analysed as in the previous experiments. Compared to the control samples, the induction of MKK5 DD resulted in decreased endocytosis of PIN2-EGFP (**figure 2.9 D**). The combined results suggest that the activated MAPK module MKK5-MPK3/6 negatively regulates the internalization of the CME cargo PIN2, even though overall endocytotic activity seems to be slightly increased upon flg22 treatment.

2.6.2 Flg22 perception inhibits endocytosis of RbohD in root protoplasts expressing PIP5K6-mCherry

PIN2-EGFP was included in this study, because it is so far the only well characterized CME cargo protein which is internalized from the plasma membrane via CME in a PtdIns(4,5)P₂-dependent manner (Ischebeck et al., 2013). However, no immediate correlation to pathogen defence has been described for PIN proteins, so experiments were performed to test for PtdIns(4,5)P₂-dependent endocytosis of a more relevant cargo, RbohD. RbohD is a transmembrane NADPH-oxidase that is rapidly activated upon PAMP-perception (see **figure 1.2**). The activation of RbohD upon flg22 perception is known to be independent of MPK3/MPK6 but requires multiple phosphorylation events by a number of protein kinases, including BIK1 and CDPK5 (Li et al. 2014, Dubiella et al., 2013). Previous studies have shown that RbohD recycles from the plasma membrane via CME (Hao et al., 2014). Furthermore, RbohD-EYFP accumulates in FM 4-64 stained endosomal bodies upon salt stress. Still it is unclear, whether the endocytosis of RbohD is affected by flg22 treatment. In analogy to the analyses of PIN2-EGFP endocytosis, experiments were designed to test for effects of flg22 on the internalisation of fluorescence-tagged RbohD in Arabidopsis root protoplasts expressing PI4P 5-kinases. In all experiments described in this section, the expression of fusion proteins was driven by the *pCaMV35S* promoter and protein integrity was tested by Western blot and immunodetection (**suppl. figure 8.5**). Fluorescent proteins were detected using a primary anti-GFP (for EYFP detection) or anti-mCherry antibody. Luminol-based detection was enabled by a secondary anti-rabbit antibody coupled to HRP. When RbohD-EYFP was expressed, the marker localized almost exclusively at the plasma membrane of untreated and water treated transgenic protoplasts (**figure 2.10**). Residual intracellular EYFP-fluorescence probably represents ER or TGN/EE localized fusion protein and may be an artefact of the *pCaMV35S*-driven overexpression. As in previous studies, mCherry-tagged PI4P 5-kinases showed plasma membrane and cytosolic localization (**figure 2.10**). Transgenic protoplasts were treated with 1 μ M flg22 or water as a control for 1 h prior to incubation with 25 μ M BFA and 10 μ M CHX for 1 h. Z stack micrographs were taken with a confocal laser scanning microscope, and the fluorescence intensities of endosomal bodies (EB) and plasma membrane (PM) were monitored respectively from z projections of the image stacks. Based on these intensity values, the (EB/PM) ratios were calculated. Measured differences between samples were tested for statistical significance using a 2-tailed student's t-test based on the deviation of variance between sample setups. The first experiments were performed to test whether the endocytosis of RbohD-EYFP was affected by PAMP treatment, and upon flg22 treatment, root protoplasts expressing only RbohD-EYFP showed significantly reduced endocytosis compared to the mock controls (**figure 2.10**). This observation is consistent with the results on the endocytosis of PIN2-EGFP (**figure 2.9**).

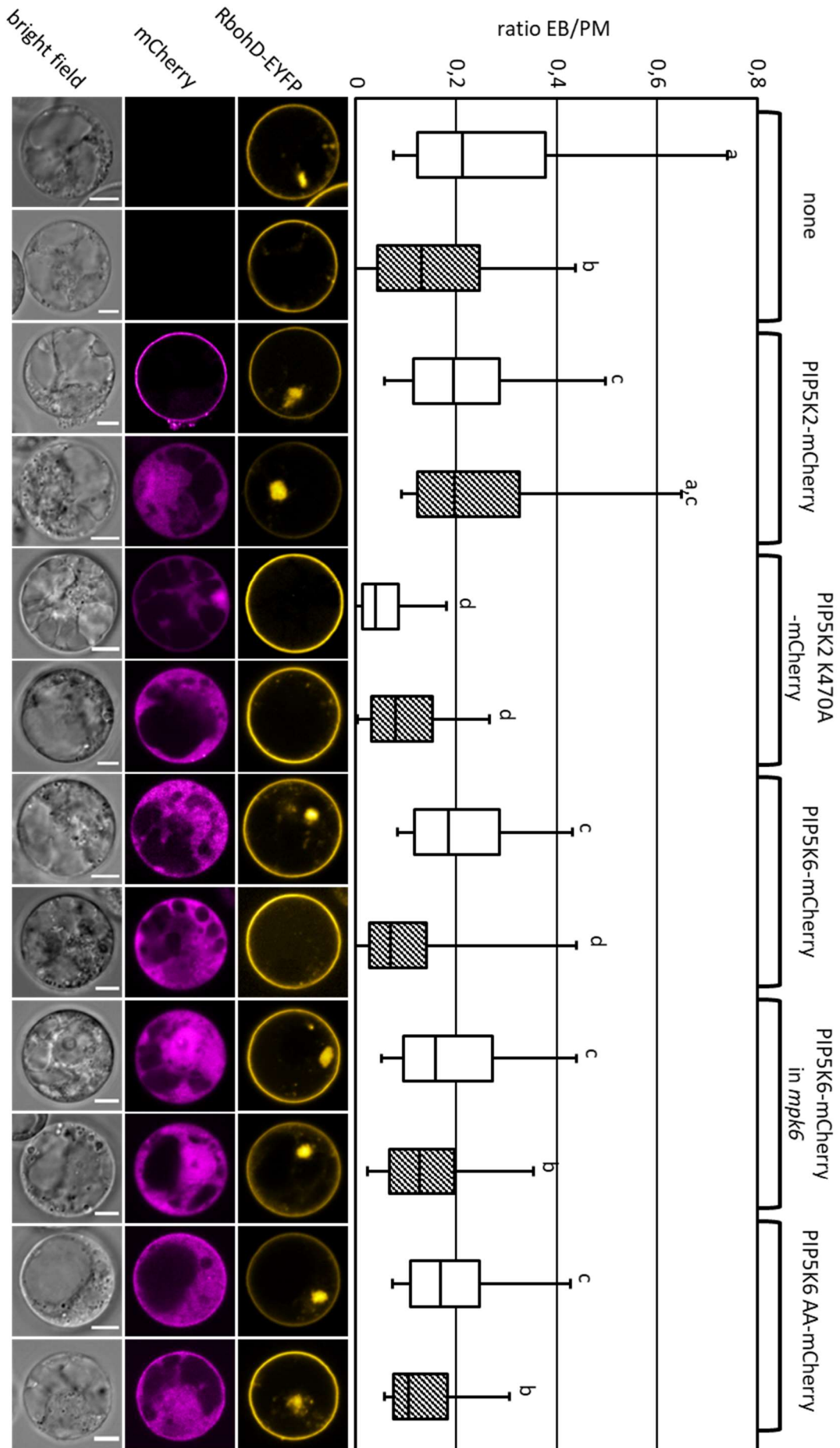


Figure 2.10: Systematic analyses of PtdIns(4,5)P₂-dependent and flg22-sensitive endocytosis of RbohD-EYFP. Upon flg22 perception, PtdIns(4,5)P₂-dependent endocytosis of RbohD-EYFP is reduced. RbohD-EYFP endocytotic rate correlates negatively with the activity of ectopically overexpressed PI4P 5-kinases. Integrity of ectopically expressed of fusion proteins was verified by SDS-PAGE and Western blot-based immunodetection (**suppl. figure 8.5**). Inhibition of PIP5K6-driven CME of RbohD-EYFP requires MPK6 and T590/T597. Transgenic Arabidopsis root protoplasts were treated with 1 μ M flg22 (patterned) or water as a control (plain) for 1 h prior incubation with 25 μ M BFA and 10 μ M CHX for 1 h. Z stack micrographs were taken using confocal microscopy. Computer-based quantification of endosomal bodies (EB) and plasma membrane (PM) localized EYFP intensity from z stack projections and calculation of the EB/PM-ratio. Significant differences were statistically verified by unpaired student's t-test based on calculated variances and are indicated by different letters for global comparison. N = 3. For each transformation and treatment, 6 cells were analysed. Bars, 5 μ m.

For further characterization of the impact of PtdIns(4,5)P₂ on RbohD internalization, flg22-triggered changes in the endocytotic rate were tested upon overexpression of mCherry-tagged PI4P 5-kinases. PIP5K2-mCherry was used as a control construct, because PIP5K2 is known to be a regulator of CME (Ischebeck et al., 2013), and a catalytically dead variant, PIP5K2 K470A, was available (Stenzel et al., 2012). Furthermore, earlier experiments had indicated that PIP5K2 is not phosphorylated upon flg22 perception (**suppl. figure 8.3**), suggesting this enzyme might not be regulated in response to the PAMP treatment. Root protoplasts expressing PIP5K2-mCherry displayed no significant changes in the endocytotic rate of RbohD-EYFP upon flg22 treatment compared to the mock control (**figure 2.10**). Furthermore, these samples were comparable to water treated cells that expressed only RbohD-EYFP, indicating that overexpressed PIP5K2 can fully support CME of RbohD. Interestingly, the overexpressed PIP5K2-mCherry was able to abolish the inhibitory effect of flg22 perception on the internalization of RbohD-EYFP, which had been observed when no PI4P 5-kinase was coexpressed. This observation indicates that the overexpressed PIP5K2-EYFP fusion displaced other intrinsic PI4P 5-kinases that may have been sensitive to inhibition upon flg22 treatment. Importantly, this effect can be conclusively attributed to PIP5K2 activity, because overexpression of the catalytically dead variant PIP5K2 K450A-mCherry resulted in a substantial reduction in the CME of RbohD-EYFP, regardless of whether the cells were treated with flg22 or with water (**figure 2.10**). This observation suggests a dominant negative effect exerted by the inactive PIP5K2 K470A. Together the results from the analyses of the PIP5K2-based controls indicate that PtdIns(4,5)P₂ production is required for the endocytosis of RbohD. When PIP5K6-mCherry was overexpressed in the protoplasts, the endocytosis of RbohD-EYFP was substantially present in the mock treated protoplasts but significantly decreased when cells were treated with flg22. These results are consistent with the inhibition of PIP5K6 by flg22-triggered phosphorylation. This interpretation is further supported by the attenuation of the effect, when PIP5K6-mCherry and RbohD-EYFP were coexpressed in *mpk6* mutant root protoplasts, showing a significantly weaker inhibition of RbohD-EYFP endocytosis upon flg22 treatment compared to the same setup in protoplasts from wild type plants (**figure 2.10**). Furthermore, the overexpression of PIP5K6

AA-mCherry had a similar effect as was detected in *mpk6* mutant plants (**figure 2.10**). Together these data indicate that RbohD endocytosis is PtdIns(4,5)P₂-dependent and is reduced upon flg22 perception. PIP5K6 was able to promote RbohD endocytosis in untreated cells, whereas flg22 treatment inhibited the endocytosis of RbohD. Importantly, the full inhibition of RbohD endocytosis required MPK6 and the presence of residues T590 and/or T597 in the catalytic domain of PIP5K6.

2.7 PtdIns(4,5)P₂-dependent CME of RbohD correlates with extracellular ROS production

The data so far indicate that PIP5K6 was phosphorylated by MPK6 upon flg22 treatment, resulting in the inhibition of PIP5K6 activity and reduced production of PtdIns(4,5)P₂. Likely in consequence of this inhibition, flg22 treatment also reduced the endocytosis of RbohD in transgenic mesophyll protoplasts overexpressing PIP5K6-EYFP in comparison to mock treated cells (**figure 2.10**). As RbohD is the most abundant NADPH-oxidase in vegetative tissue in Arabidopsis, and the main source of apoplastic ROS produced during PTI (Torres et al., 2002), it was tested whether reduced PtdIns(4,5)P₂-dependent endocytosis of RbohD would influence flg22-triggered ROS production. Transgenic mesophyll protoplasts overexpressing variants of PIP5K2 or PIP5K6 were treated for up to 1 h with flg22 or with water as a control, and ROS production was analyzed using a peroxidase-based ROS assay modified from Gomez-Gomez et al., 1999. In this assay, light emitted by a ROS-dependent luciferase reporter (given in relative light units, RLU) is proportional to the ROS concentration at a given time point. All constructs were expressed under the *pCaMV35S* promoter. The integrity of the expressed fusion proteins was verified by Western blot and immunodetection, and only full-length proteins were detected (**figure 2.11 H**). To test if the assay was compatible with the use of mesophyll protoplasts, a further control was included that did not contain a vector but was PEG treated according to the protoplast transformation protocol. All protoplasts treated with 1 μM flg22 displayed substantial ROS production, whereas no ROS was detected in the mock-treated controls. Immediately upon flg22 treatment of the untransformed controls, ROS production increased over a period of 5 min, followed by a decline to base level over the subsequent 40 min (**figure 2.11 A**). This pattern indicates that the PEG treatment did not interfere with the flg22-triggered NADPH-oxidase activity in protoplast cells. Flg22-triggered ROS production in protoplasts expressing EYFP was similar to that in the untransformed cells, indicating that NADPH-oxidase activity was not affected by ectopic protein expression (**figure 2.11 B**). To test the effects of altered PtdIns(4,5)P₂-formation on ROS production, EYFP-tagged fusions of PIP5K2 and PIP5K2 K470A were used as active and inactive PI4P 5-kinase controls, respectively. ROS production was strongly reduced when PIP5K2-EYFP was expressed (**figure 2.11 C and G**). By contrast, whereas expression of the catalytically dead PIP5K2 K470A-EYFP resulted in a substantial ROS burst (**figure 2.11 D and G**).

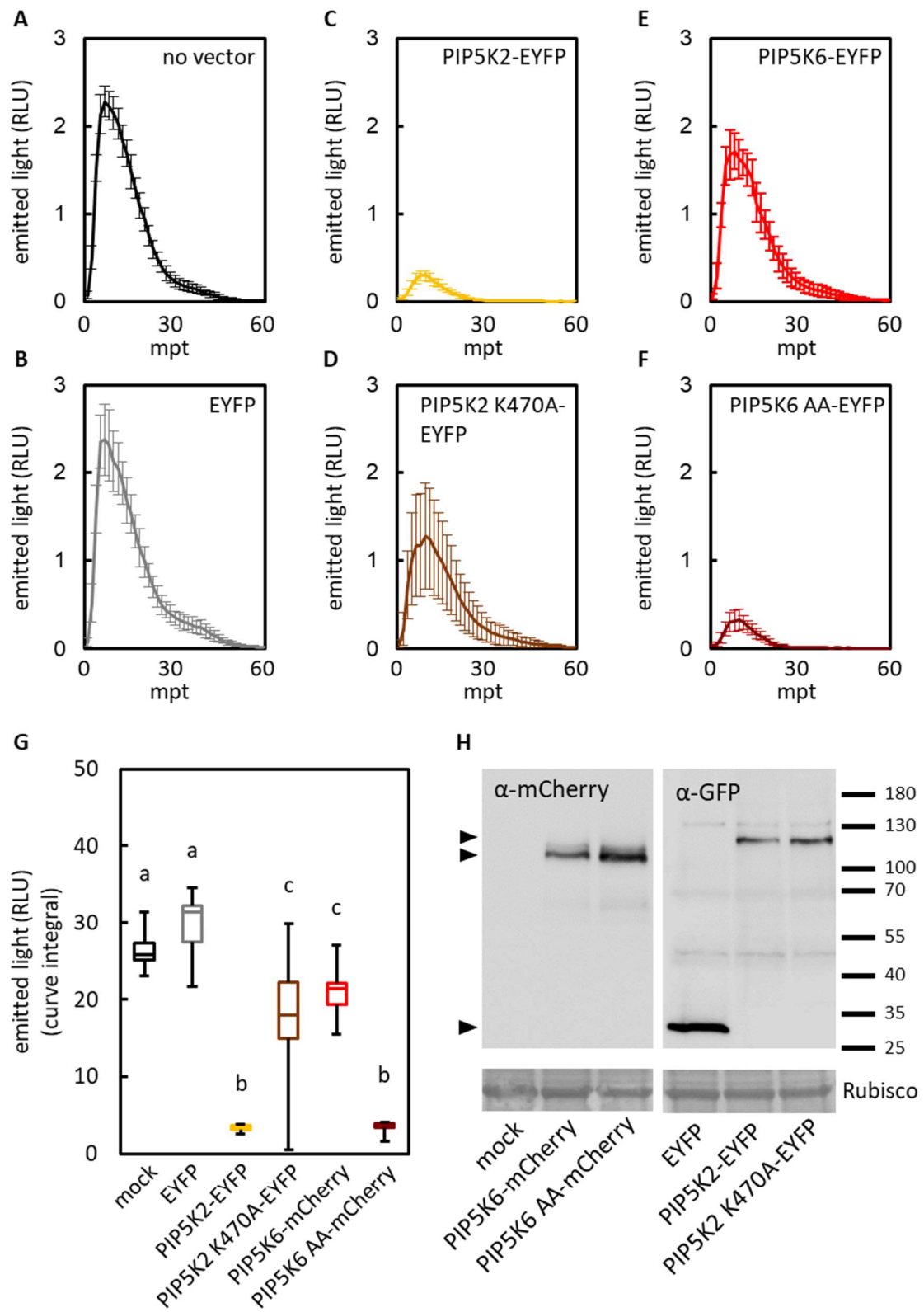


Figure 2.11: Effects of regulated PtdIns(4,5)P₂ formation on flg22-triggered apoplastic ROS production in Arabidopsis mesophyll protoplasts. Arabidopsis Col-0 mesophyll protoplasts were PEG-transformed for ectopic expression of indicated proteins. Flg22-triggered apoplastic ROS production was assessed in an HRP/luminol-based assay modified from Gomez-Gomez et al., 1999. The emitted light was measured to quantify ROS amount indirectly (relative light units; RLU). No ROS production was detected upon mock treatment. H) The integrity of ectopically expressed proteins was analysed using Western blot-based immunodetection. Immunodetection was performed using primary anti-mCherry or anti-GFP and secondary anti-rabbit antibody conjugated to HRP for luminol-based chemiluminescence assay. All proteins were expressed at full-length (arrow heads). Amido black staining was used to show equal loading amounts (showing Rubisco large subunit). A-F) Flg22-triggered ROS production was monitored over a period of 1h. Flg22-triggered ROS production was affected upon overexpression of PtdIns4P 5-kinases. Flg22-triggered ROS production negatively correlates with PtdIns4P 5-kinase activity. G) Total amount of ROS produced over a period of 1 h after flg22 perception. Statistically significant differences were verified using an acquainted variance-based unpaired students t-test. Different letters to enable global comparison indicate statistical differences. N = 3. For each experiment and transformation, 8 replicates were analysed.

These results suggest that overexpression of an active PI4P 5-kinase correlates with decreased ROS production, possibly due to the promotion of RbohD endocytosis. In protoplasts expressing PIP5K6-mCherry, ROS production was substantially decreased in comparison to untransformed cells (**figure 2.11 E and G**), and the pattern of ROS production was similar to that observed in protoplasts expressing the inactive PIP5K2 K470A-EYFP. This observation is consistent with the earlier data on the inhibition of PIP5K6 by flg22-triggered and MPK6-mediated phosphorylation. Importantly, ROS production was strongly reduced in protoplasts expressing PIP5K6 AA-mCherry (**figure 2.11 F and G**), which can no longer be inhibited by flg22-triggered phosphorylation (**figure 2.8 C**). Together the results support the hypothesis that upon flg22 treatment PIP5K6 is inhibited by MPK6-mediated phosphorylation at T590 and/or T597. As a consequence, PtdIns(4,5)P₂ production by PIP5K6 is reduced, resulting in reduced endocytosis of RbohD from the plasma membrane and concomitantly increased apoplastic ROS production.

3 Discussion

In recent years, the regulatory functions of PIs in plants have received increasing attention in the field. As our understanding of the PI-system and its essential roles in plant physiology grows (Gerth et al., 2017), new questions arise about the spatiotemporal dynamics of PIs, about the modes of regulation of PI biosynthesis, and about the interconnection of PIs with other key signalling pathways in plants. Data in this thesis demonstrate that the formation of PtdIns(4,5)P₂, a PI with important regulatory roles in the control of membrane trafficking, can be modulated by a MAPK-cascade that is triggered by the activation of a cell surface receptor, FLS2, binding its ligand, flg22. The ensuing signal transduction cascade influences the formation of PtdIns(4,5)P₂, resulting in changes in membrane trafficking that affect the recycling of several important proteins from the plasma membrane, such as RbohD or PIN2. The evidence presented, thus, expands our understanding of the plant PI-system in two directions, both upstream and downstream of PtdIns(4,5)P₂ production.

3.1 MAPK signalling and PIs are interconnected throughout different tissues

First indications for a link between the highly conserved signalling pathways of MAPKs and PIs came from studies on the role of PIs in the control of polar tip growth of pollen tubes (Hempel et al., 2017). Pollen tubes respond to changes in PI metabolism with the manifestation of characteristic physiological phenotypes, thus making them an ideal model systems to study the regulation of the formation of PI species, such as PtdIns(4,5)P₂ (Ischebeck et al., 2008; Ischebeck et al., 2010, Ischebeck et al., 2011, Sousa et al., 2008). However, pollen tubes represent a very specialized type of gametophytic cell with unique physiology. MPK6 together with MPK3 is involved in the regulation in funicular guidance in growing pollen tubes (Guan et al., 2014). In vegetative tissue however, MPK6 acts in the MAPK cascade module MKK4/5-MPK3/6 that is known to be involved in the positive regulation of plant PTI (Meng and Zhang, 2013). Up to this point, PIP5K6 is the only PI4P 5-kinase known to be regulated by MAPKs. PIP5K6 however, has only been studied in its function as a regulator of pollen growth (Zhao et al., 2010; Hempel et al., 2017), even though the protein is ubiquitously expressed (**figure 2.1**). It is important to mention that for PIP5K6 no function in vegetative tissue has been identified yet and that the experiments in this thesis are only suitable to support a regulation of PIP5K6 upon flg22 treatment. To conclusively define the biological function of PIP5K6 during PTI, the experiments performed are not sufficient. With these limitations, the focus of this thesis was on the integration of the MAPK-PI signalling network in vegetative tissue. Upon flg22-treatment, reduced plasma membrane association of the PtdIns(4,5)P₂ marker mCITRINE_{2xPH(PLCδ1)} was observed in Arabidopsis seedlings (**figure 2.4**). While the dissociation of the fluorescence reporter from the plasma membrane indicates a decrease in PtdIns(4,5)P₂ abundance upon elicitation, no significant changes were observed when flg22-treated or

PST DC3000 infected seedlings were subjected to biochemical PtdIns(4,5)P₂ quantification (**figure 2.5 and 2.6**). Since PtdIns(4,5)P₂ is a low abundant lipid, direct quantification is performed closely to the limits of detection and therefore, detection of significant changes can be difficult especially when a treatment is expected to cause a further reduction of the respective compound. Still, a transient increase in PtdIns(4,5)P₂ that would be restricted to the first minutes after elicitor perception cannot be precluded. Furthermore, another possible scenario would be that overall PtdIns(4,5)P₂ levels are not changed at all upon elicitor perception. In this case the observed effect of flg22 treatment on the PtdIns(4,5)P₂ reporter localization could be explained by the reporter competing with intrinsic PtdIns(4,5)P₂-binding protein, that have not been identified yet and are expressed or activated during PTI. Such an effect does not necessarily impact global PtdIns(4,5)P₂ turnover but may rather be restricted to specific PtdIns(4,5)P₂ pools involved in the regulation of processes connected to this particular response. Still it has been suggested that PIs may be organized in functional pools that exert regulation on unique sets of cellular processes independently from each other (Heilmann & Heilmann 2015; Gerth et al., 2017). Such PI pools could be formed or degraded by specific isoforms of PI4P 5-kinases or other members of respective enzyme families. While the results from the biochemical analyses of unlabelled PI species may remain inconclusive, the observed decrease of intrinsic PI4P 5-kinase activity upon both, flg22 perception and chemically induced activation of the MKK5-MPK6 module, supports the results obtained using the mCITRINE_{2xPH(PLCδ1)} biosensor (**figure 2.4 A+B**). Together these results point towards a negative regulation of PtdIns(4,5)P₂ formation upon flg22 treatment or biotic stress. This notion contrasts with dynamic patterns of PI changes that have been reported for plant responses to abiotic stress. Salt stress for example leads to a transient accumulation of PtdIns(4,5)P₂ at the plasma membrane in different plant models (Heilmann et al., 1999; Heilmann et al., 2001; DeWald et al., 2001; König et al., 2007; König et al., 2008). Both types of stress, hyperosmotic stress and to encounter a pathogen might require a different kind of response. While the application of salt revealed an increased association of PtdIns(4,5)P₂ with clathrin (König et al., 2008) possibly to mediate the bulk-flow endocytosis of plasma membrane area, defence-relevant PMPs might require reduced endocytotic recycling and stabilization at the plasma membrane upon induction of the plant immune response. That both stimuli transduce their respective signal through PIs is also suggested by experimental data using a SD microscope to assess the distribution of mCITRINE_{2xPH(PLCδ1)} within the plasma membrane. NaCl-application to Arabidopsis hypocotyl cells has previously been shown to trigger PtdIns(4,5)P₂-formation (König et al., 2007; König et al., 2008) and also causes the association of a PtdIns(4,5)P₂ reporter with distinct foci at the plasma membrane (**figure 2.4 C**). This distribution pattern was no longer present when cells were subjected to pretreatment with 1 μM flg22 for 1 h (**figure 2.4 C**), indicating that a pretreatment of Arabidopsis cells with flg22 can suppress the effect of high salt treatment on the formation of PtdIns(4,5)P₂. This

observation suggests hierarchical crosstalk between signalling pathways competing for effects on PtdIns(4,5)P₂ production. As currently the formation and maintenance of plasma membrane microdomains containing PtdIns(4,5)P₂ is poorly understood, the interpretation of some of the observations in this thesis remains difficult.

3.2 Phosphorylation of PIP5K6 by MPK6 and inhibition of catalytic activity upon flg22 treatment

Upon flg22 treatment of mesophyll protoplasts, PIP5K6 was phosphorylated at threonine residues T590 and/or T597 (**figure 2.3**). While the phosphorylation event could be detected by observing the retarded electrophoretic mobility of phosphorylated PIP5K6-HA protein (**figure 2.3**), the band shift appeared differently in the Phos-tag gel, depending on the presence of the protein, myc-MVQ1. Upon coexpression of myc-MVQ1 the band shift of PIP5K6-HA appeared more pronounced compared to samples not coexpressing myc-MVQ1 (**figure 2.3 A and C**). This effect might be due to the presence of myc-MVQ1, which is phosphorylated by MPK3/6 at multiple sites and competes with phosphorylated PIP5K6-HA for Phos-tag binding sites, resulting in a lower resolution of electrophoretic separation. Refinement of this method is still required, since the advantages of an intrinsic control outrun the drawbacks as long as true phosphorylation is still detectable. Higher concentrations of the incorporated Phos-tag constituent could probably enhance the gel shift of both proteins, while possibly increasing the sensitivity of the method to salt contamination in the samples. The observation that flg22-triggered phosphorylation of PIP5K6 in *mpk6* mutant protoplasts was reduced but still substantial indicates that other protein kinases besides MPK6 may also target PIP5K6. For instance, MPK3 acts together with MPK6 in the same MAPK module, and both MAPKs are activated by upstream MKK5-mediated phosphorylation (Asai et al., 2002). It has been shown that MPK3 and MPK6 share an overlapping subset of substrates (Rayapuram et al., 2018). The fact that PIP5K6 AA was not phosphorylated anymore upon flg22 treatment suggests that T590 and T597 are the only target sites that are phosphorylated by MPK6 and an MPK6-redundant kinase, likely MPK3. However, data from *mpk6* mutant protoplasts are preliminary and should be viewed with caution. Additional investigations that also include the usage of an *mpk3* knockout mutant are necessary. While it has been demonstrated that PIP5K6 can also be a substrate for CDPKs (Hempel et al., 2017), some of which are activated upon flg22 treatment as well (Boudsocq et al., 2010), experiments shown in this thesis do not indicate CDPK-mediated phosphorylation of PIP5K6 upon flg22 perception. The combined results provide evidence that PIP5K6 is phosphorylated upon flg22 treatment and that MPK6 is required for maximum phosphorylation efficiency. Flg22-triggered phosphorylation of PIP5K6 decreases catalytic activity of the enzyme. This effect can likely be attributed to an inhibition of the PIP5K6 protein by the

phosphorylation, because neither the accumulation of PIP5K6 transcript nor PIP5K6 protein abundance were changed upon flg22 treatment (**figure 2.7**). Considering that PTI is a process that is triggered within minutes and persists for only a relatively short time, phosphorylation-mediated degradation of PIP5K6 at later time points than assessed in this thesis appears unlikely, but cannot be excluded, since it has been shown that MPK3/6-mediated phosphorylation can affect the stability of some target proteins up to 24 h post elicitor treatment (Wang et al., 2014). *In vitro* radiolabelling assays using immunoprecipitated PIP5K6-HA from protoplasts support a reduction of "specific" PI4P 5-kinase activity when the protoplasts were treated with flg22 (**figure 2.8 C**). For PIP5K6-HA and PIP5K6 AA-HA no statistical significant differences in activity were detected when cells were mock treated, indicating that the T590A and T597A substitutions did not affect the overall function of the enzyme. These data correlate with previous studies that detected an inhibitory effect of MPK6-mediated phosphorylation of recombinant PIP5K6 at T590 and T597 (Hempel et al., 2017). In both pollen tube cells and mesophyll protoplasts, the effect of ectopic PIP5K6 overexpression was reduced by coexpression of MPK6 or activation of an flg22-triggered MAPK cascade, respectively (Hempel et al., 2017, this thesis). Still, the contribution of the reported inhibition of PIP5K6 to the physiology of a native biological system remains unclear, considering the redundancy between PI4P 5-kinase isoforms. Six out of 11 PtdIns4P 5-kinases are expressed ubiquitously in Arabidopsis and can probably act redundantly to a certain extent. There also may be additional compensatory effects, which are currently not understood. For instance, an Arabidopsis *pip5K1* mutant showed increased transcriptional activity for the PIP5K2 gene and vice versa, indicating that the plant may compensate the loss of one kinase through increased expression of the other (Ischebeck et al., 2013). At the level of posttranslational modifications, there may be subsets of PI4P 5-kinase isoforms that might be subject to similar or different modes of regulation. For instance, PIP5K4 and PIP5K5 also possess one of the MPK6-targeted TP-motifs that were identified in the variable insert in the sequence of PIP5K6 (**figure 3.1**).

```

PIPK1 589 AERIMDYSLLVGVHFRDD--NTGKMKGLSPFVLRSGRIDSYQNEKFMRGCRFLEAELQDM
PIPK2 591 AERIMDYSLLVGVHFRDD--NTGDKMGLSPFVLRSGKIESYQSEKFMRGCRFLEAELQDM
PIPK3 563 AERIMDYSLLIGLHFRES--GMRDDISLG-----IGRRD--QEDKLMRG-----
PIPK4 627 QERIMDYSLLVGIHFREA--SVAGELIP-----SGARTTPIGEFEDESAPRISRADV-DQ
PIPK5 620 QERIMDYSLLVGIHFREA--SVAGELIP-----SGARTTPIGESEEEESGPRISRAEV-DE
PIPK6 566 QERIMDYSLLVGLHFRFA--AIKSATPT-----SGARTTPTGNSET----RLSRAEM-DR
PIPK7 566 SLNIIDYSLLIGLHFRAP--GQLNDIIEPPNAMSDQES--VSSVIVGLTQEHSPKGLL
PIPK8 579 SLQIIDYSLLIGLHFRAP--DPLTDIIEPPNEMSDQESDSVGSVIVNLPREESIPKGLL
PIPK9 628 AQNIMDYSLLIGVHHFRAP--QHLSQIVRSQSITIDALESVAEDIT-IEDDMLSYHEGLV
PIPK10 205 EEGIMDYSLLVGLQSKGSCQGSIDGINPVYGSFAPPSSFKSNSTKSMKTASSSPDRSSVA
PIPK11 213 DEGIMDYSLLIGLVQVKGSGCHGSIDELIPVYDSFTSRGSVDSNSSKFMKTASNSPDRSSST

```

Figure 3.1: PIP5K6 MPK6-target sites T₅₉₀P₅₉₁/T₅₉₇P₅₉₈ are partially conserved among Arabidopsis PI4P 5-kinases. Alignment of the sequence segment of PIP5K6 that comprises the MPK6-target sites with all Arabidopsis PI4P 5-kinases. PIP5K6 T₅₉₀P₅₉₁-motif is not present in other PI4P 5-kinases. PIP5K4 and PIP5K5 share sequence identity with PIP5K6 at T₅₉₇P₅₉₈-motif (red). Ubiquitously expressed enzymes are written in black. Enzymes with restricted expression are written in grey.

This particular motif comprises the threonine at position 597, which has been shown to affect PIP5K6 activity when phosphorylated by MPK6 (Hempel et al., 2017). Both show a similar expression pattern to PIP5K6 and are mainly expressed in the mature pollen and growing pollen tube (eFP browser, Winter et al., 2007, **suppl. figure 8.1**). A certain redundancy between these kinases therefore is suggested but has not been verified yet. By contrast, PIP5K1 or PIP5K2 do not possess the motifs targeted by MPK6.

3.3 Protoplast expression system: a matter of control

Investigations on enzymes that display key regulators of a cellular processes have always been a challenge. PIs are low abundant regulatory lipids that control numerous membrane-associated pathways, thus requiring tight spatiotemporal regulation of formation and degradation. For that reason, generating stable transgenic Arabidopsis lines ectopically expressing enzymes with functions in PI metabolism has proven to be difficult. This thesis is built on experiments that required overexpression of the PI4P 5-kinase PIP5K6 and other PI4P 5-kinases. Since no stable PIP5K6 expressing Arabidopsis line has been successfully established yet, a transient expression system was required. Due to the nature of the object of interest in this thesis, transient *Agrobacterium*-mediated transformation was no option, as it would trigger pathogen response immediately upon bacteria-cell-contact in the inoculated tissue. To be able to investigate the role of PIP5K6 in a homologous expression system without stable expression lines available, Arabidopsis mesophyll and root protoplasts have become a useful tool. Protoplasts have been shown to respond to a wide range of stresses including salt stress and PAMP-treatment. Still, the drawbacks of this system need to be taken into consideration. The preparation and transformation of protoplasts including cell wall digestion and PEG-mediated endocytosis puts stress on the cells, therefore a well-defined set of controls was applied to every experiment to minimize bias of interpretation.

However, the use of protoplasts allowed significant progress in all fields of plant research due to the advantages of the system that were as well exploited in this very thesis. Transgenic protoplasts obtained from different Arabidopsis tissues such as leaves and roots can be subjected to a number of experimental approaches including electrophoretic protein separation for Western blot and immunodetection, immunoprecipitation of expressed proteins and microscopic analyses. Protoplasts respond in a similar way to chemical or stress treatment as whole seedlings. Except for they require lower substance dosage compared to intact plants, providing a more gentle and precise treatment. For example, the susceptibility of the elicitor peptide flg22, which is completely soluble in water, is much higher and does not depend on the tissue depth. Like other Chemicals, flg22 can be added directly into the cell suspension medium, allowing an equal treatment of every cell within. In this thesis protoplast were subjected to a wide variety of applications. While usage of this system for *in vivo* assays to study

phosphorylation, degradation and localization is well established, only a few examples exist that assessed endocytosis in protoplasts. Depletion of cell wall is critical when it comes to the study endocytosis and membrane trafficking. These processes have been shown to depend on cell wall structure and compound composition (Liu et al., 2015). However, endocytosis has already been studied in different protoplast systems (Onelli et al., 2008, Bandmann et al., 2011, Bandmann and Homann, 2012).

3.4 Flg22-treatment or activation of the MKK5-MPK3/6 module attenuate PtdIns(4,5)P₂-dependent membrane trafficking

The impact of earlier findings on plant endocytosis was first assessed according to uptake experiments using the lipophilic fluorescent dye, FM 4-64. FM 4-64-staining of Arabidopsis root tip cells revealed a very slight increase in overall endocytotic activity upon perception of flg22 (**figure 2.9 A**). At first sight, this observation is contrasted by a decreased uptake of FM 4-64-stained membrane material when cells expressed MKK5 DD compared to cells that expressed MKK5 KR control construct. Elicitors trigger numerous cellular processes including receptor-triggered endocytosis. The observation of a slight but significant increase in endocytosis of FM 4-64-stained membrane upon treatment with flg22 (**figure 2.9 A**) could be due to an induction of the internalization of flg22-bound FLS2 that is required to induce the immune response (Robatzek et al., 2006). It is possible that different subsets of endocytotic events might be triggered and/or regulated upon either flg22 perception or MKK5 DD induction. The activation of the MKK5-MPK3/6 module by the induced expression of constitutively active MKK5 DD bypasses the activation of the upstream RLK FLS2. Therefore, it can be assumed that the internalization of flg22-bound FLS2 may mask an inhibitory effect that is executed by the activated MKK5-MPK3/6 module (**figure 2.9 B**) on different endocytotic events, possibly through regulation of PtdIns(4,5)P₂ metabolism. This hypothesis is supported by the observation of the reduced endocytosis of a specific CME cargo PIN2-EGFP upon both flg22 perception and induction of MKK5 DD (**figure 2.9 C and D**). A similar effect was observed in a *pip5k1 pip5k2* double mutant, in which perturbed PtdIns(4,5)P₂ metabolism strongly affected clathrin recruitment and the CME of PIN2-EGFP, while the overall endocytosis of FM 4-64-stained membrane was much less severely affected (Ischebeck et al., 2013). As PIN2 is the only PMP that has been shown to recycle from the plasma membrane in a PtdIns(4,5)P₂-dependent manner, it was included in this thesis, even though no immediate relation to immune responses has been reported for this protein. To investigate the endocytosis of a CME cargo with reported function in PTI, the NADPH-oxidase RbohD was analysed. To study the internalization of fluorescence-tagged RbohD, transiently transformed root protoplasts were used for a number of reasons. A transient expression system was required because of the lack of stable transgenic

Arabidopsis lines expressing PI4P 5-kinases or RbohD-EYFP (A previously reported Arabidopsis line expressing RbohD-EYFP (Hao et al., 2014) was obtained but did not display fluorescence in our hands). Furthermore, protoplast cells from the root tip are not highly vacuolated and favouring the imaging of cytoplasmic endosomal bodies. The endocytosis of RbohD-EYFP was reduced upon flg22 treatment, giving rise to the hypothesis that the protein might be stabilized at the plasma membrane for efficient apoplastic ROS production. The endocytosis of RbohD-EYFP was positively correlated with PI4P 5-kinase activity in transgenic root protoplasts (**figure 2.10**). Interestingly, RbohD was shown previously to internalize and accumulate in FM 4-64-stained endosomal bodies upon salt stress (Hao et al., 2014), which in turn induces transiently increased PtdIns(4,5)P₂ formation (DeWald et al., 2001; König et al., 2007; König et al., 2008). Together, these data support the notion that RbohD is internalized from the plasma membrane by PtdIns(4,5)P₂-dependent CME. Moreover, previous analyses of the distribution and dynamics of fluorescence-tagged RbohD revealed an increased molecule density at the plasma membrane upon flg22 treatment (Hao et al., 2014), which is consistent with the findings in this thesis. A reduction of RbohD-EYFP internalization upon flg22 treatment in cells expressing a PIP5K6-mCherry variant was more severe, when MPK6 and the target sites T₅₉₀P₅₉₁/ T₅₉₇P₅₉₈ were present and available for phosphorylation, in comparison with the results obtained with the PIP5K6 AA-HA variant (**figure 2.10**). From this observation, it can be concluded 1) that PIP5K6 is able to promote PtdIns(4,5)P₂-dependent CME of RbohD and 2) that PIP5K6 might be inhibited by MPK6-mediated phosphorylation to stabilize RbohD at the plasma membrane for efficient ROS production upon elicitor-triggered immunity. However, as a note of caution, all results supporting a PIP5K6-mediated regulation of RbohD internalization were obtained from an overexpression system. To verify the biological relevance of these results, endocytosis of RbohD upon flg22 perception should be assessed in a *pip5k6* mutant background. While such a mutant was isolated, it did not show an obvious growth phenotype and requires further characterization (data not shown). It can be expected that the *pip5k6* single mutant must be crossed with other PI4P 5-kinase mutants to overcome redundancy issues within the PI4P 5-kinase family. Functional redundancy among PI4P 5-kinases might be further complicated because of partial functional overlap of isoforms. For instance, it has been demonstrated that both PIP5K1/PIP5K2 (Ischebeck et al., 2013) and PIP5K6 (Zhao et al., 2010) are important for CME in plant cells. In this thesis, both PIP5K2-mCherry and PIP5K6-mCherry, were able to promote internalization of RbohD-EYFP, but only PIP5K6 was inhibited upon flg22 treatment, suggesting an isoform-specific mode of regulation. To judge the impact of this observation, more information about the true abundance and functional interactions of different PI4P 5-kinase isoforms is required. Recent data suggest that PIP5K1 and PIP5K2, which represent the predominant PI4P 5-kinase activities in Arabidopsis embryos and young seedlings (Ischebeck et al., 2013; Tejos et al., 2014) may be less abundant in fully developed tissues (personal communication, Dr. Praveen Krishnamoorthy & Prof. Dr. Ingo Heilmann).

Reciprocally, PIP5K6 appears to be expressed at substantially higher rates in 6 to 8-week old plants compared to seedlings (**figure 2.1 L**). Considering these expression dynamics with the age of the plant, it is possible that PIP5K6 plays a more important role in the regulation of PAMP-triggered ROS production than anticipated from its low expression as suggested by the *efp* browser.

3.5 PtdIns(4,5)P₂ may impact on RbohD recycling from the plasma membrane and on ROS production

The overexpression of PI4P 5-kinases heavily impacts the flg22-triggered production of apoplastic ROS in transgenic mesophyll protoplasts (**figure 2.11**). This effect correlated with the extent of endocytosis observed for RbohD-EYFP in transgenic protoplasts expressing active or inactive variants of PI4P 5-kinases. By using fluorescence-tagged PIP5K2 or PIP5K2 K470A for an active and inactive PI4P 5-kinase control, respectively, it was shown that endocytosis of RbohD-EYFP was correlated with the presence of PI4P 5-kinase activity. By contrast, apoplastic ROS production was increased in cells that expressed a PI4P 5-kinase of low or no enzymatic activity. These observations support the hypothesis that inhibited PtdIns(4,5)P₂ production upon flg22 treatment blocks CME of activated RbohD, allowing for a longer plasma membrane half life of RbohD and fostering more efficient ROS production. PIP5K6 is a confirmed MPK6 target and may play a role in this process. It is worth to mention that these data support the idea of a rapid and transient decrease in PtdIns(4,5)P₂ abundance upon elicitor perception, since PAMP-induced apoplastic ROS production is a rapid process and correlates with RbohD endocytotic rate in a diametrical opposed manner. The activation of a PtdIns(4,5)P₂-depleting enzyme upon PAMP treatment has been observed in an independent study (personal communication, Juliane Rausche, Prof. Dr. Sabine Rosahl and Prof. Dr. Ingo Heilmann), which might contribute an additional layer of regulation to limit PtdIns(4,5)P₂ production during PTI.

Some data shown in this thesis contrast with previous reports on the possible connection between the MAPK signalling and the induction of apoplastic ROS production. A knock out of both *MPK3* and *MPK6* leads to embryo lethality and a severe growth phenotype and can thus not be studied. To avoid a developmental phenotype, stable transgenic Arabidopsis plants were generated that expressed an MPK6 variant (MPK6 YG), which can be inhibited by NA-PP1 application in an *mpk3 mpk6* double mutant background. In the MPK6 YG sequence a tyrosine within the ATP binding pocket was mutated to a glycine to enable binding of NA-PP1, which cannot be hydrolysed (Xu et al., 2014). This chemically induced Arabidopsis *mpk3 mpk6* double knock out displayed flg22-triggered apoplastic ROS production similar to wild type controls (Xu et al., 2014), leading Xu and coworkers to conclude that RbohD might be regulated independently of MPK3/6. However, MPK6^{YG} inhibition by NA-PP1 was only confirmed *in vitro*, therefore residual *in vivo* activity cannot be excluded. Still, various investigations on flg22-

triggered ROS production do not immediately support the idea that RbohD function is regulated by MPK6-controlled formation/degradation of PtdIns(4,5)P₂ (Xu et al., 2014). Production of ROS can be harmful to the producing cell itself. Therefore, it requires strict regulation, which is obvious from the fact that multiple signalling cascades jointly control the activity of the most abundant NADPH-oxidase RbohD in Arabidopsis. These cascades involve several protein kinases downstream of FLS2 and calcium signalling (Ogasawara et al. 2008, Dubiella et al. 2013, Kadota et al. 2014, Li et al. 2014). Besides protein factors, also phospholipids can contribute to this regulation, and it has been shown that the signalling lipid PtdOH binds to the N-terminal cytosolic domain of RbohD (Zhang et al., 2009). Furthermore, phospholipase Dα1 (PLDα1) is a positive regulator of ROS production during stomatal closure (Zhang et al., 2009). Whether this mode of regulation is unique to guard cells is currently unknown and RbohD interaction with different PI species has never been tested. From the experiments in this thesis, an effect of PtdIns(4,5)P₂ on the activity of RbohD by direct protein-lipid-interaction is not supported, but cannot be excluded. Based upon the data on the endocytosis of RbohD in PI4P 5-kinase-expressing root protoplasts, PtdIns(4,5)P₂ effects on the endocytosis of RbohD appear more likely, thus modulating the subcellular distribution of RbohD and thus impacting ROS production. The data can be summarized in a model of an in parts speculative mechanism how the plasma membrane association of RbohD might be regulated by modulating PtdIns(4,5)P₂ production (**figure 3.2**). In this model, the perception of different stimuli, such as salt or flg22, impact on PI metabolism to promote or suppress the endocytosis of RbohD from the plasma membrane. For example, salt stress leads to an increased internalization of RbohD and induces the production of intracellular ROS (Hao et al., 2014). Application of high concentrations of NaCl causes a transient increase in PtdIns(4,5)P₂ levels, which is a positive regulator of CME (König et al. 2008, Ischebeck et al., 2013). By contrast, apoplastic ROS production is required upon recognition of a pathogen. Activation of a the PAMP-triggered MAPK module MKK4/5-MPK3/6 inhibits PtdIns(4,5)P₂ production by PIP5K6, thus reducing endocytosis of RbohD and increasing ROS production to the apoplast. A regulation of additional key enzymes that either produce PtdIns(4,5)P₂ or use it as a substrate, such as PI-lipases or PI-phosphatases, is possible. With regard to the more detailed effects of flg22-mediated signalling, the data obtained in this thesis are summarized in a second model (**figure 3.3**). In untreated Arabidopsis plants, RbohD recycles from the plasma membrane by CME (Hao et al., 2014), a process requiring PtdIns(4,5)P₂. Upon perception of flg22 by the RLK complex FLS2/BAK1, the downstream MAPK module MKK4/5-MPK3/6 is activated by an unknown protein kinase. MPK6 phosphorylates PIP5K6 to inhibit PtdIns(4,5)P₂ production by that enzyme. Reduced PtdIns(4,5)P₂ formation then leads to a decreased rate of endocytotic recycling of RbohD. Upon stabilization at the plasma membrane, RbohD mediates more efficient ROS production to the apoplast.

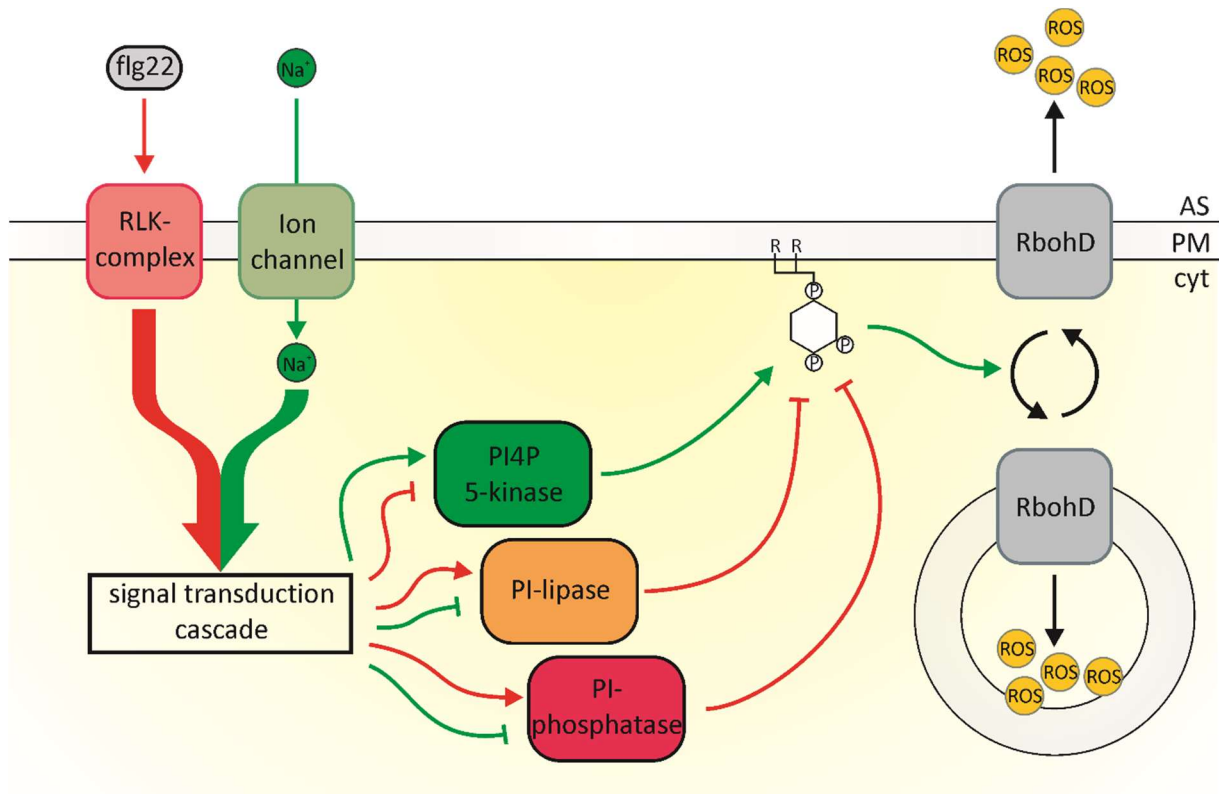


Figure 3.2: Model: Different inputs may affect RbohD localization through effects on PtdIns(4,5)P₂-dependent endocytosis. RbohD-mediated ROS production takes place in different cellular compartments. PtdIns(4,5)P₂ promotes CME of intramembrane cargoes including RbohD. RbohD localization to the plasma membrane or endomembrane system is balanced by the abundance of PtdIns(4,5)P₂. Signalling cascades transduce different stimuli regulate the activity of key enzymes in PtdIns(4,5)P₂ metabolism. Application of high concentrations of NaCl is accompanied by transiently increased formation of PtdIns(4,5)P₂. Upon salt stress, RbohD endocytosis and intracellular ROS production is triggered. When flg22 is perceived, PtdIns(4,5)P₂ production is inhibited causing RbohD to be stabilized at the plasma membrane for apoplatic ROS burst. Green arrows indicate processes that favour endocytosis. Red arrows indicate processes that suppress endocytosis and might favour exocytosis. Apolastic space (AS), plasma membrane (PM), cytosol (cyt).

While the data from this thesis might in parts be interpreted differently than shown in the model, overall they provide ample new evidence for the functional crosstalk between two ancient eukaryotic signalling pathways, MAPK cascades and PI signalling. PtdIns(4,5)P₂ is introduced as a new regulator that connects the MAPK module MKK4/5-MPK3/6 to elicitor-triggered ROS production mediated by RbohD, two pathways that have previously been thought to act independently from each other. RbohD emerges as a CME cargo that is dependent on PtdIns(4,5)P₂ for its correct trafficking at the plasma membrane.

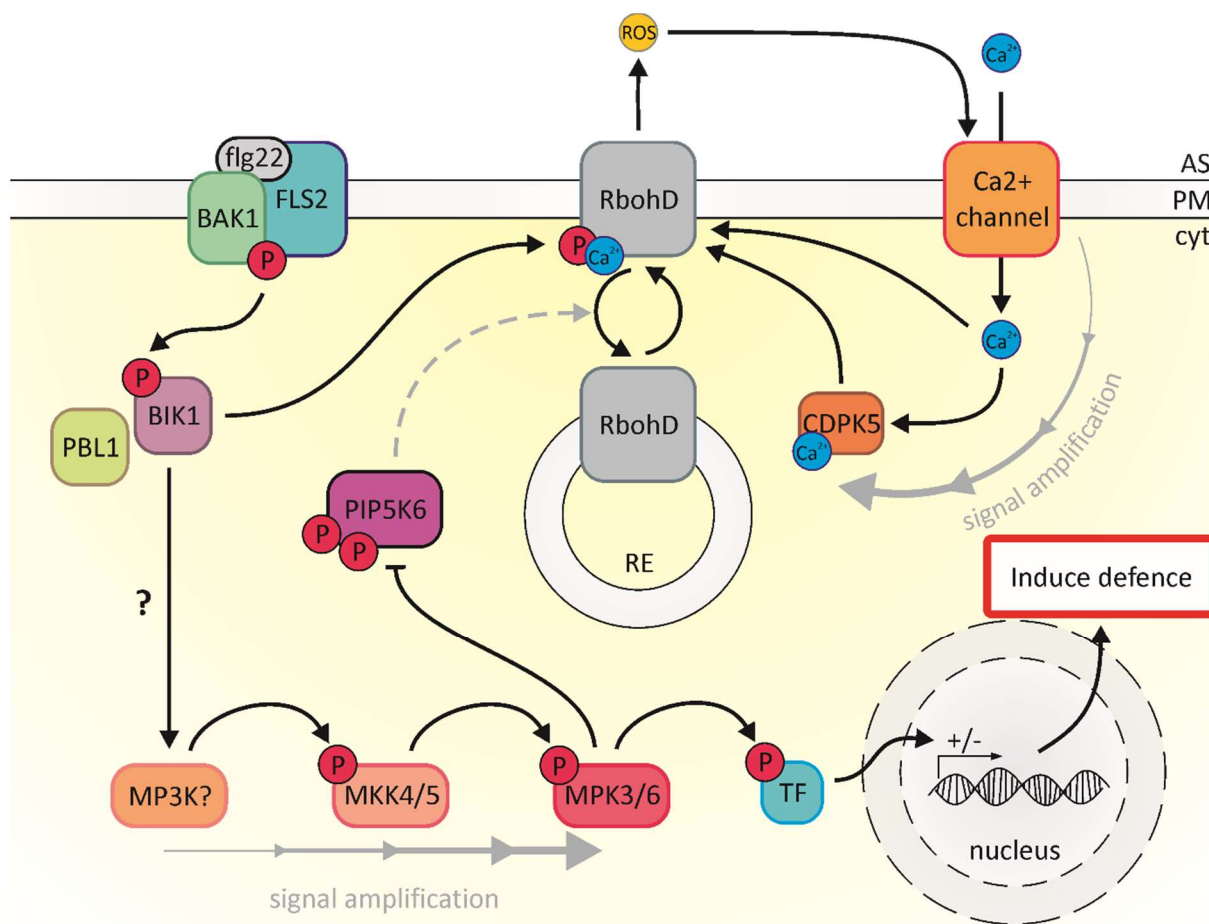


Figure 3.3: Model: PIP5K6 and PtdIns(4,5)P₂-formation is controlled by an flg22-triggered MAPK cascade and might regulate localization of RbohD for efficient apoplastic ROS burst. The FLS2-associated MAPK module MKK4/5-MPK3/6 negatively regulates the enzymatic activity of PIP5K6 upon flg22 perception. RbohD recycles from the plasma membrane via PtdIns(4,5)P₂-dependent CME. Upon flg22 perception, reduced formation of PtdIns(4,5)P₂ leads to a stabilization and accumulation of activated RbohD at the plasma membrane and enables substantial ROS burst to the apoplast. Cytosolic enzyme (CE), transcription factor (TF), apoplast space (AS), plasma membrane (PM), cytosol (cyt). The model was created after Bigeard et al. (2015) with data obtained from Hao et al. (2014) and this thesis.

3.6 A model to be completed: Further complexity and open questions

As mentioned before, the conclusions drawn from the data in this thesis have to be confirmed in further experiments that avoid dominant effects of overexpression. Several observations in this thesis were perceived as surprises and raised new and exciting questions for future investigation. For instance, it appears a surprise that flg22 treatment and the induction of the MAPK-cascade exerted apparently opposing effects on the endocytosis of the dye, FM 4-64. This observation might be related to the apparent contradiction that flg22 treatment has on one hand been shown to induce the endocytosis of FLS2 (Robatzek et al., 2006), but on the other hand is found to reduce the levels of PtdIns(4,5)P₂ required for endocytosis (Ischebeck et al., 2013; Zhao et al., 2010; Hempel et al., 2017).

It will be exciting to see whether future experiments might reveal evidence for localized and potentially contrapuntal modes of controlling endocytosis of certain subgroups of CME cargoes, an explanation currently favoured by our group. Another topic for future investigations will be the analyses of the contribution of individual PI4P 5-kinase isoforms to the trafficking of certain protein cargoes, and of their individual modes of regulation upon external inputs. Such studies might extend also to other enzymes of PI metabolism, such as PI4-kinases, as have been shown to also impact on the control of endocytosis in plants (Preuss et al., 2006; Kang et al., 2011), even with participation of MAPKs (Lin et al., 2019).

At a larger scale, results from this thesis touch on the question how plant signalling pathways (or even eukaryotic signalling pathways) are interconnected to provide an integrated system for the acquisition and "interpretation" of information from the environment, even without a brain.

4 Material and methods

4.1 Chemical compounds and antibiotics

If not stated otherwise, all chemicals were supplied by the companies Carl Roth (Karlsruhe, Germany), Merck (Darmstadt, Germany), Fluka (Steinheim, Germany) or Sigma-Aldrich (Taufkirchen, Germany).

Table 4.1: Chemical compounds and antibiotics.

Compound	Solvent	Stock concentration	Working concentration	Supplier
PhosSTOP, Phosphatase Inhibitor Cocktail	H ₂ O	10 x (according to supplier)	1 x (according to supplier)	Roche Diagnostics GmbH, Mannheim, Germany
Agarose	H ₂ O	No stock	1 % (w/v)	Biozym, Hessisch Oldendorf, Germany
Agar	H ₂ O	No stock	0.8 – 1 % (w/v)	Duchefa Biochemie, Haarlem, The Netherlands
Carbenicilin	H ₂ O	50 mg/ml	50 µg/ml	Duchefa Biochemie, Haarlem, The Netherlands
Flg22	H ₂ O	1 mM	0.1 – 10 µM	IPB Halle (Saale)
Kanamycin	H ₂ O	50 mg/ml	50 µg/ml	Duchefa Biochemie, Haarlem, The Netherlands
Lyso-PC	chloroform	5 mg/ml	5 mg/ml	Avanti Polar Lipids Inc., Alabaster, AL, USA
PtdIns(4,5)P ₂	chloroform	5 mg/ml	0.1 mg/ml	Avanti Polar Lipids Inc., Alabaster, AL, USA
PtdIns4P	chloroform	5 mg/ml	5 mg/ml	Avanti Polar Lipids Inc., Alabaster, AL, USA
γ-[³² P]-ATP	Aqueous buffer (supplier)		10 µCi/reaction	Hartmann Analytics, Braunschweig, German
Dexamethasone	DMSO	100 mM	1 µM/20 µM	Sigma-Aldrich, Taufkirchen, Germany

4.2 Enzymes and molecular size markers

All enzymes and molecular size markers were used according to manufacturer's instructions and are listed in **table 4.2**.

Table 4.2: Enzymes and molecular size markers.

Item	Supplier
Restriction endonucleases	NEB, Frankfurt, Germany
Gateway™ BP Clonase™ II enzyme mix	Thermo Fisher Scientific, Dreieich, Germany
Gateway™ LR Clonase™ II enzyme mix	Thermo Fisher Scientific, Dreieich, Germany
T4 DNA ligase	NEB, Frankfurt, Germany
Phusion High Fidelity DNA-Polymerase	NEB, Frankfurt, Germany
Prestained Protein Molecular Weight Marker (PAGERULER™)	Thermo Fisher Scientific, Dreieich, Germany
Cellulose R-10	Serva, Heidelberg, Germany
Macerozyme R-10	Serva, Heidelberg, Germany

4.3 Kits and single-use material

Kits were used according to manufacturer's instructions.

Table 4.3 Kits and single-used material.

Kit	Supplier
GeneJET™ Gel Extraction Kit	Thermo Fisher Scientific, Dreieich, Germany
GeneJET™ Plasmid Miniprep Kit	Thermo Fisher Scientific, Dreieich, Germany
Plasmid Midi Kit	Qiagen, Hilden, Germany
Nylon mesh filters (pore size 20 µm or 100 µm)	Carl Roth, Karlsruhe, Germany

4.4 Equipment

Equipment was used according to manufacturer's instructions. Safety advisory was obeyed at all time.

Table 4.4: Equipment.

Equipment	Supplier
Fujifilm BAS-1500 phosphorimager	Fujifilm, Düsseldorf, Germany
Confocal Laser Scanning Microscope LSM 780	Carl Zeiss, Jena, Germany
Microcentrifuge 5424	Eppendorf, Hamburg, Germany
Cooling microcentrifuge 5424 R	Eppendorf, Hamburg, Germany
Cooling microcentrifuge 5810 R	Eppendorf, Hamburg, Germany
Thermomix comfort	Eppendorf, Hamburg, Germany
pH meter 691	Metrohm, Herisau, Swiss
Photometer Ultrospec 2100 pro	Thermo Fisher Scientific, Dreieich, Germany
Real time PCR cycler Rotor-Gene Q	Qiagen, Hilden, Germany
PCR cycler Biometra Tadvanced	AnalytikJena, Jena, Germany

4.5 Software and online tools

Different offline and online programs were used for data analyses, figure configuration and image analyses, quantification and processing.

Table 4.5: Software and online tool.

Program or online tool	features
Fiji (ImageJ 2)	Image processing and analyses
Coral Draw X5	Figure processing, Graphics
TINA (Raytest, Straubenhardt, Germany)	Phospho image quantification
Arabidopsis eFP-browser http://bar.utoronto.ca/ (Winter et al., 2007)	Visualization tool for Arabidopsis gene expression data

4.6 Antibodies

Primary and secondary antibodies were used for immunodetection and immunoprecipitation of epitope-tagged proteins ectopically expressed in Arabidopsis mesophyll and root protoplasts.

Table 4.6: Primary and secondary antibodies.

Antibody	Dilution	Host organism	Supplier
Anti-HA, 16B12	1:1000	Mouse	Biologend, San Diego, CA, USA
Anti-myc, C3956	1:1000	Rabbit	Sigma-Aldrich, Taufkirchen, Germany
Anti-GFP, A11122	1:1000	Rabbit	Thermo Fisher Scientific, Dreieich, Germany
Anti-mCherry, ab16745	1:2000	Rabbit	Abcam, Cambridge, United Kingdom
Anti-IgG mouse, A4416	1:10000	Goat	Sigma-Aldrich, Taufkirchen, Germany
Anti-IgG rabbit, MAP201P	1:10000	Mouse	Merk Millipore, Darmstadt, Germany

4.7 Microorganisms

Table 4.7: Microorganisms

Organism, Strain	Purpose	Supplier
<i>E.coli</i> , NEB5 α	Cloning and plasmid generation	New England Biolabs, Frankfurt, Germany
<i>E. coli</i> , DB3.1	Proliferation of Gateway TM -plasmids	Thermo Fisher Scientific, Dreieich, Germany
<i>Pseudomonas syringae</i> pv. tomato DC3000	Infection of Arabidopsis leaf tissue (virulent strain)	Dr. Justin Lee, IPB Halle(Saale)
<i>Pseudomonas syringae</i> pv. tomato DC3000 <i>hrpA</i>	Infection of Arabidopsis leaf tissue (non-virulent strain, Wei et al., 2000)	Dr. Justin Lee IPB Halle(Saale)

4.8 Plant material

All transgenic *Arabidopsis* lines generated from Columbia-0 (Col-0) background.

Table 4.8: *Arabidopsis* lines used in this thesis.

Plant line	Features	Source
MKK5 DD	Dexamethasone-induced GVG-mediated expression of PcMKK5 DD (Aoyama and Chua, 1997, Lee et al., 2004, Lassowskat et al., 2014)	Dr. Justin Lee, IPB Halle (Saale)
MKK5 KR	Dexamethasone-induced GVG-mediated expression of PcMKK5 KR (Aoyama and Chua, 1997, Lee et al., 2004, Lassowskat et al., 2014)	Dr. Justin Lee, IPB Halle (Saale)
pPIP5K6-GUS	Glucuronidase (GUSPlus) expression controlled by a 1500 bp native <i>pPIP5K6</i> promotor	Dr. Irene Stenzel, Department of cellular Biochemistry, MLU Halle (Saale)
PIN2-EGFP	Expression of PIN2-EGFP controlled by a 1500 bp native <i>pPIN2</i> promotor (Ischebeck et al., 2013)	Prof. Dr. Ingo Heilmann, Department of Cellular Biochemistry, MLU Halle (Saale)
P24Y	<i>pUBC10</i> -driven expression of mCITRINE _{2xPH(mPLCδ1)} (Simon et al., 2014)	Nottingham Arabidopsis Stock Centre (NASC)
PIN2-EGFPxMKK5 DD	<i>pPIN2</i> -driven expression of PIN2-EGFP in the MKK5 DD background (Ischebeck et al., 2013, Lassowskat et al., 2014)	Generated in this thesis
<i>mpk6</i>	T-DNA insertion line (Alonso, J.M. et al. 2003), complete knock out of At2g43790	Dr. Justin Lee, IPB Halle (Saale)

4.9 cDNA manipulation and molecular biology techniques

4.9.1 RNA isolation from plant material

Total RNA was isolated from 100-200 mg *Arabidopsis* Col-0 leaf material was grinded to a fine powder using a mortar and a pestle under constant cool with N₂. The frozen powder was transferred into 1.5 ml reaction tube and was mixed with 1 ml TRIZOL (38 % (v/v) phenol, saturated with 0.1 M Citrat-Puffer pH 4,3 (Sigma-Aldrich), 0.8 M guanidinium thiocyanate, 0.4 M Ammonium thiocyanate, 133.6 mM sodium acetate pH 5.0, 5 % (v/v) glycerol). Samples were allowed to slowly thaw on ice before cell

debris were pelleted by centrifugation at 20000 x g and 4 °C for 10 min. Supernatant was transferred into a fresh reaction tube and thoroughly mixed with 200 µl chloroform. After incubating samples for 3 min at RT, phase separation was induced by centrifugation at 20000 x g and 4 °C for 15 min. The upper aqueous phase was transferred into a fresh reaction tube and mixed successively with 0.5 volumes of propane-2-ol and 0.5 volumes high salt precipitation buffer (0.8 M sodium citrate, 1.2 M NaCl). Samples were allowed to rest for 10 min at RT before centrifugation at 20000 x g and 4 °C for 10 min. The supernatant was discarded and RNA pellets were washed twice with 75 % (v/v) ethanol. The dried RNA was resuspended in sterile ddH₂O. RNA quality was verified by agarose gel electrophoresis.

4.9.2 cDNA synthesis from Arabidopsis total RNA preparation

For cDNA synthesis, total RNA preparations were normalized to the lowest concentration. The reaction was performed using RevertAid H Minus First Strand cDNA Synthesis Kit (Thermo Fisher Scientific) according manufacturer's instructions.

4.9.3 cDNA amplification by polymerase-chain reaction (PCR)

Amplification of cDNAs was performed by PCR using gene-specific primers. All reactions were performed using the Phusion[®] High Fidelity Polymerase (NEB) according to manufacturer's instructions. All cDNAs were amplified with the following temperature gradient used for standard PCR, except for cDNAs harbouring Gateway[™]-compatible attachment sites, which were amplified using a 2-step PCR protocol. Primer that were used in this thesis are listed in **table 8.3**.

Standard PCR

- | | |
|-------------------------|--------------------|
| 1. Initial denaturation | 98 ° C for 5 min |
| 40 x step 2.-4. | |
| 2. Denaturation | 98 °C for 30 s |
| 3. Annealing | 58 °C for 30 s |
| 4. Elongation | 72 °C for 1 min/kb |
| 5. Final elongation | 72 °C for 10 min |

2-step PCR

- | | |
|-------------------------|------------------|
| 1. Initial denaturation | 98 ° C for 5 min |
|-------------------------|------------------|
- 10 x step 2.-4.
- | | |
|-----------------|---------------------|
| 2. Denaturation | 98 ° C for 30 s |
| 3. Annealing | 58 ° C for 30 s |
| 4. Elongation | 72 ° C for 1 min/kb |
- 30 x step 5.-7.
- | | |
|---------------------|---------------------|
| 5. Denaturation | 98 ° C for 30 s |
| 6. Annealing | 62 ° C for 30 s |
| 7. Elongation | 72 ° C for 1 min/kb |
| 8. Final elongation | 72 ° C for 10 min |

4.9.4 Analysing transcript levels by quantitative real time PCR (qPCR)

Transcript levels were analysed from different Arabidopsis Col-0 plant tissues at indicated time points using quantitative qPCR. Approximately 100 ng of cDNA (see **4.9.2**) and 1 μ M primer were mixed with 1x Maxima SYBR Green qPCR Master Mix (Thermo Fisher Scientific) according to manufacturer's instructions. Primer used for qPCR are listed in **table 8.3**. The reaction was performed using a qPCR-Thermocycler Rotor-Gene Q (Qiagen) with the following temperature gradient.

RT-PCR

- | | |
|-------------------------|-------------------|
| 1. Initial denaturation | 95 ° C for 10 min |
|-------------------------|-------------------|
- 40x step 2.-4.
- | | |
|-----------------|-----------------|
| 2. Denaturation | 95 ° C for 10 s |
| 3. Annealing | 60 ° C for 15 s |
| 4. Elongation | 72 ° C for 20 s |

As reference genes, UBC10, EUKARYOTIC TRANSLATION INITIATION FACTOR 4 A1 (EIF4A1) or Actin were used. qPCR data were analysed using LinRegPCR (Ramakers et al., 2003).

4.9.5 Analytical and preparative electrophoretic separation of cDNA

RNA and DNA samples were analysed or purified using Agarose gel electrophoretic separation. Samples were loaded into agarose gel (1 % (w/v) agarose, 40 mM Tris/HCl pH 7.6, 20 mM acetate, 1 mM EDTA) and subjected to horizontal electrophoresis in TAE-buffer (40 mM Tris/HCl pH 7.6, 20 mM acetate, 1 mM EDTA) under constant voltage at 130 V. For visualization of separated nucleic acids, agarose gels

were soaked in ethidium bromide solution and detection was performed using Gel iX Imager 20 (INTAS Science Imaging) and a 12-bit CCD camera. For preparation of separated DNA, the respective band was cut from agarose gel and DNA was reobtained from agarose using GeneJET Gel Extraction Kit (K0692, Thermo Fisher Scientific).

4.9.6 Measuring the concentration of nucleic acid solutions

For determination of the DNA or RNA concentration in an aqueous solution, the absorption at a wavelength of 260 nm (A_{260}) was measured using an Ultrospec 3000 UV/Vis photometer (Amersham Pharmacia Biotech).

4.9.7 Assembly of DNA constructs

T4 DNA Ligase-mediated assembly

PCR amplified cDNA fragments and plasmid vectors were restricted using the indicated restriction enzymes according to the manufacturer's protocol. Restricted cDNA fragments were introduced into the plasmid vector using the T4 DNA ligase (NEB) according to manufacturer's instructions.

Gateway cloning

The technique of Gateway™ cloning enables introduction of cDNAs by site-specific recombination. PCR amplified cDNA fragments harbouring the attachment sites attB1 and attB2 at 5'-end and 3'-end, respectively, were introduced into Gateway™-compatible plasmid vectors according to the manufacturer's protocol for BP Clonase II®- or LR Clonase II®-mediated ligation to obtain an entry clone or expression clone, respectively.

4.9.8 DNA sequencing

Generated cDNA constructs were verified for correct sequences using the sequencing service of Eurofins Genomics. Gateway-compatible plasmid constructs were sequenced using M13.for and M13.rev primer. Primer used for sequencing are listed in **table 8.3**.

4.9.9 Preparation of competent *E. coli* cells

Competent *E. coli* cells were prepared using a modified protocol from Inoue et al. (1990). Antibiotic-free liquid lysogeny broth (LB) medium (1 % (w/v) peptone, 0.5 % (w/v) yeast extract, 1 % (w/v) NaCl) was inoculated with a single colony of *E. coli* NEB5α or DB3.1. The preculture was grown overnight at

37°C under continuous shaking. For the main culture, 500 ml LB-medium was inoculated with preculture cells at OD₆₀₀ 0.05 and allowed to grow to OD₆₀₀ 0.6-0.8 at 30 °C under continuous shaking. The culture was prechilled on ice for 10 min before cells were sedimented by centrifugation at 1000 x g and 4 °C for 10 min. Cell pellets were resuspended in cold TFB-buffer (10 mM PIPES pH 6.7, 250 mM KCl, 55 mM MnCl₂, 15 mM CaCl₂) and were allowed to rest on ice for 10 min. Washed cells were sedimented by centrifugation at 100 x g and 4°C for 10 min and supernatant was discarded. The pellet was resuspended in TFB-buffer containing 7 % DMSO before resting on ice for 10 min. Aliquots were snap frozen in liquid N₂ and stored at -80 °C.

4.9.10 Transformation of competent *E. coli* with plasmid DNA

For transformation of plasmid DNA into *E. coli*, competent DH5α cells were used. Competent cells were slowly thawed on ice. Cells were mixed with an appropriate amount of plasmid DNA and rested on ice for 30 min. After heat shock treatment at 42 °C for 90 s, cells were immediately transferred to ice and rested for 2 min. Antibiotic-free liquid LB-medium was added and cells were incubated at 37 °C for 2 h before being transferred to solid LB-medium petri dishes containing an appropriate antibiotic to select for positive clones.

4.9.11 Plasmid DNA extraction from *E. coli* cells

For cloning purpose, plasmid DNA was extracted from transgenic *E. coli* NEB5α or DB3.1 cells according to the GeneJET Plasmid Miniprep Kit (Thermo Fisher Scientific) protocol. Plasmid DNA that was subjected to protoplast transformation was obtained from transgenic *E. coli* NEB5α cells using Plasmid DNA Midi Kit (Qiagen).

4.10 Cloning strategies

Plasmid constructs that were used in this thesis are listed in **table 8.2**. The sequences of all primers that were used for cloning the following constructs are listed in **table 8.3**.

4.10.1 Epitope-tagged protoplast expression and BiFC clones

PIP5K6-HA, *PIP5K6 AA-HA* and *HA^C-YFP-PIP5K6*

PIP5K6 and *PIP5K6 AA* cDNAs were PCR amplified from pENTRY:pLat52::PIP5K6:EYFP and pENTRY:pLat52::PIP5K6 AA:EYFP (Hempel et al 2017) using the primer combination attB1_PIP5K6.for and attB2_PIP5K6.rev to fuse Gateway™-compatible attachment sites attB1 and attB2 sites to the 5'-

and 3'-ends, respectively. The cDNA was introduced into pDONR™221 resulting in the entry clones pDONR™221:PIP5K6 and pDONR™221:PIP5K6 AA, which were used for subcloning into the pUGW14 (Nakagawa *et al.*, 2007) plasmid for *pCaMV35S*-driven expression as a fusion with a triple hemagglutinin (HA) tag. The resulting constructs were pUGW14:PIP5K6 and pUGW14:PIP5K6 AA. All Gateway™ reactions were performed as described previously. Furthermore, pDONR™221:PIP5K6 was used for Gateway™-mediated subcloning of the PIP5K6 cDNA into pUC-SPYCE (Walter *et al.*, 2004) for *pCaMV35S*-driven expression of HA-^CYFP-PIP5K6 fusion protein.

PIP5K2-HA

PIP5K2 cDNA was amplified using the primer combination attB1_PIP5K2.for/attB2_PIP5K2.rev to fuse Gateway™-compatible attachment sites attB1 and attB2 to the 5'- and 3'-ends, respectively. The plasmid construct pEntryA:pCaMV35S::PIP5K2:EYFP was used as a template. PCR amplified cDNA was introduced into pDONR™221 to generate the entry clone pDONR™221:PIP5K2, which was used for subcloning *PIP5K2* cDNA into pUGW14 (Nakagawa *et al.*, 2007) to obtain the expression clone pUGW14:PIP5K2.

RBCL-^NYFP-myc and HA-^CYFP-RBCL

The cDNA of the large subunit of *ribulose (1,5)-bisphosphate carboxylase/oxygenase (RBCL)* was PCR amplified from Arabidopsis cDNA (see 4.9.2). Gateway™-compatible attachment sites attB1 and attB2 were introduced into the sequence by using the primer combinations attB1_RBCL.for/ attB2_RBCL.rev and attB1_RBCL.for /attB2_RBCL(noSTOP).rev for amplification with or without STOP-codon, respectively. *RBCL* cDNAs with or without STOP-codon were introduced into pDONR™221 plasmid by Gateway™-mediated ligation. The resulting constructs pDONR™221:RBCL(+STOP) and pDONR™221:RBCL(-STOP) were used for LR-Clonase II™-mediated subcloning into pE-SPYNE or pUC-SPYCE (Walter *et al.*, 2004) to obtain the constructs pE-SPYNE:RBCL and pUC-SPYCE:RBCL.

MVQ1-myc

MVQ1 cDNA was PCR amplified using the primer combination attB1_MVQ1.for/attB2_MVQ1(+STOP).rev to fuse Gateway™-compatible attachment sites attB1 and attB2 to the 5'- and 3'-ends, respectively. As template, the plasmid construct pUGW14:MVQ1 (Pecher *et al.*, 2014) was used. Agarose gel-purified cDNA was subjected to BP Clonase II™-mediated insertion of the cDNA into pDONR™221 to obtain pDONR™221:MVQ1, which was used for LR Clonase II™-mediated subcloning of the *MVQ1* cDNA into pUGW15 (Nakagawa *et al.*, 2007) plasmid vector resulting in pUGW15:MVQ1 construct.

4.10.2 Plasmid constructs for protoplast expression of fluorescence-tagged PI4P 5-kinases

PIP5K6-mCherry and PIP5K6 AA-mCherry

PIP5K6 or *PIP5K6 AA* cDNA were PCR amplified from pUGW14:*PIP5K6* and pUGW14:*PIP5K6 AA* as templates using the primer combination At*PIP5K6* Ascl.for/At*PIP5K6* XhoI.rev to fuse Ascl and XhoI restriction sites. cDNAs were purified from agarose gel as described before and were restricted according to manufacturer's protocol. T4 DNA ligase-mediated ligation into restricted pEntryD:pCaMV35S::mCherry plasmid vector to obtain pEntryD:pCaMV35S::*PIP5K6*:mCherry and pEntryD:pCaMV35S::*PIP5K6 AA*:mCherry cDNA constructs.

PIP5K2-mCherry and PIP5K2 K470A-mCherry

PIP5K2 and *PIP5K2 K470A* cDNAs were PCR amplified using the primer combination *PIP5K2*.Ascl.for/*PIP5K2*.XhoI.rev and pEntryA:pCaMV35S::*PIP5K2*:EYFP and pEntryA:pCaMV35S::*PIP5K2 K470A* (Dr. Angela Katharina Gerth, Dr. Mareike Heilmann) as templates. Primers provided Ascl and XhoI restriction sites at the 5'- and 3'-end, respectively. Agarose gel-purified cDNAs were restricted according to manufacturer's instructions and were ligated into restricted pEntryD:pCaMV35S::mCherry plasmid to generate pEntryD:pCaMV35S::*PIP5K2*:mCherry pEntryD:pCaMV35S::*PIP5K2 K470A*:mCherry constructs.

PIP5K2 K470A-EYFP

PIP5K2 K470A cDNA was PCR amplified from pEntryD:pCaMV35S::*PIP5K2 K470A*:mCherry with the primer pair *PIP5K2*.Ascl.for/*PIP5K2*.XhoI.rev to fuse Ascl and XhoI restriction sites to 5'- and 3'-end, respectively. Agarose gel-purified and restricted cDNA was ligated into restricted pEntryA:pCaMV35S::EYFP plasmid to obtain pEntryA:pCaMV35S::*PIP5K2 K470A*:EYFP.

4.10.3 Plasmid constructs for protoplast expression of EYFP-tagged RbohD

RBOHD-EYFP

RBOHD cDNA was PCR amplified from total Arabidopsis cDNA (see 4.9.2) using the primer combination *RBOHD*_NdeI.for/*RBOHD*_NotI.rev to fuse NdeI- and NotI-restriction sites to the 5'- and 3'-end, respectively. Amplified *RBOHD* cDNA was purified from agarose gel and restricted according to manufacturer's instructions. T4 DNA ligase-mediated ligation into restricted pEntryA:pCaMV35S::EYFP plasmid vector was performed to obtain pEntryA:pCaMV35S::*RBOHD*:EYFP construct.

4.11 Seed sterilization

Arabidopsis seeds were sterilized using 6 % (v/v) sodium hypochlorite and 0.1 % (v/v) Triton X-100 for 8 min at RT in a 1.5 ml reaction tube. The sterilization solution was discarded and seeds were washed six times with 1 ml sterile double-distilled water (ddH₂O). Sterile seed were taken into 0.1 % agarose and placed at 4 °C overnight for vernalisation.

4.12 Plant growth conditions

Seedlings that were subjected to microscopic analyses were cultivated at long-day conditions (16 h light, 22 °C, 7000 Lux/8 h dark, 18 °C) for the indicated time on ½ MS-medium (Murashige and Skoog, 1969) with 1 % (w/v) sucrose and 0.5 % (w/v) MES (pH 5.7). Plants that were used for the preparation of leaf protoplasts were grown on soil at short day conditions (8 h light, 7000 Lux/16 h dark) for at least six weeks to maximize leaf rosette size. Arabidopsis root culture was used for the preparation of root protoplasts. Sterile vernalisation seeds were transferred into liquid MS-medium with 3 % (w/v) sucrose and 0.5 (w/v) MES (pH 5.7) and were grown for 3 weeks under normal-day conditions (12 h light, 7000 Lux/12 h dark).

4.13 GUS assay

Activities of the *pPIP5K6* promotor-driven expression of the *uidA* gene of *PIP5K6* in transgenic Arabidopsis Col-0 seedlings was analysed by GUS staining. The 1500 bp genomic sequence upstream of the *PIP5K6* coding sequence was cloned in front of the *uidA* gene and introduced into Arabidopsis Col-0 by Agrobacterium-mediated transformation (Dr. Irene Stenzel). 14-day old seedlings were treated as described above and incubated in GUS-staining solution (100 mM NaH₂PO₄ pH 7.0, 10 mM EDTA, 0.5 mM ferricyanide, 0.5 mM ferrocyanide, 0.1 % Triton X-100, 2 mM X-Gluc substrate) overnight at 37 °C. Staining solution was discarded before seedlings were washed with four times with 70 % (v/v) ethanol for 45 min at RT. Stained seedlings were subjected to microscopic analyses using a stereo microscope.

4.14 Protoplast preparation and transformation

Preparation

Mesophyll leaf protoplast preparation and transformation was performed according to Yoo et al. (2007). Well-expanded leaves of not shooting Arabidopsis Col-0 plants were cut into stripes (ca. 0.5 – 1 mm). Leaf stripes were transferred into enzyme solution (0.4 mM mannitol, 20 mM KCl, 10 mM CaCl₂, 20 mM MES pH 5.7, 1.5 % (w/v) cellulose R-10, 0.4 % (w/v) macerozyme R-10, 0.1 % (w/v) BSA) and

were vacuum-infiltrated in a desiccator for 30 min at RT before being incubated for 2.5 h at 20 °C. Protoplasts were released from leaf stripes by gently shaking for 30 min at 20 °C. The cell suspension was filtered through a 100 µm mesh size nylon filter and harvested by centrifugation at 200 x g and 4 °C for 1 min. Supernatant was discarded and cells were resuspended in W5-buffer solution (125 mM CaCl₂, 5 mM KCl, 154 mM NaCl, 2 mM MES pH 5.7). Cells were washed twice with W5-buffer solution for 40 min at 20 °C to remove residual enzyme solution and to allow for regeneration. In-between wash steps, cells sedimented by gravity. After washing, protoplasts were taken into MMg-buffer solution (0.4 mM mannitol, 15 mM MgCl₂, 4 mM MES pH 5.7) and suspension density was adjusted to 2x10⁵ cells/ml. For the preparation of Arabidopsis root protoplasts, the protocol was adjusted to increase the amount of obtained cells. For that purpose, roots were incubated in an enzyme solution for 6 h at RT under constant shaking. Due to their smaller size, root protoplasts were filtered using a 20 µm mesh size nylon filter and required sedimentation by centrifugation to reobtain cells from buffer solutions.

Transformation

For transformation, leaf or root protoplast suspension was mixed with a total amount of 10 µg plasmid DNA per 100 µl cell suspension and rested for 5 min. Reaction was mixed thoroughly with 1.1 volume of 40 % PEG-solution (40 % (w/v) PEG, 0.2 M mannitol, 100 mM CaCl₂) followed by incubation at 20 °C for 15-30 min. Especially for root protoplasts, prolonged incubation times led to improved transformation rate. The reaction was terminated by adding 4.4 volumes of W5-buffer solution and cells were harvested by centrifugation at 200 x g and 4 °C for 1 min. For root protoplasts, 8.8 volumes of W5-buffer solution were added to further decrease viscosity of the suspension. After centrifugation at 200 x g and 4 °C for 8 min, the supernatant was discarded and cells were suspended in 1 volume WI-buffer solution (0.5 mM mannitol, 20 mM KCl, 4 mM MES pH 5.7). Transformed cells were stored in the dark at 20 °C overnight.

4.15 Treatment of Arabidopsis seedlings and protoplasts

Both, Arabidopsis seedlings and protoplasts, were subjected to a variety of treatments including histochemical staining, pharmacological and elicitor treatment.

4.15.1 FM4-64 staining of Arabidopsis seedlings

Arabidopsis seedlings were grown from sterile seeds in liquid ½MS-medium for 5 days. Seedlings were transferred to liquid ½MS-medium containing 2 µM FM4-64 and were stained for 10 min before washing once with ½MS-medium without FM4-64 for 5 min.

4.15.2 Pharmacological treatment

To assess overall endocytotic rate in Arabidopsis, FM4-64-stained 5-day old seedlings were transferred into liquid ½MS-medium containing 50 µM BFA 30 min before microscopic imaging. To examine endocytotic rate of EGFP-tagged PIN2, Arabidopsis seedling root tips were incubated in liquid ½MS-medium containing 25 µM BFA and 10 µM CHX for 1 h prior microscopic imaging. The endocytotic rate of EYFP-tagged RbohD in transgenic Arabidopsis root protoplasts was analysed after treatment with 25 µM BFA and 10 µM CHX in WI-buffer for 1 h.

4.15.3 Elicitor treatment

For elicitor treatment, Arabidopsis seedlings were transferred to liquid ½MS-medium containing flg22 at a concentration of 1-10 µM for either 1 h or overnight. Arabidopsis protoplasts derived from leaf or root tissue were treated with flg22, added to the sample at a final concentration of 0.1-1 µM for the indicated time. The exact concentrations and incubation times are indicated at the respective experiment. Liquid ½MS-medium or ddH₂O without flg22 was applied as control.

4.15.4 Chemical induction of MKK5 KR and MKK5 DD expression

Stable transgenic Arabidopsis lines for dexamethasone induced expression of a catalytically dead variant, MKK5 KR, and a constitutively active variant, MKK5 DD, were provided by Dr. Justin Lee (IPB, Halle (Saale)). Expression is controlled by a dexamethasone-activated trans-acting chimeric transcription factor, GVG, composed of the DNA-binding domain of yeast transcription factor GAL4, the transactivating domain of the herpes viral protein 16 (VP16) and the receptor domain of the rat glucocorticoid receptor (GR) (Aoyama and Chua, 1997). Expression of MKK5 DD or MKK5 KR in stable transgenic Arabidopsis seedlings was induced by treatment with 10 µM dexamethasone for either 4 h or maximum 12 hours (Lassowskat et al., 2014). Due to the lack of a PIN2-EGFP Arabidopsis line in the MKK5 KR background, seedlings of PIN2-EGFPxMKK5 DD Arabidopsis line were treated with DMSO without dexamethasone as a control.

4.16 Bimolecular fluorescence complementation assay (BiFC)

In vivo protein-protein-interaction was tested using BiFC assay (Hu et al., 2002). The cDNAs of the genes to be tested for *in vivo* protein-protein-interaction were clone into BiFC-plasmids (see 4.10.1). Transgenic protoplasts coexpressing candidate genes fused to N-terminal ^CYFP or C-terminal ^NYFP respectively were subjected to microscopic investigations.

4.17 Microscopy and image analysis

Confocal laser scanning microscopy (cLSM)

Live cell imaging of transgenic Arabidopsis Col-0 seedlings or transgenic protoplasts was performed using a LSM 880 and AxioObserver (Carl Zeiss, Jena, Germany) with an immersion oil-assisted 63x objective. All fluorophores were excited and detected according to their specific wavelength (**table 8.4**). If more than one fluorophore were used in the same experiment, the detector was adjusted to detect signals separately. Overexposition was avoided using a digital saturation indicator to adjust detector gain. EGFP and EYFP and YFP fluorophore signals were collected using a 488/514 nm dual band multi pass filter. Signal from mCherry fluorescence tag or FM4-64 membrane dye were collected using a 561 nm single pass filter. For investigations on the plasma membrane-affinity of the PtdIns(4,5)P₂ reporter mCITRINE_{2xPH(PLCδ1)} and quantitative analyses of the internalization of FM4-64-stained plasma membrane and PIN2-EGFP the fluorescence signal intensities for cytosol (cyt) and plasma membrane (PM) were measured separately to calculate the cyt/PM-ratio (**figure 4.1 A**). For investigations on the endocytotic rate of RbohD-EYFP in Arabidopsis root protoplasts, z stacks of 20 single planes per cell were combined to a z projection image before quantification. The signal intensities of endosomal bodies (EB) and plasma membrane (PM) were quantified and EB/PM-ratio (**figure 4.1 B**) was calculated and blotted to the respective diagram.

Spinning-disc (SD) microscopy

Plasma membrane distribution of mCITRINE_{2xPH(PLCδ1)} in transgenic Arabidopsis Co-0 seedlings was analysed using Zeiss Cell observer microscope (Carl Zeiss, Jena, Germany) with a Yokogawa CSU-X1 spinning disc head and an immersion oil-assisted 100x objective. Images were acquired using a Photometrics Evolve 512 Delta EM-CCD camera. The mCITRINE fluorophore was excited at 488 nm and a DBP 527/54+645/60 band pass filter (Chroma Technology) was used.

Stereomicroscopy

For promotor GUS studies, transgenic Arabidopsis Col-0 seedlings were imaged using a Discovery.V8 fluorescence Stereo Microscope (Carl Zeiss Jena, Germany) equipped with an AxioCam Color (Carl Zeiss, Germany).

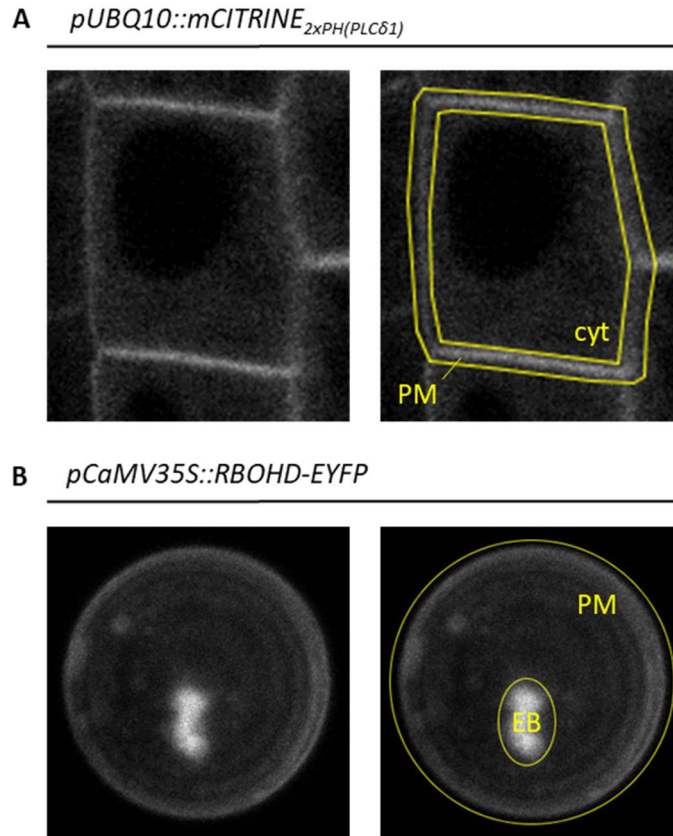


Figure 4.1: Analyses and quantification of the subcellular distribution or endocytotic rate of different fluorescence markers.

A) The subcellular distribution of the $\text{PtdIns}(4,5)\text{P}_2$ reporter $m\text{CITRINE}_{2x\text{PH}(\text{PLC}\delta 1)}$ or the endocytotic rate of FM4-64-stained plasma membrane and EGFP-tagged PIN2 were analysed by measuring fluorescence intensities of the plasma membrane (PM) and the cytosol (cyt) separately. The cyt/PM-ratio was calculated and gives a value for the relative subcellular distribution or relative endocytotic rate. B) The endocytotic rate of RbohD-EYFP was analysed using z projection images from 20-plane z stacks. Fluorescence intensities from plasma membrane (PM) and endosomal bodies (EB) was measured separately to calculate the EB/PM-ratio as the endocytotic rate.

4.18 Electrophoretic separation of ectopically expressed proteins

Proteins that were ectopically expressed in transgenic Arabidopsis protoplasts were analysed by sodium dodecyl sulfate polyacrylamide gel electrophoresis (SDS-PAGE). Acrylamide gels were composed of a 10 % resolving gel (10 % (v/v) acrylamide/bisacrylamide (37.5:1), 0.39 M Tris/HCl pH 8.8, 0.1 % (w/v) SDS, 0.1 % (w/v) APS, 0.0075 % (v/v) TEMED) and a 5 % stacking gel (5 % (v/v) acrylamide/bisacrylamide (37.5:1), 0.126 M Tris/HCl pH 6.8, 0.1 % (w/v) SDS, 0.01 % (w/v) APS, 0.1 % (v/v) TEMED). Protoplast samples were lysed in SDS sample buffer 50 mM Tris-HCl, pH 6.8, 2 % (w/v) SDS, 6 % (v/v) glycerol, 0.001 % (w/v) bromophenol blue, 1 % (v/v) mercaptoethanol at 95 °C for 10 min and loaded onto the gel. Electrophoresis was performed in TGS-buffer (25 mM Tris/HCl, 19.2 mM glycine, 0.1 % (w/v) SDS) at constant 25 mA until prestained marker was completely separated. Gels were further subjected to Western blotting.

4.19 Analysing protein phosphorylation by gel shift assay

Phosphorylation status of ectopically expressed proteins from transgenic *Arabidopsis* mesophyll protoplasts was analysed using a 6 % acrylamide resolving gel (6 % (v/v) acrylamide/bisacrylamide (37.5:1), 0.39 M Tris/HCl pH 8.8, 0.1 % (w/v) SDS, 0.1 % (w/v) APS, 0.0075 % (v/v) TEMED) and a 5 % stacking gel (5 % (v/v) acrylamide/bisacrylamide (37.5:1), 0.126 M Tris/HCl pH 6.8, 0.1 % (w/v) SDS, 0.01 % (w/v) APS, 0.1 % (v/v) TEMED) that contained 50 mM of Phos-tag Acrylamide AAL-107 (WAKO Pure Chemical Ind.) and 50 mM of MnCl₂. The stacking gel was equal to standard SDS-PAGE. Protoplast samples were lysed in sample buffer by shaking at 1400 rpm for 10 min and were loaded to Phos-tag acrylamide gel. Electrophoresis was performed in TGS-buffer at 6 mA and 8 °C for approximately 5 h depending on protein size. After separation, the gel was washed three times in blotting buffer (25 mM Tris/HCl, 19.2 mM glycine, 20 % (v/v) methanol) containing 10 mM EDTA for 30 min constant shaking. Residual EDTA was removed from the gel by washing once with blotting buffer containing no EDTA for 30 min under constant shaking to avoid interference with Western blotting (see 4.18).

4.20 Immunodetection of epitope-tagged proteins

For immunodetection, proteins were transferred from polyacrylamide gels onto a 0.45 µm nitrocellulose membrane using a tank blot apparatus. Blotting sandwich was prepared according to manufacturer's instructions. Blotting was performed in blotting buffer at constant voltage of 90 V for 1.5 h or at 20 V overnight. Blotting procedure was adjusted, when Phos-tag PAGE was used. To compensate poor blotting efficiency, voltage was increased to 100 V for 2 h at 8 °C. After blotting, membranes were washed in TBST-buffer (50 mM Tris/HCl pH 7.6, 150 mM NaCl, 0.5 % Tween) and were subjected to saturation of unspecific binding sites on the membrane by incubating in TBST-buffer containing 5 % (w/v) non fat dry milk for 1 h under constant shaking. Antibodies for immunodetection were always diluted in TBST-buffer containing 3 % (w/v) non-fat dry milk. Dilution of antibodies are indicated in **table 8.4**. Saturated membranes were incubated with the primary antibody for 1 h under constant shaking. After washing the membrane thrice with TBST-buffer for 10 min under constant shaking, the corresponding secondary antibody was applied for 1 h under constant shaking. Secondary antibodies used in this thesis were always horseradish peroxidase (HRP) conjugates, enabling for luminol-based detection. Membranes were coated with luminol substrate solution and chemiluminescent signals were detected using a Fusion Solo S chemiluminescence imaging system (VWR) featuring a 16-bit CCD camera. Exposure times were adjusted for every experiment to avoid overexposure. Loading amounts were estimated by staining with 4-amino-5-hydroxy-3-((E)-(4-nitrophenyl) diazenyl)-6-((E)-phenyldiazenyl) naphthalene-2,7-disulfonate (amido black). After immunodetection, membranes were washed with TBST-buffer once before incubation in amido black

staining solution (0.5 % (w/v) amido black, 25 % (v/v) isopropanol, 10 % (v/v) acetic acid). For images in this thesis, the band related to Rubisco large subunit is displayed. Amido black staining was only performed for quantitative assays using mesophyll protoplasts. No amido black staining was performed for gel shift assays due to poor staining efficiency and band resolution and distortion.

4.21 Immunoprecipitation of epitope-tagged proteins from transgenic protoplasts

Preparation of anti-HA protein G sepharose® immune complex (anti-HA protein G beads)

Protein G sepharose® beads (Sigma-Aldrich) were washed three times with sterile ddH₂O for 10 min under constant shaking. Washed protein G beads were dried on a 0.2 µm cellulose acetate filter using a desiccator to remove residual ethanol. Dry protein G beads were scraped into a reaction tube and 2 volumes of buffer A (50 mM Tris/HCl pH 7.6, 250 mM NaCl, 5 mM EDTA, 5 mM EGTA, 5 mM NaF, 0.1 % (v/v) Tween20) were added. Immune complex assembly was performed by adding 20 µl anti-HA antibody (Biolegend) to 500 µl protein G bead suspension followed by incubation for 2 h at 8 °C under constant mixing. The immune complex was washed thrice with buffer A and was stored in 2 volumes of buffer A at 8 °C.

Protein binding to anti-HA protein G bead immune complex

Transgenic protoplasts expressing either PIP5K6-HA or PIP5K6 AA-HA fusions were harvested by pulse centrifugation for 6 s. Supernatant was discarded and cells were snap frozen in liquid N₂. Frozen cell pellets were resuspended in kinase extraction buffer (25 mM Tris/HCl pH 7.5, 75 mM NaCl, 15 mM EGTA, 10 mM MgCl₂, 1 mM NaF, 0.5 mM Na₃VO₄, 1 mM DTT, 15 mM glycerophosphate, 1x protease inhibitor cocktail (Sigma-Aldrich), 1 % Triton X-100) and were incubated on ice for 30 min. Cells were lysed by three rounds of snap freezing in liquid N₂ and thawing at 25 °C. Cell debris were pelleted by centrifugation at 20000 x g and 4 °C for 10 min before anti-HA protein G beads were added to the supernatant. Binding was performed at 8 °C overnight under constant mixing. Unbound protein was eliminated by washing the anti-HA protein G beads thrice with buffer B (20 mM Tris/HCl pH 7.6, 100 mM NaCl, 5 mM EDTA, 1 % Triton X-100) for 10 min at 8 °C under constant mixing. In between the washing steps, the anti-HA protein G beads were sedimented by centrifugation at 2000 x g and 4°C for 10 min. Washed anti-HA protein G beads-bound PIP5K6-HA and PIP5K6AA-HA were resuspended in kinase extraction buffer and was snap frozen in liquid N₂ and stored at -80 °C.

4.22 PI4P 5-kinase activity assay

To assess intrinsic PI4P 5-kinase activity upon flg22 perception or expression of a constitutively active MKK5, untransformed or transgenic Arabidopsis Col-0 mesophyll protoplasts were treated as

described above (see **4.15**) and were harvested by pulse centrifugation for 6 s before snap freezing in liquid N₂. Frozen cells were resuspended in kinase extraction buffer (see **4.21**) and incubated on ice for 30 min. Cells were lysed by rapid freeze-thaw cycles (see **4.18**). Cell debris were pelleted by centrifugation at 2000 x g and 4°C for 10 min and supernatant was transferred to a fresh reaction tube. Arabidopsis total protein extract or immunoprecipitation purified PIP5K6-HA and PIP5K6 AA-HA were subjected to PI4P 5-kinase assay. Substrates for the reaction were prepared by incorporating PtdIns4P substrate into Triton X-100 micelles. 100 nmol PtdIns4P solved in chloroform were transferred to a 1.5-ml reaction tube and air dried before adding 5 µl of a 2 % (v/v) Triton X-100. Micelle formation was induced by sonification for 10 min and emulsion was used to complete reaction mix (30 mM Tris/HCl pH 7.6, 37.5 mM MgCl₂, 2.5 mM Na₂MoO₄, 10 µCi γ[³²P]-ATP). For PI4P 5-kinase assays using immunoprecipitated PIP5K6-HA or PIP5K6 AA-HA, 2.5 mM non-radioactive ATP was added to the reaction. Reaction was initiated by thoroughly mixing 30 µl protein sample with 20 µl reaction mix and incubating samples for 2 h at RT under pipette mixing every 10 min. For every experiment a control reaction was performed with recombinantly expressed and purified MBP-PIP5K6 (Dr. Mareike Heilmann). The formed radiolabelled product was used as a positive control and a standard to identify the PtdIns(4,5)P₂ band in sample reactions. Reaction was terminated by adding chloroform/methanol (1:2, v/v) and samples were subjected to acidic phospholipid extraction. To reobtain immunoprecipitated protein the anti-HA protein G beads-bound PIP5K6-HA and PIP5K6 AA-HA were sedimented by gravity, before carefully transferring supernatant into fresh glass tube. To increase lipid product yield, the sediment was reextracted with 1 % (v/v) Triton X-100 in sterile ddH₂O twice. The combined supernatants were used for acidic phospholipid extraction. Protein amounts for each sample were quantified using Western blotting and immunodetection (see **4.20**).

4.23 Lipid analysis

Lipid analysis was performed to assess PtdIns4P and PtdIns(4,5)P₂ levels in Arabidopsis seedlings upon infection or activation of the MAPK module MKK5-MPK3/6.

4.23.1 Acidic phospholipid extraction

100-200 µg of leaf material from Pseudomonas-infected Arabidopsis Col-0 or whole seedlings from Arabidopsis MKK5 DD or MKK5 KR lines were harvested and snap frozen in liquid N₂. Plant material was grind to a fine powder under constant liquid N₂ cooling using mortar and pestle. Grinded material was taken into 4 ml chloroform/methanol (1:2, v/v) and was transferred to a screw-lidded glass tube. Samples were stored at 4 °C overnight for consistent extraction before adding 250 µl 0.5 M EDTA, 500 µl 2.4 M HCl and 1 ml chloroform successively, while mixing samples in between. Samples were

centrifuged at 600 x g and 4 °C for 2 min to initiated phase separation. The lower organic phase was transferred to a clean glass tube before reextracting aqueous phase twice with 1 ml chloroform. Organic phases were combined and washed with 1.5 ml 0.5 M HCl in 50 % methanol. Phase separation was achieved by centrifugation at 600 x g and 4 °C for 1 min. The organic phase was transferred to a fresh glass tube and evaporated under air flow.

4.23.2 Lipid separation by thin-layer chromatography (TLC)

Dried lipids were dissolved in 50 µl chloroform and spotted onto the bottom of a standard silica S60 plate together with authentic lipid standards for Lyso-PC, PtdIns4P and PtdIns(4,5)P₂. TLCs were developed in a 200x200x100 mm vertical glass chamber in development solvent (chloroform/methanol/ammonium hydroxide/H₂O (45:45:4:11, v/v/v/v)) until solvent front was close to the top edge of the plate. Developed plates were dried before severing lipid standard section from the sample section of the plate using a glass cutter. Lipid standards were visualized by submerging dry TLC plates in CuSO₄-solution (10 % (w/v) CuSO₄, 0.8 % (w/v) H₃PO₄). After drying, the plate was cautiously heated to 180 °C on a heating plate until bands were clearly visible.

4.23.3 Isolation and transesterification of separated PIs from silica plates

Isolation and transesterification protocol was modified from Heilmann and Heilmann (2013). Positions of the lipids within every lane were determined using lipid standards before carefully scraping the respective areas and collect lipids containing silica powder in a fresh glass tubes. Lipids were reobtained from silica powder by adding 333 µl toluene/methanol (1:2, v/v) and 5 µg tripentadecanoin (15:0 triacylglycerol) as an internal standard. For GC measurements, lipid-associated fatty acids were transesterified to methanol to form fatty acid (FA) methyl esters (FAMES). Transesterification was initiated by adding 167 µl 0.5 M NaOCH₃. The reaction was mixed thoroughly and was incubated 1 h at RT. To terminate reaction, 0.1 ml 5 M NaCl-solution were added to samples. FAME extraction from the reaction was performed by mixing with 2 ml hexane before centrifugation at 600 x g and 4 °C for 1 min. The hexane phase was transferred into a fresh glass tube for evaporation under constant air flow. FAMES were resuspended in 10 µl acetonitrile and subjected to analytical gas chromatography.

4.23.4 FAME quantification by analytical gas chromatography

FA-derived FAMES were analysed by gas chromatography using a 30 m x 250 µm DB-23 capillary column (Agilent) and an FID-coupled GC-2010 (Shimadzu). 1 µl sample solution was loaded into the gas-chromatograph at an injector temperature of 220 °C. Chromatography was performed using the

following temperature gradient: hold for 1 min at 150 °C, raise temperature at a rate of 8 °C/min to a maximum of 200 °C. FAME species amounts were quantified using the internal tripentadecanoin standard and were normalized to sample fresh weight.

4.24 Statistical evaluation

For all experiments, biological and technical replicates were used for evaluation of the statistical significance of difference using an independent-samples two-tailed student's t-test based on variances that were calculated for every sample set separately. The confidence interval for statistical significant difference was $p = 0.05$. Asterisks or different letters indicate statistical verified differences in the respective images.

5 Summary

Plant cells perceive cues from their environment partially via surface receptors that transduce the exogenous stimuli by triggering a complex network of interconnecting signalling cascades. The integration of signalling pathways in eukaryotic cells is an active and important field of current research. A recent study identified the phosphatidylinositol 4-phosphate 5-kinase (PI4P 5-kinase) PIP5K6 from *Arabidopsis thaliana* (*Arabidopsis*) as a new substrate for the mitogen-activated protein kinase (MAPK) MPK6. It was previously shown that MPK6-mediated phosphorylation of PIP5K6 inhibits PtdIns(4,5)P₂-production by the enzyme *in vitro* and impacts on membrane trafficking and cell expansion in growing pollen tubes. Promotor-GUS analyses and RT-PCR data confirmed expression of PIP5K6 in vegetative tissues at different times of *Arabidopsis* growth, suggesting a role in MAPK-mediated processes outside of pollen tubes. In this thesis, MPK6-mediated regulation of PIP5K6 was investigated upon activation of the cell surface receptor-like kinase (RLK) FLAGELLIN SENSITIVE 2 (FLS2) by treatment with its synthetic ligand, flg22. PIP5K6 protein expressed in *Arabidopsis* mesophyll protoplasts was phosphorylated and inhibited in its activity upon flg22 treatment. This effect could not be detected when the MPK6-target sites T₅₉₀P₅₉₁/ T₅₉₇P₅₉₈ were substituted for A₅₉₀P₅₉₁ and A₅₉₇P₅₉₈, respectively, or when protoplasts from an *Arabidopsis* mpk6 knock out mutant were used. The abundance of PIP5K6 transcript or PIP5K6 protein did not change upon flg22 treatment, suggesting flg22-triggered regulation by inhibition of enzymatic activity of PIP5K6. The inhibitory effect of flg22 or the chemical activation of the MPK6 cascade on intrinsic and PIP5K6-mediated PI4P 5-kinase activity in *Arabidopsis* mesophyll protoplasts correlated with the a decreased plasma membrane association of the fluorescent PtdIns(4,5)P₂ reporter, mCITRINE_{2xPH(PLCδ1)} in hypocotyl cells. Together, these experiments indicate that the flg22-activated MAPK-cascade limited PtdIns(4,5)P₂ production in *Arabidopsis*. Even though no apparent changes in abundance and FA composition of PtdIns4P and PtdIns(4,5)P₂ were detected upon flg22 treatment of intact *Arabidopsis* seedlings, PtdIns(4,5)P₂-dependent downstream processes were substantially altered. Treatment with flg22 or the activation of the MAPK module MKK5-MPK3/6 resulted in reduced clathrin-mediated endocytosis (CME) of a PIN-formed 2 (PIN2)-EGFP marker in *Arabidopsis* root tip cells. Furthermore, the CME of the NADPH-oxidase RESPIRATORY BURST OXIDASE HOMOLOG D (RbohD) was also reduced upon flg22 treatment or induction of the MPK6-cascade in a PIP5K6-dependent fashion. These findings are consistent with previous reports on the effects of reduced PtdIns(4,5)P₂ formation in *Arabidopsis* mutants. Importantly, the reduced recycling of RbohD from the plasma membrane was correlated with increased apoplastic production of reactive oxygen species (ROS). The combined data indicate that the activation of the cell surface receptor FLS2 by treatment with flg22 triggers MPK6-mediated phosphorylation of PIP5K6 that limits a functional PtdIns(4,5)P₂ pool reducing endocytotic recycling of

RbohD from the plasma membrane, possibly to optimize ROS production during PAMP-triggered immunity of Arabidopsis.

6 Zusammenfassung

Pflanzliche Zellen besitzen Oberflächenrezeptoren, die Umweltreize wahrnehmen, in biochemische Signale übersetzen und auf ein Netzwerk aus Signalkaskaden übertragen. Das Zusammenfügen verschiedener Prozesse der Signalverarbeitung zu einem Netzwerk in eukaryotischen Zellen ist ein interessantes Feld der gegenwärtigen Forschung. Im Rahmen einer systematischen Suche nach möglichen Regulatoren einer Phosphatidylinositol 4-phosphat 5-Kinase (PI4P 5-Kinase) PIP5K6 aus *Arabidopsis thaliana* (*Arabidopsis*), wurde eine Mitogen-aktivierte Proteinkinase (MAPK) MPK6 identifiziert. Die MPK6-vermittelte Phosphorylierung und Inhibierung von PIP5K6 reguliert den Membranverkehr in elongierenden *Arabidopsis* Pollenschlauchzellen. Promotor-GUS und qPCR Studien bestätigten die Expression von PIP5K6 in vegetativen Geweben zu unterschiedlichen Zeitpunkten in der Entwicklung von *Arabidopsis*. Das weist auf ein Zusammenspiel beider von MPK6 und PIP5K6 außerhalb des Pollenschlauchsystems hin. In der vorliegenden Arbeit wurde eine mögliche Regulation von PIP5K6 durch MPK6 nach Aktivierung von FLAGELLIN SENSITIVE 2 (FLS2) durch die Erkennung von flg22 und der Einfluss auf Phosphatidylinositol-(4,5)-bisphosphat-abhängige Prozesse untersucht. In transgenen Mesophyll-Protoplasten wurde eine Phosphorylierung und Inhibierung der enzymatischen Aktivität von PIP5K6 nach Behandlung der Zellen mit flg22 gezeigt werden. Dieser Effekt war nichtvorhanden, wenn eine Variante von PIP5K6 exprimiert wurde, in der die MPK6-Phosphorylierungsstellen T₅₉₀P₅₉₁/ T₅₉₇P₅₉₈ zu A₅₉₀P₅₉₁ and A₅₉₇P₅₉₈ verändert wurden. Eine Verringerung der Menge an phosphoryliertem PIP5K6 Protein wurde beobachtet in *mpk6* Knockout Protoplasten. Die Abundanz von *PIP5K6* Transkript und Protein zeigte keine Veränderung nach der Behandlung mit flg22, was auf eine Regulation des Proteins durch Inhibierung der enzymatischen Aktivität hinweist. Eine Inhibierung der intrinsischen oder PIP5K6-vermittelten PI4P 5-Kinase Aktivität in Mesophyll-Protoplasten nach Behandlung mit flg22 oder chemischer Aktivierung von MKK5 korrelierte mit einer Verringerung der Plasmamembran-Affinität eines PtdIns(4,5)P₂ Reporters, mCITRINE_{2xPH(PLCδ1)}. Zusammen genommen zeigen beide Experimente, dass die FLS2-vermittelte Aktivierung einer MAPK-Kaskade die Produktion von PtdIns(4,5)P₂ in *Arabidopsis* beschränkt. Obwohl eine direkte Quantifizierung von Phosphatidylinositol-4-phosphate (PtdIns4P) und PtdIns(4,5)P₂ Gehalten und Fettsäure-Zusammensetzung nach flg22-Behandlung keine Änderungen ergab, konnten Effekte auf PtdIns(4,5)P₂-abhängige Prozesse beobachtet werden. Die Behandlung mit flg22 und die chemisch induzierte Expression von einer konstitutiv aktiven MKK5 Variante (MKK5 DD) führten zu einer Reduktion der Endozytose des Membranfarbstoffes FM4-64 und von PIN-FORMED 2 (PIN2)-EGFP in Wurzelspitzenzellen von *Arabidopsis* Setzlingen. PIP5K6 konnte die Endozytose der NADPH-abhängigen Oxydase RESPIRATORY BURST OXIDASE HOMOLOG D (RbohD) in Wurzelprotoplasten fördern. Eine Inhibierung von PIP5K6 durch das FLS2-assoziierte MAPK-Modul MKK4/5-MPK3/6 führte

zu einer Stabilisierung von RbohD an der Plasmamembran und zu einer Steigerung der apoplastischen Produktion von reaktive Sauerstoffspezies. Zusammengenommen verweisen die Daten in dieser Arbeit auf eine Reduktion eines funktionalen Anteils von $\text{PtdIns}(4,5)\text{P}_2$ durch die MPK6-vermittelte Inhibierung von PIP5K6 nach Erkennung von flg22 durch FLS2.

7 Literature

Abe H, Urao T, Ito T, Seki M, Shinozaki K, Yamaguchi-Shinozaki K. 2003. **Arabidopsis AtMYC2 (bHLH) and AtMYB2 (MYB) function as transcriptional activators in abscisic acid signaling.** Plant Cell 15:63-78.

Alfano JR, and Collmer A. 1997. **The type III (Hrp) secretion pathway of plant pathogenic bacteria: trafficking harpins, Avr proteins, and death.** J Bacteriol 179:5655-5662.

Alonso JM, Stepanova AN, Leisse TJ, Kim CJ, Chen H, Shinn P, Stevenson DK, Zimmerman J, Barajas P, Cheuk R, Gadrinab C, Heller C, Jeske A, Koesema E, Meyers CC, Parker H, Prednis L, Ansari Y, Choy N, Deen H, Geralt M, Hazari N, Hom E, Karnes M, Mulholland C, Ndubaku R, Schmidt I, Guzman P, Aguilar-Henonin L, Schmid M, Weigel D, Carter DE, Marchand T, Risseuw E, Brogden D, Zeko A, Crosby WL, Berry CC, Ecker JR. 2003. **Genome-wide insertional mutagenesis of *Arabidopsis thaliana*.** Science 301:653-657.

Aoyama T, Chua N. 1997. **A glucocorticoid-mediated transcriptional induction system in transgenic plants.** Plant J 11:605-612.

Asai T, Tena G, Plotnikova J, Willmann MR, Chiu W, Gomez-Gomez L, Boller T, Ausubel FM, Sheen J. 2002. **MAP kinase signalling cascade in Arabidopsis innate immunity.** Nature 415:977-983.

Audhya A, Scott D, Emr SD. 2003. **Regulation of PI4,5P₂ synthesis by nuclear–cytoplasmic shuttling of the Mss4 lipid kinase.** EMBO J 22:4223-4236.

Bandmann V and Homann U. 2012. **Clathrin-independent endocytosis contributes to uptake of glucose into BY-2 protoplasts.** Plant J 70:578-584

Bandmann V, Kreft M, Homann U. 2011. **Modes of exocytotic and endocytotic events in tobacco BY-2 protoplasts.** Mol Plant 4:241-251.

Beck M, Zhou J, Faulkner C, MacLean D, Robatzek S. 2012. **Spatio-temporal cellular dynamics of the Arabidopsis flagellin receptor reveal activation status-dependent endosomal sorting.** Plant Cell 24:4205-4219.

Boudsocq M, Willmann MR, McCormack M, Lee H, Shan L, He P, Bush J, Cheng S, Sheen J. 2010. **Differential innate immune signalling via Ca²⁺ sensor protein kinases.** Nature 464:418-423.

Bradley DJ, Kjellbom P, Lamb CJ. 1992. **Elicitor- and wound induced oxidative cross-linking of a proline-rich plant cell wall protein: a novel, rapid defense response.** Cell 70:21-30.

Brand U, Fletcher JC, Hobe M, Meyerowitz EM, Simon R. 2000. **Dependence of stem cell fate in Arabidopsis on a feedback loop regulated by CLV3 activity.** Science 289:617-619.

Chalkley RJ, Bandeira N, Chambers MC, Clauser KR, Cottrell JS, Deutsch EW, Kapp EA, Lam HH, McDonald WH, Neubert TA. 2014. **Proteome informatics research group (iPRG)_2012: a study on detecting modified peptides in a complex mixture.** Mol Cell Proteomics 13:360-371.

Chang L, Karin M. 2001 **Mammalian MAP kinase signalling cascades.** Nature 410:37-40.

Chappie JS and Dyda F. 2013. **Building a fission machine—structural insights into dynamin assembly and activation.** J Cell Sci 126:2773-84.

Chinchilla D, Zipfel C, Robatzek S, Kemmerling B, Nurnberger T, Jones JD, Felix G, Boller T. 2007. **A flagellin-induced complex of the receptor FLS2 and BAK1 initiates plant defence.** Nature 448:497-500.

Colcombet J and Hirt H. 2008. **Arabidopsis MAPKs: a complex signalling network involved in multiple biological processes.** Biochem J 413:217-226.

Cui H, Tsuda K, Parker JE. 2015. **Effector-triggered immunity: from pathogen perception to robust defense.** Annu Rev Plant Biol 66:487-511.

Danquah A, Zélicourt A, Colcombet J, Hirt H. 2015. **The role of ABA and MAPK signaling pathways in plant abiotic stress responses.** Biotechnol Adv 32:40-52.

Denoux C, Galletti R, Mammarella N, Gopalan S, Werck D, De Lorenzo G, Ferrari S, Ausubel FM, Dewdney J. 2008. **Activation of defense response pathways by OGs and flg22 elicitors in Arabidopsis seedlings.** Mol Plant 1:423-445.

DeWald DB, Torabinejad J, Jones CA, Shope JC, Cangelosi AR. 2001. **Rapid accumulation of phosphatidylinositol 4,5-bisphosphate and inositol 1,4,5-trisphosphate correlates with calcium mobilization in salt-stressed Arabidopsis.** Plant Physiol 126:759-769.

Ercetin ME, Ananieva EA, Safaee NM, Torabinejad J, Robinson JY, Gillaspay GE. 2008. **A phosphatidylinositol phosphate-specific myo-inositol polyphosphate 5-phosphatase required for seedling growth.** Plant Mol Biol 67:375-388.

König S, Ischebeck T, Lerche J, Stenzel I, Heilmann I. 2008. **Salt-stress-induced association of phosphatidylinositol 4,5-bisphosphate with clathrin-coated vesicles in plants.** Biochem J 415:387-399.

König S, Mosblech A, Heilmann I. 2007. **Stress-inducible and constitutive phosphoinositide pools have distinctive fatty acid patterns in Arabidopsis thaliana.** FASEB J 21:1958-1967.

Doke N. 1983. **Generation of superoxide anion by potato tuber protoplasts during hypersensitive response to hyphal wall components of Phytophthora infestans and specific inhibition of the reaction with suppressors of hypersensitivity.** Physiol Plant Pathol 23:359-367.

Dubiella U, Seybold H, Durian G, Komander E, Lassig R, Witte CP. 2013. **Calcium-dependent protein kinase/NADPH oxidase activation circuit is required for rapid defense signal propagation.** Proc Natl Acad Sci USA 110:8744-8749.

Feng F, Yang F, Rong W, Wu X, Zhang J, Chen S, He C, Zhou J. 2012. **A Xanthomonas uridine 5'-monophosphate transferase inhibits plant immune kinases.** Nature 485:114-118.

Fritz-Laylin LK, Krishnamurthy N, Tör M, Sjölander KV, Jones JDG. 2005. **Phylogenomic analyses of the receptor-like proteins of rice and Arabidopsis.** Plant Physiol 138:611-623.

Furt F, König S, Bessoule JJ, Sargueil F, Zallot R. 2010. **Polyphosphoinositides are enriched in plant membrane rafts and form microdomains in the plasma membrane.** Plant Physiol 152:2173-2187.

Gadeyne A, Sánchez-Rodríguez C, Vanneste S, Di Rubbo S, Zauber H, Vanneste K, Van Leene J, De Winne N, Eeckhout D, Persiau G, Van De Slijke E, Cannoot B, Vercruyssen L, Mayers JR, Adamowski M, Kania U, Ehrlich M, Schweighofer A, Ketelaar T, Maere S, Bednarek SY, Friml J, Gevaert K, Witters E, Russinova

E, Persson S, De Jaeger G, Van Damme D. 2014. **The TPLATE adaptor complex drives clathrin-mediated endocytosis in plants.** Cell 156:691-704.

Geldner N, Friml J, Stierhof YD, Jürgens G, Palme K. 2001. **Auxin transport inhibitors block PIN1 cycling and vesicle trafficking.** Nature 413:425-428.

Geldner N, Anders N, Wolters H, Keicher J, Kornberger W, Müller P, Delbarre A, Ueda T, Nakano A, Jürgens G. 2003. **The Arabidopsis GNOM ARF-GEF mediates endosomal recycling, auxin transport, and auxin-dependent plant growth.** Cell 112:219-230.

Gendre D, Jonsson K, Boutté Y, Bhalerao RP. 2015. **Journey to the cell surface-the central role of the trans-Golgi network in plants.** Protoplasma 252:385-98.

Gerth K, Lin F, Menzel W, Krishnamoorthy P, Stenzel I, Heilmann M, Heilmann I. 2017. **Guilt by association: a phenotype-based view of the plant phosphoinositide network.** Annu Rev Plant Biol 68:349-374.

Gomez-Gomez L, Felix G, Boller T. 1999. **A single locus determines sensitivity to bacterial flagellin in *Arabidopsis thaliana*.** Plant J 18:277-284.

Gomez-Gomez L and Boller T. 2000. **FLS2: an LRR receptor-like kinase involved in the perception of the bacterial elicitor flagellin in Arabidopsis.** Mol Cell 5: 1003-1011.

Griffiths G and Simon K. 1986. **The trans Golgi network: sorting at the exit site of the Golgi complex.** Science 234:438-443.

Guan Y, Lu J, Xu J, McClure B, Zhang S. 2014. **Two mitogen-activated protein kinases, MPK3 and MPK6, are required for funicular guidance of pollen tubes in Arabidopsis.** Plant Physiol 165:528-533.

Hamilton DA, Roy M, Rueda J, Sindhu RK, Sanford J, Mascarenhas JP. 1992. **Dissection of a pollen-specific promoter from maize by transient transformation assays.** Plant Mol Biol 18:211-218.

Harper JF, Breton G, Harmon A. 2004. **Decoding Ca²⁺ signals through plant protein kinases.** Annu Rev Plant Biol 55:263-288.

Heilmann I. 2016. **Phosphoinositide signaling in plant development.** Development 143:2044-2055.

Heilmann I, Perera IY, Gross W, Boss WF. 1999. **Changes in phosphoinositide metabolism with days in culture affect signal transduction pathways in *Galdieria sulphuraria*.** Plant Physiol 119:1331-1339.

Heilmann I, Perera IY, Gross W, Boss WF. 2001. **Plasma membrane phosphatidylinositol 4,5-bisphosphate levels decrease with time in culture.** Plant Physiol 126:1507-1518.

Heilmann M and Heilmann I. 2013. **Mass measurement of polyphosphoinositides by thin-layer and gas chromatography.** Methods Mol Biol 1009:25-32.

Heilmann M and Heilmann I. 2015. **Plant phosphoinositides - complex networks controlling growth and adaptation.** Biochim Biophys Acta 185:759-769.

Hempel F, Stenzel I, Heilmann M, Krishnamoorthy P, Menzel W, Golbik R, Helm S, Dobritsch D, Baginsky S, Lee J, Hoehenwarter W, Heilmann I. 2017. **MAPKs influence pollen tube growth by controlling the formation of phosphatidylinositol 4,5-bisphosphate in an apical plasma membrane domain.** Plant Cell 29: 3030-3050.

Hettenhausen C, Schuman MC, Wu J. 2014. **MAPK signaling - a key element in plant defense response to insects.** Insect Sci 22:157–164.

Higashiyama T and Yang W. 2017. **Gametophytic pollen tube guidance: attractant peptides, gametic controls, and receptors.** Plant Physiol 173:112-121.

Hao H, Fan L, Chen T, Li R, Li X, He Q, Botella MA, Lin J. 2014. **Clathrin and membrane microdomains cooperatively regulate RbohD dynamics and activity in Arabidopsis.** Plant Cell 26:1729-1745.

Honing S, Ricotta D, Krauss M, Spate K, Spolaore B. 2005. **Phosphatidylinositol-(4,5)-bisphosphate regulates sorting signal recognition by the clathrin-associated adaptor complex AP2.** Mol Cell 18:519-531.

Ichimura K, Casais C, Peck SC, Shinozaki K, Shirasu K. 2006. **MEKK1 is required for MPK4 activation and regulates tissue-specific and temperature-dependent cell death in Arabidopsis.** J Biol Chem 281:36969-36976.

Ischebeck T, Seiler S, Heilmann I. 2010. **At the poles across kingdoms: phosphoinositides and polar tip growth.** *Protoplasma* 240:13-31.

Ischebeck T, Stenzel I, Heilmann I. 2008. **Type B phosphatidylinositol-4-phosphate 5-kinases mediate *Arabidopsis* and *Nicotiana tabacum* pollen tube growth by regulating apical pectin secretion.** *Plant Cell* 20:3312-3330.

Ischebeck T, Stenzel I, Hempel F, Jin X, Mosblech A, Heilmann I. 2011. **Phosphatidylinositol-4,5-bisphosphate influences Nt-Rac5-mediated cell expansion in pollen tubes of *Nicotiana tabacum*.** *Plant J* 65:453-468.

Ischebeck T, Werner S, Krishnamoorthy P, Lerche J, Meijon M. 2013. **Phosphatidylinositol 4,5-bisphosphate influences PIN polarization by controlling clathrin-mediated membrane trafficking in *Arabidopsis*.** *Plant Cell* 25:4894-4911.

Jia, W, Li B, Li S, Liang Y, Wu X, Ma M. 2016. **Mitogen-activated protein kinase cascade MKK7-MPK6 plays important roles in plant development and regulates shoot branching by phosphorylating PIN1 in *Arabidopsis*.** *PLoS Biol* 14:e1002550.

Jones JDG and Dangl JL. 2006. **The plant immune system.** *Nature* 444:323-329.

Joo S, Liu Y, Lueth A, Zhang S. 2008. **MAPK phosphorylation-induced stabilization of ACS6 protein is mediated by the non-catalytic C-terminal domain, which also contains the cis-determinant for rapid degradation by the 26S proteasome pathway.** *Plant J* 54:129-140.

Kadota Y, Sklenar J, Derbyshire P, Stransfeld L, Asai S, Ntoukakis V, Jones JD, Shirasu K, Menke F, Jones A. 2014. **Direct regulation of the NADPH oxidase RBOHD by the PRR-associated kinase BIK1 during plant immunity.** *Mol Cell* 54:43-55.

Kang BH, Nielsen E, Preuss ML, Mastronarde D, Staehelin LA. 2011. **Electron tomography of RabA4 band PI-4K β 1-labeled trans Golgi network compartments in *Arabidopsis*.** *Traffic* 12:313-329.

Hu C, Chinenov Y, Kerppola TK. 2002. **Visualization of interactions among bZIP and Rel family proteins in living cells using bimolecular fluorescence complementation.** *Mol Cell* 9:789-798.

Kinoshita E, Kinoshita-Kikuta E, Takiyama K, Koike T. 2006. **Phosphate-binding tag, a new tool to visualize phosphorylated proteins.** Mol Cell Proteomics 5:749–757.

Konopka CA, Backues SK, Bednarek SY. 2008. **Dynamics of Arabidopsis dynamin-related protein 1C and a clathrin light chain at the plasma membrane.** Plant Cell 20:1363-1380.

Kost B, Lemichez E, Spielhofer P, Hong Y, Tolias K, Carpenter C, Chua N. 1999. **Rac homologues and compartmentalized phosphatidylinositol 4,5-bisphosphate act in a common pathway to regulate polar pollen tube growth.** J Cell Biol 145:317-330.

Koyama T, Mitsuda N, Seki M, Shinozaki K, Ohme-Takagi M. 2010. **TCP transcription factors regulate the activities of ASYMMETRIC LEAVES1 and miR164, as well as the auxin response, during differentiation of leaves in Arabidopsis.** Plant Cell 22:3574-88.

Kusano H, Testerink C, Vermeer JE, Tsuge T, Shimada H, Oka A, Munnik T, Aoyama T. 2008. **The Arabidopsis Phosphatidylinositol Phosphate 5-Kinase PIP5K3 is a key regulator of root hair tip growth.** Plant Cell 20:367-380.

Lam BC, Sage TL, Bianchi F, Blumwald E. 2001. **Role of SH3 domain-containing proteins in clathrin-mediated vesicle trafficking in Arabidopsis.** Plant Cell 13:2499-512.

Lambeth JD. 2004. **NOX enzymes and the biology of reactive oxygen.** Nat Rev Immunol 4:181-189.

Langhans M, Förster S, Helmchen G, Robinson DG. 2011. **Differential effects of the Brefeldin A analogue (6R)-hydroxy-BFA in tobacco and Arabidopsis.** J Exp Bot 62:2949-2957.

Lassowskat I, Bottcher C, Eschen-Lippold L, Scheel D, Lee J. 2014. **Sustained mitogen-activated protein kinase activation reprograms defense metabolism and phosphoprotein profile in Arabidopsis thaliana.** Front Plant Sci 5:554.

Lee J, Rudd JJ, Macioszek VK, Scheel D. 2004. **Dynamic changes in the localization of MAPK cascade components controlling pathogenesis-related (PR) gene expression during innate immunity in parsley.** J Biol Chem 279:22440-22448.

Lemmon MA. 2003. **Phosphoinositide recognition domains**. *Traffic* 4:201-213.

Li J and Chory J. 1997. **A putative leucine-rich repeat receptor kinase involved in brassinosteroid signal transduction**. *Cell* 90:929-938.

Li L, Li M, Yu L, Zhou Z, Liang X, Liu Z. 2014. **The FLS2-associated kinase BIK1 directly phosphorylates the NADPH oxidase RbohD to control plant immunity**. *Cell Host Microbe* 15:329-338.

Li R, Liu P, Wan Y, Chen T, Wang Q, et al. 2012. **A membrane microdomain-associated protein, Arabidopsis Flot1, is involved in a clathrin-independent endocytotic pathway and is required for seedling development**. *Plant Cell* 24:2105-2122.

Lin F, Krishnamoorthy P, Schubert V, Hause G, Heilmann M, Heilmann I. 2019. **A dual role for cell plate-associated PI4K β in endocytosis and phragmoplast dynamics during plant somatic cytokinesis**. *EMBO J* 38:e100303.

Liu Z, Persson S, Sánchez-Rodríguez C. 2015. **At the border: the plasma membrane–cell wall continuum**. *J Exp Bot* 66:1553-1563.

Löfke C, Ischebeck T, König S, Freitag S, Heilmann I. 2008. **Alternative metabolic fates of phosphatidylinositol produced by PI-synthase isoforms in Arabidopsis thaliana**. *Biochem J* 413:115-124.

Lu D, Wu S, Gao X, Zhang Y, Shan L, He P. 2010. **A receptor-like cytoplasmic kinase, BIK1, associates with a flagellin receptor complex to initiate plant innate immunity**. *Proc Natl Acad Sci USA* 107:496-501.

Lu D, Lin W, Gao X, Wu S, Cheng C, Avila J, Heese A, Devarenne TP, He P, Shan L. 2011. **Direct ubiquitination of pattern recognition receptor FLS2 attenuates plant innate immunity**. *Science* 332:1439-1442.

Luna E, Pastor V, Robert J, Flors V, Mauch-Mani B, Ton J. 2011. **Callose deposition: a multifaceted plant defense response**. *Mol. Plant Microbe Interact* 24:183-193.

Ma X, Xu G, He P, Shan L. 2016. **SERKing coreceptors for receptors**. *Trends Plant Sci* 21:1017-1033.

- Macho AP, Boutrot F, Rathjen JP, Zipfel C. 2012. **Aspartate oxidase plays an important role in Arabidopsis stomatal immunity.** *Plant Physiol* 159:1845-1856.
- Mayank P, Grossman J, Wuest S, Boisson-Dernier A, Roschitzki B, Nanni P, Nuhse T, Grossniklaus U. 2012. **Characterization of the phosphoproteome of mature Arabidopsis pollen.** *Plant J* 72:89-101.
- Mbengue M, Bourdais G, Gervasi F, Beck M, Zhou J, Spallek T, Bartels S, Boller T, Ueda T, Kuhn H. 2016. **Clathrin-dependent endocytosis is required for immunity mediated by pattern recognition receptor kinases.** *Proc Natl Acad Sci USA* 113:11034-11039.
- McMahon HT, Boucrot E. 2011. **Molecular mechanism and physiological functions of clathrin-mediated endocytosis.** *Nat Rev Mol Cell Biol* 12:517-533.
- Memon AR and Durakovic C. 2014. **Signal perception and transduction in plants.** *PEN* 2:15-29.
- Meng X and Zhang S. 2013. **MAPK cascades in plant disease resistance signaling.** *Annu Rev Phytopathol* 51:245-266.
- Mersmann S, Bourdais G, Rietz S, Robatzek S. 2010. **Ethylene signaling regulates accumulation of the FLS2 receptor and is required for the oxidative burst contributing to plant immunity.** *Plant Physiol* 154:391-400.
- Meyer D, Pajonk S, Micali C, O'Connell R, Schulze-Lefert P. 2009. **Extracellular transport and integration of plant secretory proteins into pathogen-induced cell wall compartments.** *Plant J* 57:986-999.
- Mueller-Roeber B and Pical C. 2002. **Inositol phospholipid metabolism in Arabidopsis. Characterized and putative isoforms of inositol phospholipid kinase and phosphoinositide-specific phospholipase C.** *Plant Physiol.* 130:22-46.
- Murashige T and Skoog F. 1962. **A revised medium for rapid growth and bio assays with Tobacco tissue cultures.** *Physiol Plant* 15:473-497.

Nakagawa T, Kurose T, Hino T, Tanaka K, Kawamukai M, Niwa Y, Toyooka K, Matsuoka K, Jinbo T, Kimura T. 2007. **Development of series of gateway binary vectors, pGWBs, for realizing efficient construction of fusion genes for plant transformation.** J Biosci Bioeng 104:34-41.

Nuhse TS, Bottrill AR, Jones AM, Peck SC. 2007. **Quantitative phosphor proteomic analyses of plasma membrane proteins reveals regulatory mechanisms of plant innate immune responses.** Plant J 51:931-940.

Ogasawara Y, Kaya H, Hiraoka G, Yumoto F, Kimura S, Kadota Y. 2008. **Synergistic activation of the Arabidopsis NADPH oxidase AtRbohD by Ca²⁺ and phosphorylation.** J Biol Chem 283:8885-8892.

Ogawa M, Shinohara H, Sakagami Y, Matsubayashi Y. 2008. **Arabidopsis CLV3 peptide directly binds CLV1 ectodomain.** Science 319:294.

Olsen JV, Blagoev B, Gnäd F, Macek B, Kumar C, Mortensen P, Mann M. 2006. **Global, *in vivo*, and site-specific phosphorylation dynamics in signalling networks.** Cell 127:635-648.

Onelli E, Prescianotto-Baschong C, Caccianiga M, Moscatelli A. 2008. **Clathrin-dependent and independent endocytic pathways in tobacco protoplasts revealed by labelling with charged nanogold.** J Exp Bot 59:3051-3068.

Park SJ, Itoh T, Takenawa T. 2001. **Phosphatidylinositol 4-phosphate 5-kinase type I is regulated through phosphorylation response by extracellular stimuli.** J Biol Chem 276:4781-4787.

Pecher P, Eschen-Lippold L, Herklotz S, Kuhle K, Naumann K, Bethke G, Uhrig J, Weyhe M, Scheel D, Lee J. 2014. **The Arabidopsis thaliana mitogen activated protein kinases MPK3 and MPK6 target a subclass of 'VQ-motif' containing proteins to regulate immune responses.** New Phytol 203:592-606.

Preuss ML, Schmitz AJ, Thole JM, Bonner HK, Otegui MS, Nielsen E. 2006. **A role for the RabA4b effector protein PI-4Kbeta1 in polarized expansion of root hair cells in Arabidopsis thaliana.** J Cell Biol 172:991-998.

Pribat A, Sormani R, Rousseau-Gueutin M, Julkowska MM, Testerink C, et al. 2012. **A novel class of PTEN protein in Arabidopsis displays unusual phosphoinositide phosphatase activity and efficiently binds phosphatidic acid.** *Biochem J* 441:161-171.

Ramakers C, Ruijter JM, Deprez RH, Moorman AF. 2003. **Assumption-free analysis of quantitative real-time polymerase chain reaction (PCR) data.** *Neurosci Lett* 339:62-66.

Rayapuram N, Bonhomme L, Bigeard J, Haddadou K, Przybylski C, Hirt H, Pflieger D. 2014. **Identification of novel PAMP-triggered phosphorylation and dephosphorylation events in *Arabidopsis thaliana* by quantitative phosphoproteomic analyses.** *J Proteome Res* 13:2137-2151.

Rayapuram N, Bigeard J, Alhoraibi H, Bonhomme L, Hesse A, Vinh J, Hirt H, Pflieger D. 2018. **Quantitative phosphoproteomic analyses reveals shared and specific targets of Arabidopsis mitogen-activated protein kinases (MAPKs) MPK3, MPK4, and MPK6.** *Mol Cell Proteomics* 17:61-80.

Ren D, Yang H, Zhang S. 2002. **Cell death mediated by MAPK is associated with hydrogen peroxide production in Arabidopsis.** *J Biol Chem* 277:559-565.

Robatzek S, Chinchilla D, Boller T. 2006. **Ligand-induced endocytosis of the pattern recognition receptor FLS2 in Arabidopsis.** *Genes Dev* 20:537-542.

Rodriguez MC, Petersen M, Mundy J. 2010. **Mitogen-activated protein kinase signaling in plants.** *Annu Rev Plant Biol* 61:621-649.

Seaman MNJ, McCaffery JM, Emr SD. 1998. **A membrane coat complex essential for endosome-to-Golgi retrograde transport in yeast.** *J Cell Biol* 142:665-681.

Seki, M., Narusaka, M., Ishida, J., Nanjo, T., Fujita, M., Oono, Y., Kamiya, A., Nakajima, M., Enju, A., Sakurai, T., Satou, M., Akiyama, K., Taji, T., Yamaguchi-Shinozaki, K., Carninci, P., Kawai, J., Hayashizaki, Y., Shinozaki, K. 2002. **Monitoring the expression profiles of 7000 Arabidopsis genes under drought, cold and high-salinity stresses using a full-length cDNA microarray.** *Plant J* 31:279-292.

Simon ML, Platre MP, Assil S, van Wijk R, Chen WY. 2014. **A multi-colour/multi-affinity marker set to visualize phosphoinositide dynamics in Arabidopsis.** *Plant J* 77:322-337.

Singh R, Singh S, Parihar P, Mishra RK, Tripathi DK, Singh VP, Chauhan DK, Prasad SM. 2016. **Reactive oxygen species (ROS): Beneficial companions of plants' developmental processes.** *Front Plant Sci* 7: 1299.

Smith JM, Salamango DJ, Leslie ME, Collins CA, Heese A. 2014. **Sensitivity to flg22 is modulated by ligand-induced degradation and *de novo* synthesis of the endogenous flagellin-receptor FLAGELLIN-SENSING2.** *Plant Physiol* 164:440-454.

Sousa E, Kost B, Malho R. 2008. **Arabidopsis phosphatidylinositol-4-monophosphate 5-kinase 4 regulates pollen tube growth and polarity by modulating membrane recycling.** *Plant Cell* 20:3050-3064.

Steinmann T, Geldner N, Grebe M, Mangold S, Jackson CL. 1999. **Coordinated polar localization of auxin efflux carrier PIN1 by GNOM ARF GEF.** *Science* 286:316-318.

Stenzel I, Ischebeck T, König S, Holubowska A, Sporysz M. 2008. **The type B phosphatidylinositol 4-phosphate 5-kinase 3 is essential for root hair formation in *Arabidopsis thaliana*.** *Plant Cell* 20:124-141.

Stenzel I, Ischebeck T, Quint M, Heilmann I. 2012. **Variable regions of PI4P 5-kinases direct PtdIns(4,5)P₂ towards alternative regulatory functions in tobacco pollen tubes.** *Front Plant Sci* 2:1-14.

Suarez-Rodriguez MC, Adams-Phillips L, Liu Y, Wang H, Su SH, Jester PJ, Zhang S, Bent AF, Krysan PJ. 2007. **MEKK1 is required for flg22-induced MPK4 activation in Arabidopsis plants.** *Plant Physiol* 143:661-669.

Takeuchi H and Higashiyama T. 2016. **Tip-localized receptors control pollen tube growth and LURE sensing in Arabidopsis.** *Nature* 531:245-248.

Tebar F, Sorkina T, Sorkin A, Ericsson M, Kirchhausen T. 1996. **Eps15 is a component of clathrin-coated pits and vesicles and is located at the rim of coated pits.** *J Biol Chem* 271:28727-28730.

Teige M, Scheikl E, Eulgem T, Dóczi R, Ichimura K, Shinozaki K, Dangl JL, Hirt H. 2004. **The MKK2 pathway mediates cold and salt stress signaling in Arabidopsis.** *Mol Cell* 15:141-152.

Tejos R, Sauer M, Vanneste S, Palacios-Gomez M, Li H. 2014. **Bipolar plasma membrane distribution of phosphoinositides and their requirement for auxin-mediated cell polarity and patterning in *Arabidopsis***. *Plant Cell* 5:2114-2128.

Thole JM, Vermeer JE, Zhang Y, Gadella TW Jr, Nielsen E. 2008. **ROOT HAIR DEFECTIVE4 encodes a phosphatidylinositol-4-phosphate phosphatase required for proper root hair development in *Arabidopsis thaliana***. *Plant Cell* 20:381-395.

Torres MA, Dangl JL, Jones JD. 2002. ***Arabidopsis* gp91phox homologues AtrbohD and AtrbohF are required for accumulation of reactive oxygen intermediates in the plant defense response**. *Proc Natl Acad Sci USA* 99:517-522.

Traub LM and Bonifacino JS. 2013. **Cargo recognition in clathrin-mediated endocytosis**. *Cold Spring Harb Perspect Biol* 5:a016790.

Vajrala N, Bottomley PJ, Stahl DA, Arp DJ, Sayavedra-Soto LA. 2014. **Cycloheximide prevents the *de novo* polypeptide synthesis required to recover from acetylene inhibition in *Nitrosopumilus maritimus***. *FEMS Microbiol Ecol* 88:495-502.

Valencia JP, Goodman K, Otegui MS. 2016. **Endocytosis and endosomal trafficking in plants**. *Annu Rev Plant Biol* 67:309-335.

Van Leeuwen W, Ökrész L, Bögre L, Munnik T. 2004. **Learning the lipid language of plant signalling**. *Trends Plant Sci* 9:378-384.

Van Leeuwen W, Vermeer JEM, Gadella TW Jr, Munnik T. 2007. **Visualization of phosphatidylinositol 4,5-bisphosphate in the plasma membrane of suspension-cultured tobacco BY-2 cells and whole *Arabidopsis* seedlings**. *Plant J* 52:1014-1026.

Varnai P and Balla T. 1998. **Visualization of phosphoinositides that bind pleckstrin homology domains: calcium- and agonist-induced dynamic changes and relationship to myo-[³H]inositol-labeled phosphoinositide pools**. *J Cell Biol* 143:501-510.

Vermeer JE, Thole JM, Goedhart J, Nielsen E, Munnik T, Gadella TW Jr. 2009. **Imaging phosphatidylinositol 4-phosphate dynamics in living plant cells.** *Plant J* 57:356-372.

Vermeer JE, van Leeuwen W, Tobin-Santamaria R, Laxalt AM, Jones DR, Divecha N, Gadella TW Jr, Munnik T. 2006. **Visualization of PtdIns3P dynamics in living plant cells.** *Plant J* 47:687-700.

Viotti C, Bubeck J, Stierhof Y, Krebs M, Langhans M, van den Berg W, van Dongen W, Richter S, Geldner N, Takano J, Jürgens G, de Vries SC, Robinson DG, Schumacher K. 2010. **Endocytotic and secretory traffic in Arabidopsis merge in the trans-Golgi network/early endosome, an independent and highly dynamic organelle.** *Plant Cell* 22:1344-1357.

Walter M, Chaban C, Schütze K, Batistic O, Weckermann K, Näke C, Blazevic D, Grefen C, Schumacher K, Oecking C, Harter K, Kudla J. 2004. **Visualization of protein interactions in living plant cells using bimolecular fluorescence complementation.** *Plant J* 40:428-438.

Wang C, Yan X, Chen Q, Jiang N, Fu W. 2013. **Clathrin light chains regulate clathrin-mediated trafficking, auxin signaling, and development in Arabidopsis.** *Plant Cell* 25:499-516.

Wei W, Plovianich-Jones A, Deng W, Jin Q, Collmer A, Huang H, He SY. 2000. **The gene coding for the Hrp pilus structural protein is required for type III secretion of Hrp and Avr proteins in *Pseudomonas syringae* pv. Tomato.** *Proc Natl Acad Sci USA* 97:2247-2252.

Welters P, Takegawa K, Emr SD, Chrispeels MJ. 1994. **AtVSP34, a phosphatidylinositol 3-kinase of *Arabidopsis thaliana* is an essential protein with homology to a calcium-dependent lipid binding domain.** *PNAS* 91:11398-11402.

Westergren T, Dove SK, Sommarin M, Pical C. 2001. **AtPIP5K1, an *Arabidopsis thaliana* phosphatidylinositol phosphate kinase, synthesizes PtdIns(3,4)P₂ and PtdIns(4,5)P₂ *in vitro* and is inhibited by phosphorylation.** *Biochem J* 359:583-589.

Williams ME, Torabinejad J, Cohick E, Parker K, Drake EJ. 2005. **Mutations in the Arabidopsis phosphoinositide phosphatase gene SAC9 lead to overaccumulation of PtdIns(4,5)P₂ and constitutive expression of the stress-response pathway.** *Plant Physiol* 138:686-700.

Winter D, Vinegar B, Nahal H, Ammar R, Wilson GV, Provart NJ. 2007. **An “Electronic Fluorescent Pictograph” browser for exploring and analyzing large-scale biological data sets.** PLoS One 2:e718.

Xu J, Xie J, Yan C, Zou X, Ren D, Zhang S. 2014. **A chemical genetic approach demonstrates that MPK3/MPK6 activation and NADPH oxidase-mediated oxidative burst are two independent signaling events in plant immunity.** Plant J 77: 222-234.

Zarsky V, Cvrckova F, Potocky M, Hala M. 2009. **Exocytosis and cell polarity in plants - exocyst and recycling domains.** New Phytol 183:255-272.

Zhang Y, Zhu H, Zhang Q, Li M, Yan M, Wang R, Wang L, Welti R, Zhang W, Wang X. 2009. **Phospholipase α 1 and phosphatidic acid regulate NADPH oxidase activity and production of reactive oxygen species in ABA-mediated stomatal closure in Arabidopsis.** Plant Cell 21:2357-2377.

Zhao Y, Yan A, Feijo JA, Furutani M, Takenawa T, Hwang I, Fu Y, Yang Z. 2010. **Phosphoinositides regulate clathrin-dependent endocytosis at the tip of pollen tubes in Arabidopsis and Tobacco.** Plant Cell 22:4031-4044.

Zhong R, Burk DH, Nairn CJ, Wood-Jones A, Morrison WH III, Ye ZH. 2005. **Mutation of SAC1, an Arabidopsis SAC domain phosphoinositide phosphatase, causes alterations in cell morphogenesis, cell wall synthesis, and actin organization.** Plant Cell 17:1449-1466.

Zhong R and Ye ZH. 2003. **The SAC domain-containing protein gene family in Arabidopsis.** Plant Physiol 132:544-555.

Zipfel C, Robatzek S, Navarro L, Oakeley EJ, Jones JD, Felix G, Boller T. 2004. **Bacterial disease resistance in Arabidopsis through flagellin perception.** Nature 428:764-767.

8 Appendix

8.1 Plasmids, constructs and primer

Table 8.1: Plasmid constructs used in this thesis.

Plasmid	Features	Source
pDONR™221	attP1, attP2; Kan ^R	Dr. Justin Lee, IPB Halle(Saale)
pUGW14	C-terminal 3x HA-tag fusion; attR1, attR2; Amp ^R	Dr. Justin Lee, IPB Halle(Saale)
pUGW18	N-terminal 3x myc-tag fusion; attR1, attR2; Amp ^R	Dr. Justin Lee, IPB Halle(Saale) Nakagawa et al., 2007
pE-SPYNE	C-terminal ^N YFP:3xHA fusion; attR1, attR2; Amp ^R	Dr. Justin Lee, IPB Halle(Saale) Walter et al., 2004
pUC-SPYCE	N-terminal 3xmyc: ^C YFP fusion; attR1, attR2; Amp ^R	Dr. Ju Walter et al., 2004 stin Lee, IPB Halle(Saale)
pEntryD:pCaMV35S::EYFP	C-terminal EYFP fusion; attR1, attR2; Amp ^R	Dr. Mareike Heilmann
pEntryD:pCaMV35S::mCherry	C-terminal mCherry fusion; attR1, attR2; Amp ^R	This thesis

Table 8.2: Plasmid constructs used in this thesis.

Plasmid construct	Promotor	Features	Source
pUGW14:PIP5K6	<i>pCaMV35S</i>	C-terminal 3x HA- tag fusion	This thesis
pUGW14:PIP5K6 AA	<i>pCaMV35S</i>	C-terminal3x HA-tag fusion	This thesis
pUGW14:MVQ1	<i>pCaMV35S</i>	C-terminal 3x HA- tag fusion	Dr. Justin Lee, IPB Halle(Saale)
pUGW18:MVQ1	<i>pCaMV35S</i>	N-terminal 3x myc- tag fusion	This thesis
pE-SPYNE:MPK6	<i>pCaMV35S</i>	C-terminal ^N YFP:3xHA fusion	Dr. Justin Lee, IPB Halle(Saale)
pUC-SPYCE:PIP5K6	<i>pCaMV35S</i>	N-terminal 3xmyc: ^C YFP fusion	This thesis

pE-SPYNE:RbcL	<i>pCaMV35S</i>	C-terminal N ^{YFP} :3xHA fusion	This thesis
pUC-SPYCE:RbcL	<i>pCaMV35S</i>	N-terminal 3xmyc:C ^{YFP} fusion	This thesis
pEntryD:CaMV35S::PIP5K6:EYFP	<i>pCaMV35S</i>	C-terminal EYFP fusion	This thesis
pEntryD:CaMV35S::PIP5K6 AA:EYFP	<i>pCaMV35S</i>	C-terminal EYFP fusion	This thesis
pEntryD:CaMV35S::PIP5K6:mCherry	<i>pCaMV35S</i>	C-terminal mCherry fusion	This thesis
pEntryD:CaMV35S::PIP5K6 AA:mCherry	<i>pCaMV35S</i>	C-terminal mCherry fusion	This thesis
pEntryD:CaMV35S::PIP5K2:mCherry	<i>pCaMV35S</i>	C-terminal mCherry fusion	This thesis
pEntryD:CaMV35S::PIP5K2 K470A:mCherry	<i>pCaMV35S</i>	C-terminal mCherry fusion	This thesis
pEntryA:CaMV35S::PIP5K2:EYFP	<i>pCaMV35S</i>	C-terminal mCherry fusion	Dr. Angela Katharina Gerth
pEntryA:CaMV35S::PIP5K2 K470A:EYFP	<i>pCaMV35S</i>	C-terminal mCherry fusion	This thesis
pUGW14:PIN2:EGFP	<i>pCaMV35S</i>	C-terminal 3x HA- tag fusion	This thesis
pEntryD:pCaMV35S::RbohD:EYFP	<i>pCaMV35S</i>	C-terminal EYFP fusion	This thesis

Table 8.3: Oligonucleotides used in this thesis.

Primer	Sequence 5' → 3'	Gene
PIP5K6_attB1.for	GGGGACAAGTTTGTACAAAAAAGC AGGCTTCATGTCGGTAGCACACGCA	<i>PIP5K6</i> , At3g07960
PIP5K6_attB2.rev	GGGGACCACTTTGTACAAGAAAGC TGGGTTAGCGTCTTCAACGAAGAC	<i>PIP5K6</i> , At3g07960
PIP5K6_attB2_noSTOP.rev	GGGGACCACTTTGTACAAGAAAGGT GGGTACTCTTGCCATCTAATTT	<i>PIP5K6</i> , At3g07960
PIP5K6_AscI.for	ATGCGGCGCGCCATGTCGGTAGCACACGCAGA	<i>PIP5K6</i> , At3g07960
PIP5K6_XhoI.rev	ATGCCTCGAGAGCGTCTTCAACGAAGACCC	<i>PIP5K6</i> , At3g07960

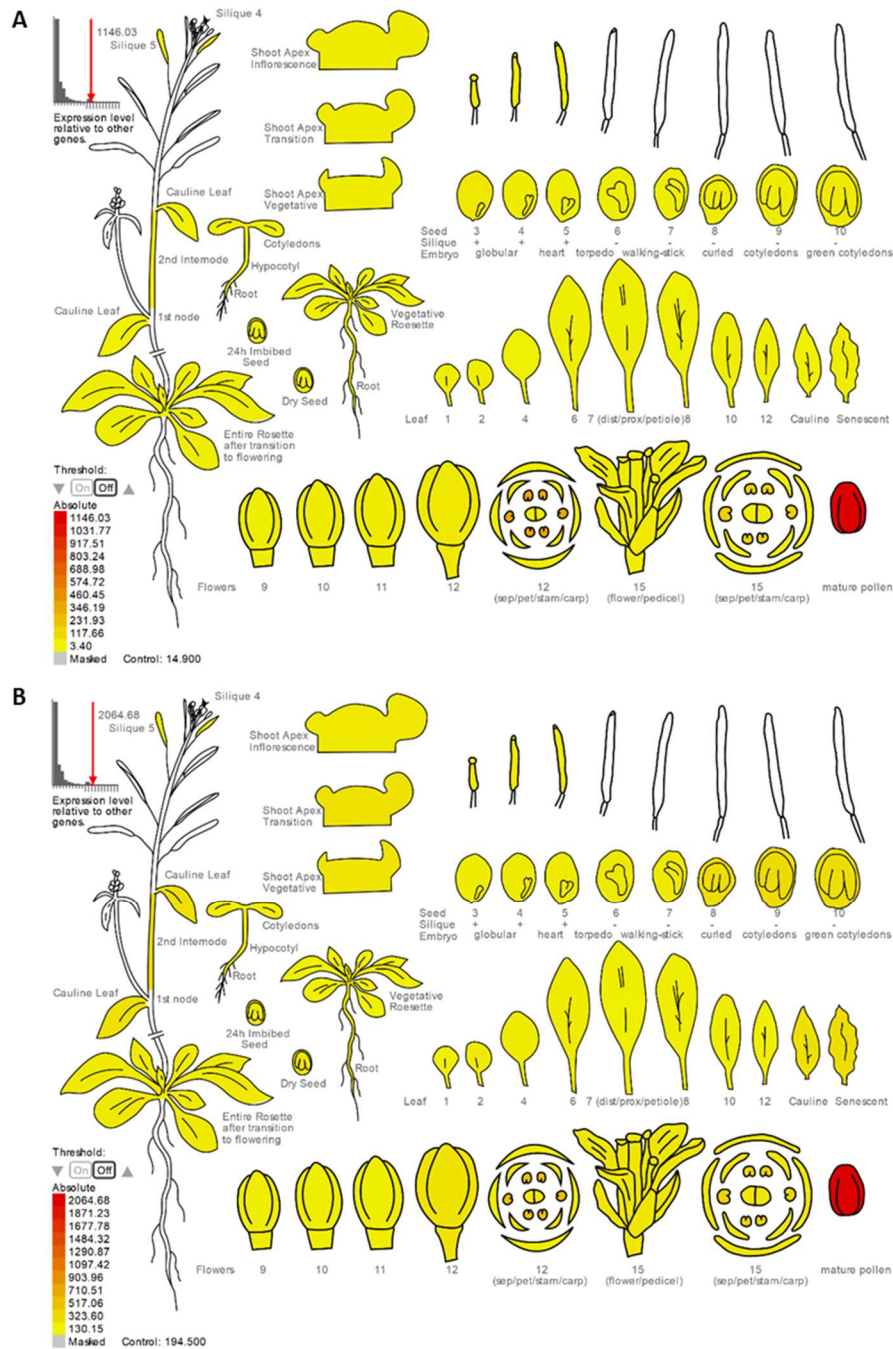
attB1PIP5K2.for	GGGGACAAGTTTGTACAAAAAAGCA GGCTTCATGATGCGTGAACCGCTT	<i>PIP5K2</i> , At1g77740
PIP5K2_attB2.rev	GGGGACCACTTTGTACAAGAAAGC TGGGTTAGCGTCTTCAACGAAGAC	<i>PIP5K2</i> , At1g77740
PIP5K2.AscI.for	ATGCGGCGCGCCATGATGCGTGAACCGCTTGTT	<i>PIP5K2</i> , At1g77740
PIP5K2.XhoI.rev	ATGCCTCGAGGCCGTCTTCGATGAAGATTCTG	<i>PIP5K2</i> , At1g77740
attB1_MVQ1.for	GGGGACAAGTTTGTACAAAAAAGCA GGCTTCATGGAGAATTCACCGAGA	<i>MVQ1</i> , At1g28280
attB2_MVQ1(+STOP).rev	GGGGACCACTTTGTACAAGAAAGCTG GGTTTCAAGAAGTAGAAGCTGA	<i>MVQ1</i> , At1g28280
RBOHD_NdeI.for	ACTGCATATGATGAAAATGAGACGAGGC	<i>RBOHD</i> , At5g47910
RBOHD_NotI.rev	CAGTGCGCCGCCTAGAAGTTCTCTTTGTG	<i>RBOHD</i> , At5g47910
qPCR_UBC10-for	ACATCATGTAGCGCAGGTCC	<i>UBC10</i> , At5g53300
qPCR_UBC10-rev	CCGGAGGGAAATGGATGGTT	<i>UBC10</i> , At5g53300
EIF4A1_qPCR.for	TCTGCACCAGAAGGCACA	<i>EIF4A1</i> , At3g13920
EIF4A1_qPCR.rev	TCATAGGATGTGAAGAACTC	<i>EIF4A1</i> , At3g13920
ERF1_qPCR.for	TCGGCGATTCTCAATTTTTC	<i>ERF1</i> , At3g23240
ERF1_qPCR.rev	ACAACCGGAGAACAACCATC	<i>ERF1</i> , At3g23240
PIPK6_qPCR.for	ATCGATCCAAACACGACGAT	<i>PIP5K6</i> , At3g07960
PIPK6_qPCR.rev	TGTCCACTTGCCTGCAGAAT	<i>PIP5K6</i> , At3g07960
M13.for	GTAAAACGACGGCCAG	Gateway plasmid sequencing
M13.rev	CAGGAAACAGCTATGAC	Gateway plasmid sequencing
RBOHD_691seq.for	ACGTCTCCGGCGATGCAA	<i>RBOHD</i> , At5g47910
RBOHD_1382seq.for	TTATTGCAAGCGGGATAG	<i>RBOHD</i> , At5g47910
RBOHD_2073seq.for	CTCCGAGGTTTGCAAACC	<i>RBOHD</i> , At5g47910
RBOHD_2534seq.rev	AACGACRGAAGCATGGCA	<i>RBOHD</i> , At5g47910
attB1_RBCL.for	GGGGACAAGTTTGTACAAAAAAGCA GGCTTTATGTCACCACAAACAGAG	<i>RBCL</i> , AtCg00490
attB2_RBCL(noSTOP).rev	GGGGACCACTTTGTACAAGAAAGCTG GGTACTACTCTTGCCATCTAA	<i>RBCL</i> , AtCg00490
attB2_RBCL.rev	GGGGACCACTTTGTACAAGAAAGGTG GGTACTCTTGCCATCTAATTT	<i>RBCL</i> , AtCg00490

8.2 Fluorophores

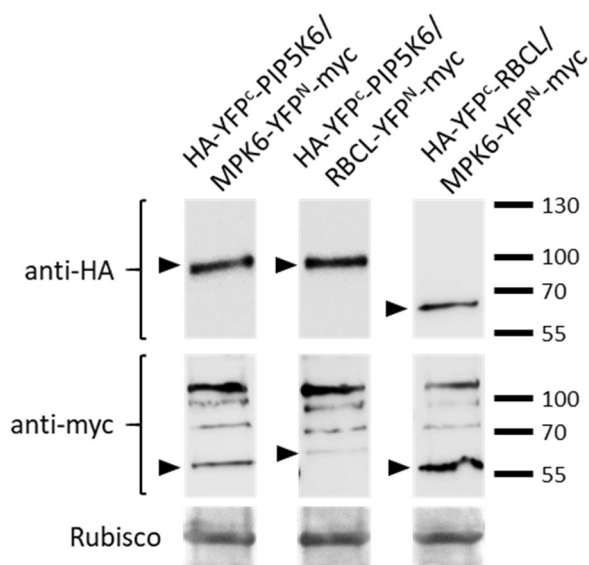
Table 8.4: Fluorophores used in cLSM.

Fluorophor	Excitation wave-length (nm)	Emission wave-length (nm)
EYFP	513	527
EGFP	488	507
mCherry	587	610
FM4-64	515	560

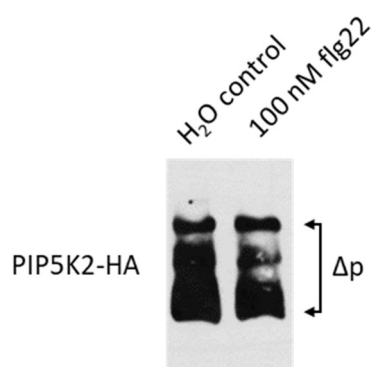
8.3 Supplementary figures



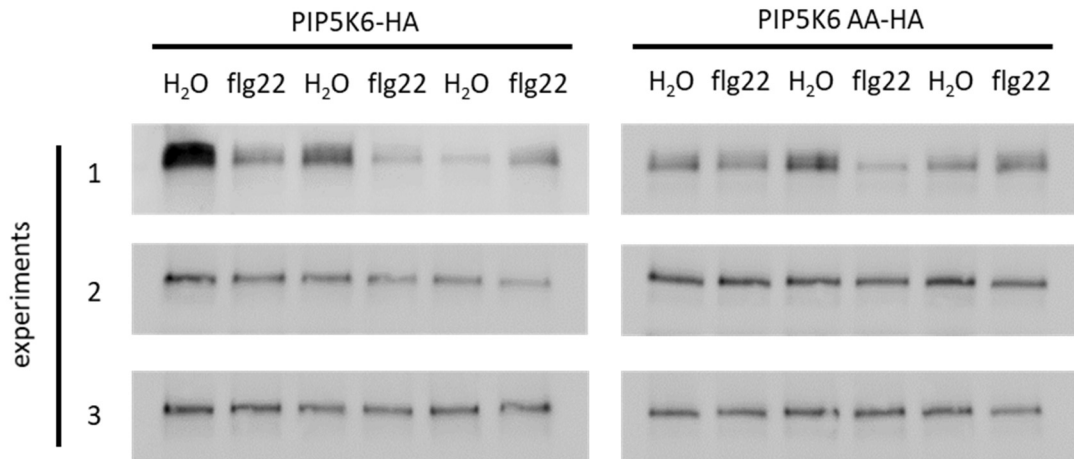
Supplementary figure 8.1: PIP5K6 and MPK6 share similar expression patterns. Expression pattern as displayed by the eFP browser (Winter et al., 2007) of PIP5K6 (At3g07960; A) and MPK6 (At3g59790; B). PIP5K6 and MPK6 display a similar expression pattern showing high expression levels in mature pollen and relatively low ubiquitous expression.



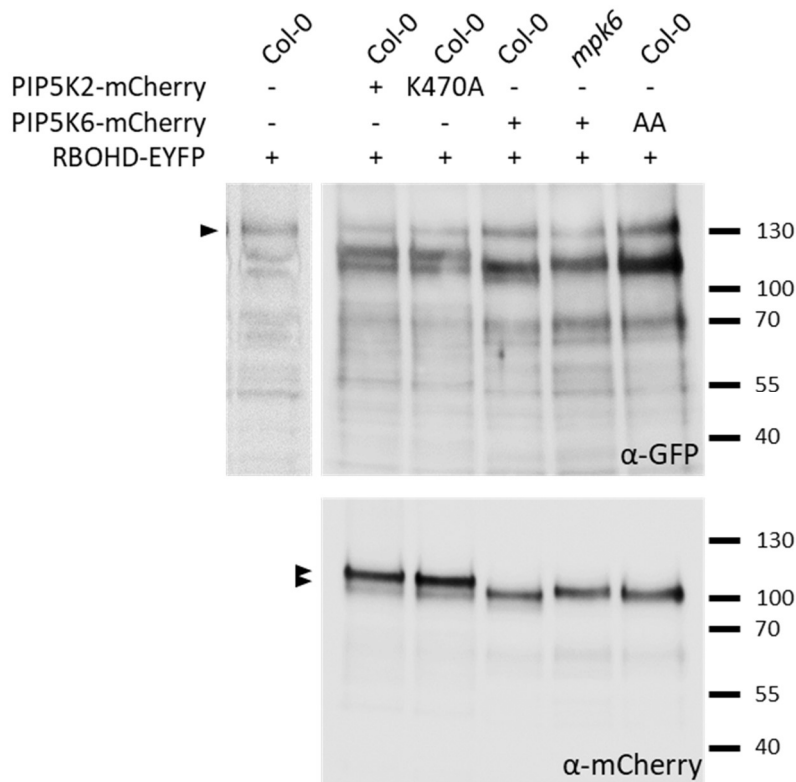
Supplementary figure 8.2: Verifying expression of full-length BiFC fusion constructs. Transgenic protoplasts were lysed and subjected to SDS-PAGE and Western blot procedure. Immunodetection of epitope-tagged proteins was performed using primary anti-HA and a secondary anti-mouse antibody for detection of HA-tagged fusion proteins or primary anti-myc and secondary anti-rabbit antibody. Secondary antibodies were conjugated to HRP for luminol-based chemiluminescence detection. All ectopically expressed proteins were expressed at full-length (arrow heads). Unspecific bands appeared in all samples when detected with an anti-myc antibody. Amido black staining was used to show equal loading amounts (showing Rubisco large subunit). $N = 3$.



Supplementary figure 8.3: Phospho-specific mobility shift analyses of PIP5K2-HA. PIP5K2 displays band shifts, indicating phosphorylation of the protein in untreated mesophyll protoplasts (Δp). No additional bands were detected from flg22-treated protoplasts that were not present in the water control, indicating no additional phosphorylation of PIP5K6 upon flg22 treatment. Transgenic mesophyll protoplasts expressing PIP5K6-HA were treated with 100 nM flg22 or water as a control for 30 min. Cell extracts were subjected to gel shift assay and Western blot procedure. Immunodetection was performed using a primary anti-HA antibody and secondary anti-mouse antibody conjugated to HRP for luminol-based chemiluminescence assay. $N = 1$.



Supplementary figure 8.4: Measuring relative protein amount used for PI4P 5-kinase assay. PI4P 5-kinase activity was assayed using immunoprecipitated PIP5K6-HA or PIP5K6 AA-HA (see **figure 2.8**) Protein amounts for each sample were analysed using SDS-PAGE and Western blot methods. Proteins were detected in a luminol-based chemiluminescence assay using a primary anti-HA antibody and a secondary anti-mouse antibody conjugated to HRP. Band intensities were quantified for relative protein amounts.



Supplementary figure 8.5: Verifying expression of full-length fluorescence-tagged fusion proteins. Protein extract from transgenic *Arabidopsis* root protoplasts was used for SDS-PAGE and Western blot procedure. Epitope-tagged proteins were detected in a luminol-based chemiluminescence assay using a primary anti-GFP or anti-mCherry antibody and a secondary anti-IgG rabbit antibody conjugated to HRP. All fusions were expressed at full-length. Expression was verified independently for every experiment. *N* = 3.

9 Abbreviations

AP-2	adaptor protein 2
APS	ammonium persulfate
Arabidopsis	Arabidopsis thaliana
BAK1	BRI1-associated receptor kinase 1
BFA	Brefeldin A
BRI1	BRASSINOSTEROID INSENSITIVE1
CBB	Coomassie Brilliant Blue
CCV	clathrin-coated vesicle
CDP-DAG	cytidine diphosphate diacylglycerol
CDPK	cyclin-dependent protein kinase
CE	cytosolic enzymes
Cer	ceramide
CHC	clathrin-heavy chain
CHX	cycloheximide
CIE	clathrin-independent endocytosis
CLC	clathrin-light chain
cLSM	confocal laser scanning microscopy
CME	clathrin-mediated endocytosis
CRP	cysteine-rich peptide
ddH ₂ O	double distilled water
DMSO	dimethyl sulfoxide
DRM	detergent-resistant membrane
DRP	DYNAMIN-RELATED PROTEIN
DTT	dithiothreitol
EE	early endosome
EGFP	enhanced green fluorescent protein
EGTA	ethylene glycol-bis(β -aminoethyl ether)-N,N,N',N'-tetraacetic acid
ER	endoplasmic reticulum
ESCRT	endosomal sorting complex required for transport
EYFP	enhanced yellow fluorescent protein
FAD	flavin adenine dinucleotide
FAME	fatty acid methyl-esters

FAPP1	phosphatidylinositol-four-phosphate adaptor protein-1
FID	flame ionization detector
FLS2	FLAGELLIN SENSING 2
FM 4-64	N-(3-triethylammoniumpropyl)-4-(6(4-(diethylamino) phenyl) hexatrienyl) pyridinium dibromide
GC	glycosylceramides
GC	gas chromatography
GEF	guanosine nucleotide exchange factor
GIPC	glycosylinositolphosphorylceramides
HCl	hydrogen chloride
HRP	horseradish peroxidase
LB	lysogeny broth
LE	late endosome
LRR	leucine-rich repeat
MAMP	microbe-associated molecular patterns
MAP3K, MEKK	mitogen-activated protein kinase kinase kinase
MAPK	mitogen-activated protein kinase
MgCl ₂	magnesium chloride
MKK, MEK	mitogen-activated protein kinase kinase
MVB	multivesicular bodies
Na ₃ VO ₄	sodium orthovanadate
NADPH	nicotinamide adenine dinucleotide phosphate
NaF	sodium fluoride
PAMP	pathogen-associated molecular patterns
PCR	polymerase chain reaction
PH domain	pleckstrin homology domain
PI	phosphoinositide
PI4K 5-kinase	phosphatidylinositol 4-phosphate 5-kinase
PIN	auxin efflux transporters-PIN FORMED
PIP5K2	phosphatidylinositol-4-phosphate 5-kinase 2
PIP5K6	phosphatidylinositol-4-phosphate 5-kinase 6
PIS	phosphatidylinositol synthase
PM	plasma membrane
PMP	plasma membrane protein
PMSF	phenylmethane sulfonyl fluoride

PRK	POLLEN RECEPTOR-LIKE KINASE
PRR	pathogen-recognition receptor
PSL	photon stimulated luminescence
PtdCho	phosphatidylcholine
PtdEtn	phosphatidylethanolamine
PtdIns	phosphatidylinositol
PtdIns	phosphatidylinositol
PtdIns(4,5)P ₂	phosphatidylinositol-(4,5)-bisphosphate
PtdIns4P	phosphatidylinositol 4-phosphate
PtdOH	phosphatidic acid
PTI	PAMP-triggered immunity
PTM	posttranslational modification
RbohD	REACTIVE OXYGEN SPECIES BURST HOMOLOGUE D
RE	recycling endosome
RHD4	ROOT HAIR DEFECTIVE4
RK	receptor kinase
RLK	receptor-like kinas
ROS	reactive oxygen species
SAC	suppressor of actin
SDS-PAGE	sodium dodecyl sulfate polyacrylamide gel electrophoresis
SERK	somatic embryogenesis receptor kinase
SH3	Src-homology 3
SV	secretory vesicle
TAE	Tris-acetate-EDTA
TEMED	tetramethylethylenediamine
TGN	trans-Golgi network
VA-TIRFM	variable-angle total internal reflection fluorescence microscopy

Acknowledgement

I find myself in the lucky position to feel obliged to gratitude to numerous people, who were there for me the past years in many ways. This very thesis would not have been written the way it is or at all without them and now, it gives me the opportunity to express my thanks.

Foremost, I want to thank my supervisor Prof. Ingo Heilmann, who of course played the most important role in my work and scientific development. During my time as a PhD student at his lab, he entrusted me with this exciting project and taught me necessities of the scientific practice. I thank him for fruitful discussion, for always being there to tackle problems and helping me to find solutions and for proof reading of this thesis.

I very much thank Dr. Lennart Eschen-Lippold for his contributions to the project and our publication in form of the PIP5K6 degradation assay and PST infiltration experiments. Furthermore, I am very thankful to him for introducing me to and teaching me everything about the protoplast expression system, which displayed a key-method to this work. I am grateful for countless times he helped me and always took his time so we could figure out a solution to another problem. And of course: "Vielen Dank, für die Blumen!"

I thank Dr. Justin Lee, who was my Mentor during the CRC648 and contributed to our publication. Due to his experience in the field of plant MAPK signalling, he pushed the project forward with ideas and suggestions and helped me many times when I would stuck. He provided me with the *mpk6*, MKK5 DD and MKK5 KR Arabidopsis lines and the plasmids and plasmid constructs pDONR™221, pUGW14, pUGW18, pE-SPYNE, pUC-SPYCE, pUGW14:MVQ1 and pUC-SPYCE:MPK6.

Many thanks to Dr. Mareike Heilmann for introducing me to the analyses of phospholipids and for contributions to the project and our publication in form of the lipid analyses on PST infected Arabidopsis tissue. I also want to thank her for everything she taught me during my time as a Master and PhD student. For always finding the time to discuss and solve problems, I encountered and patiently having an open ear and open mind whenever necessary.

I thank Dr. Praveen Krishnamoorthy for contribution to this project and our publication in form of data on the internalization of FM4-64-stained membranes and time resolved *PIP5K6* expression. He was the one to go to for any problems regarding microscopy and assisted me in SD microscopy imaging with patience.

I thank Dr. Irene Stenzel, who contributed promotor-GUS assays to our publication and this thesis. I am very thankful to Marion Sonntag, who supported me especially in the final phase of my work by providing me with buffers and media and taking some of the load off me in many other ways.

I very much thank PD Dr. Magret Köck for letting me work at the isotope lab and providing me with the needed radioactive material.

I want to thank Deutsche Forschungsgemeinschaft for funding (project HE3424 6-1) und the CRC648 (TP B10) for funding this project.

I very much thank Franziska (Hempe-) Meyer, who did the investigations on MPK6-mediated regulation of PIP5K6. She was the one who identified “New links for old pathways” and made this very project possible.

During my time as a PhD student at the lab of Ingo Heilmann, I felt blessed to work with people who would make for an atmosphere that is as professional as it is pleasing. Many thanks for the great time to Franzi, Franzi, Franzi, Praveen, Mareike, Jenny, Tobi, Lars, Feng and my students Lisa, Susanne, Lennart, Lennart and Monique.

Special thanks to Katha for all the support. Our conversations helped me a lot and I am also grateful to her for corrections on this thesis. I did not only had a good colleague but rather found a great friend in her.

Many, many thanks to my family, which is something I try to express not only on such rare occasion like this. I am ineffably grateful to my parents Christa and Werner, who gave me everything and more. They supported me in every way and would comfort me in times of misery. One cannot ask for more! Special thanks goes to my sister Grit and her husband Nils, who helped were a great support for me and my family. I very much thank my fiancée Eva and my son Anton for their endurance and all the support they gave me. I love you all.

Curriculum vitae

Name, given name	Menzel, Wilhelm Werner Reinhard Johann
Gender	male
Nationality	German
Date of birth	20th November, 1987
Place of birth	Frankfurt (Oder), Germany
Current address	Parkstraße 1, 06108, Halle (Saale), Germany

Education

Since 2014	<p>PhD, Martin-Luther-University Halle-Wittenberg</p> <p>Supervisor: Prof. Dr. Ingo Heilmann</p> <p>Thesis „ Crosstalk of ancient pathways: Phosphoinositides link receptor-triggered MAP-kinase signalling to membrane trafficking in Arabidopsis”</p>
2014	<p>Master of Science, Martin-Luther-University Halle-Wittenberg</p> <p>Supervisor: Dr. Mareike Heilmann</p> <p>Thesis “Examination of the function of putative nuclear localization signals in Arabidopsis PI4P 5-kinases”</p>
2011 - 2014	<p>Studies of Biochemistry, Martin-Luther-University Halle-Wittenberg (Master's curriculum)</p>
2011	<p>Bachelor of Science, University of Ulm</p> <p>Supervisor: Prof. Dr. Axel Brennike</p> <p>Thesis “Examinations of Mitochondrial Editing Factors in Arabidopsis thaliana”</p>
2008 - 2011	<p>Studies of Biochemistry, University of Ulm (Bachelor's curriculum)</p>

Publications

Menzel W, Stenzel I, Helbig LM, Krishnamoorthy P, Neumann S, Eschen-Lippold L, Heilmann M, Lee J, Heilmann I. 2019. **A PAMP-triggered MAPK-cascade inhibits phosphatidylinositol 4,5-bisphosphate production by PIP5K6 in *Arabidopsis thaliana***. New Phytol In press. doi: 10.1111/nph.16069.

Gerth K, Lin F, Daamen F, Menzel W, Heinrich F, Heilmann M. 2017. **Arabidopsis phosphatidylinositol 4-phosphate 5-kinase 2 contains a functional nuclear localization sequence and interacts with alpha-importins**. Plant J 92:862-878.

Gerth K, Lin F, Menzel W, Krishnamoorthy P, Stenzel I, Heilmann M, Heilmann I. 2017. **Guilt by association: A phenotype-based view of the plant phosphoinositide network**. Annu Rev Plant Biol 68:349-374.

Hempel F, Stenzel I, Heilmann M, Krishnamoorthy P, Menzel W, Golbik R, Helm S, Dobritsch D, Baginsky S, Lee J, Hoehenwarter W, Heilmann I. 2017. **MAPKs Influence pollen tube growth by controlling the formation of phosphatidylinositol 4,5-bisphosphate in an apical plasma membrane domain**. Plant Cell 29:3030-3050.

Eidesstattliche Erklärung

Ich erkläre an Eides statt, dass ich die Arbeit selbstständig und ohne fremde Hilfe verfasst, keine anderen als die von mir angegebenen Quellen und Hilfsmittel benutzt und die den benutzten Werken wörtlich oder inhaltlich entnommenen Stellen als solche kenntlich gemacht habe.

Datum

Unterschrift des Antragstellers